Post-transcriptional Regulation of Gene Expression in Response to Iron Deficiency in

Saccharomyces cerevisiae

by

Sandra Viviana Vergara

Program in Genetics and Genomics
Duke University

Date:_____
Approved:

_____
Dennis J. Thiele, Ph.D., Supervisor

_____
Matthias Gromeier, M.D.

_____
Jack Keene, Ph.D.

_____
Daniel Lew, Ph.D.

_____
William Marzluff, Ph.D.

Dissertation submitted in partial fulfillment of
the requirements for the degree of Doctor
of Philosophy in the Program in Genetics and Genomics
of Duke University

2010

ABSTRACT

Post-transcriptional Regulation of Gene Expression in Response to Iron Deficiency in

Saccharomyces cerevisiae

by

Sandra Viviana Vergara

Program in Genetics and Genomics
Duke University

Date:_____

Approved:

_____
Dennis J. Thiele, Ph.D., Supervisor

_____
Matthias Gromeier, M.D.

_____
Jack Keene, Ph.D.

_____
Daniel Lew, Ph.D.

_____
William Marzluff, Ph.D.

An abstract of a dissertation submitted in partial
fulfillment of the requirements for the degree of Doctor of Philosophy in
the Program in Genetics and Genomics
in the Graduate School of Duke University

2010

Abstract

The ability of iron (Fe) to easily transition between two valence states makes it a preferred co-factor for innumerable biochemical reactions, ranging from cellular energy production, to oxygen transport, to DNA synthesis and chromatin modification. While Fe is highly abundant on the crust of the earth, its insolubility at neutral pH limits its bioavailability. As a consequence, organisms have evolved sophisticated mechanisms of adaptation to conditions of scarce Fe availability.

Studies in the baker's yeast *Saccharomyces cerevisiae* have shed light into the cellular mechanisms by which cells respond to limited Fe-availability. In response to Fe-deficiency, the transcription factors Aft1 and Aft2 activate a group of genes collectively known as the Fe-regulon. Genes in this group encode proteins involved in high-affinity plasma membrane Fe-transport and siderophore uptake, as well as Fe-mobilization from intracellular stores and heme re-utilization. Concomitant with the up-regulation of the Fe-regulon, a large number of mRNAs encoding Fe-dependent proteins as well as proteins involved in many Fe-dependent processes are markedly down regulated. Thus, in response to low Fe-levels the cell activates the Fe-uptake and mobilization systems, while down-regulating mRNAs involved in highly Fe-demanding processes leading to a genome-wide remodeling of cellular metabolism that permits the funneling of the limiting Fe to essential Fe-dependent reactions.

The Fe-regulon member Cth2 belongs to a family of mRNA-binding proteins characterized by an RNA-binding motif consisting of two tandem zinc-fingers of the $CX_8CX_5CX_3H$ type. Members of this family recognize and bind specific AU-rich elements (AREs) located in the 3'untranslated region (3'UTRs) of select groups of mRNAs, thereby promoting their rapid degradation. In response to Fe-limitation, Cth2 binds ARE sequences within the 3'UTRs of many mRNAs encoding proteins involved in Fe-homeostasis and Fe-dependent processes, thereby accelerating their rate of decay.

Work described in this dissertation demonstrates that the Cth2 homolog, Cth1, is a *bona fide* member of the Fe-regulon, binds ARE-sequences within the 3'UTRs of select mRNAs and promotes their decay. Cth1 and Cth2 appear to be only partially redundant; Cth1 preferentially targets mRNAs encoding mitochondrial proteins, while Cth2 promotes the degradation of most of Cth1 targets in addition to other mitochondrial and non-mitochondrial Fe-requiring processes. The coordinated activity of Cth1 and Cth2 results in dramatic changes in glucose metabolism. In addition, experiments described in this dissertation indicate that the *CTH1* and *CTH2* transcripts are themselves subject to ARE-mediated regulation by the Cth1 and Cth2 proteins, creating an auto- and trans-regulatory circuit responsible for differences in their expression. Finally, work described here demonstrates that Cth2 is a nucleocytoplasmic shuttling protein and that shuttling is important for the early determination of cytosolic mRNA-fate.

Contents

List of Tables

List of Figures

Acknowledgements

I am forever thankful to my advisor Dr. Dennis J. Thiele for welcoming me in his laboratory and for providing, not only a rigorous scientific training, but also numerous opportunities to promote my professional development as a whole. His energy, enthusiasm and unwavering support offered me a very enriching graduate experience, and reinforced my desire to pursue an academic career. Most importantly, I am grateful to Dennis for teaching me that one should *work hard, AND play hard*; that *life is too short to drink bad coffee* (or bad wine), and that it is bad news to slice too thin the *prosciutto*. Without a doubt, the lessons learned at our *pizzeria* will last a life time.

I am also very grateful to my dissertation committee: Dr. Matthias Gromeier, Dr. Jack Keene, Dr. Daniel Lew, and Dr. William Marzluff (UNC-CH) for their willingness to discuss my research even outside our scheduled committee meetings, and for making me feel as their colleague. My interactions with them contributed immensely to the development of my scientific self-confidence, and I especially would like thank Danny for his time and support when I most needed it.

I also would like to thank present and past members of our *pizzeria*, in particular Dr. Sergi Puig, now at the University of Valencia (Spain), who began the studies that served as the basis for my dissertation work; my fellow iron-lady, Dr. Tracy Nevitt for her generosity; my bench-mate, Dr. Yasuhiro Nose, who continues to talk to me despite having to endure countless hours of my not-so-tuned singing and dancing; and of

course, I am very thankful to the *pizzeria's patrona*; our very own diva, Señorita Kelli Cole.

I also would like to thank my father for single-handedly raising the most rebellious and stubborn daughter anyone could have, and for introducing me to the beauty of biology at an early age; my mother for facilitating the means to come to the US to pursue my college education; my *little* brother for just that, being my *little* brother; and the rest of my family (aunts, uncles and cousins) for loving me and spoiling me without limits. I love them back without limits. And of course, there is Ted. I cannot thank him enough for his support, his patience, his love, and the mid-night Burger Truck chases and Cosmic Cantina deliveries. Never mind the mid-afternoon deliveries of frozen yogurt. How else would have I made it?

Graduate school would have not been as intellectually satisfying and as much fun without the friends that I found in Durham. I am immensely grateful to all of them for hours of interesting discussions that ranged from the existence of "God as beauty and not as an apple", to the role of women in Russian medicine, to the strange monsoons, to the new science of neuro-economics. There were times, of course, when a bunch of friends managed to talk for hours without saying anything worth remembering. Those were good times, too. I will cherish the moments we have spent together for the rest of my life.

Lastly, I would like to express my gratitude to the people in the Department of Pharmacology and Cancer Biology, to Andrea Lanahan from the program in Genetics and Genomics, and to Dean Jacqueline Looney and the staff at Graduate Student Affairs for making me part of the GSA family. I am humbly thankful to The Graduate School and the University Program in Genetics and Genomics for the opportunity of a graduate career at Duke that has far exceeded my expectations. These six years will forever remain in my mind as one of the best adventures of my life. Thank you.

1. Introduction

1.1. Co-evolution of life and transition metal bioavailability

It is estimated that about one third of all proteins require metals for function (Waldron et al., 2009). In fact, a significant percentage of each of the Enzyme Commission classes is comprised by metal-binding enzymes (Table 1)(Andreini et al., 2008). Not surprisingly, metals, in particular the transition metals Cu, Fe, Mn, and Zn participate in numerous cellular reactions that are essential for life. The essentiality of transition metals stems from their ability to interconvert between multiple oxidation states, which facilitates their participation in redox chemistry, Lewis Acid/Base chemistry, as well as hydration/dehydration reactions all of which are central to biochemistry. In addition, transition metals can serve structural roles within proteins independent of their redox activity (Table 1)(Bertini et al., 2007; Lippard and Berg, 1994) (Bertini et al., 2007; Lippard and Berg, 1994).

The biological exploitation of trace elements during the course of evolution was dramatically influenced by the solubility of the metal ions present in the primitive sea. As the chemical composition of the early atmosphere changed over time, so did the solubility of these metal ions. Consequently, the selection of metals for use by evolving proteins occurred at times when a particular metal was highly soluble, and hence, highly bioavailable . Thus, evolution is thought to have been "chemically constrained" (Williams and Frausto Da Silva, 2003). The early atmosphere was rich in H_2, CH_4, CO,

CO_2, and H_2S making it a relatively reducing medium in which elements such Fe, Mn, and Co were highly soluble, while metals such Cu and Zn were likely unavailable. Ancient photosynthetic microorganisms oxygenated the atmosphere, changing dramatically the oxidation state of trace metals. The rising levels of O_2 rendered metals such Cu and Zn more soluble therefore permitting the emergence of new metallo-proteins, and accordingly, a new repertoire of biochemical reactions or activities. Conversely, atmospheric oxygenation caused a reduction in the solubility of metals such as Fe, locking them in complexes highly insoluble at pH: 7.0 (Andreini et al., 2008). Because irreplaceable Fe-binding proteins surfaced before Fe solubility became a problem, organisms were pressured to evolve mechanisms for the scavenging of the once available, but now highly insoluble Fe. The notion that evolution was "chemically constrained" is further supported by the observation that the slope of plots comparing the number of Fe-, Mn- and Co-binding domains encoded by each genome is greater in bacteria and archaea than in eukaryotes. Conversely, the slope for Zn-binding domains is greater in eukaryotes suggesting that Zn became more important as cells became more highly specialized, likely as gene regulation became more sophisticated. In fact, Zn-finger domains and RING-finger domains are estimated to constitute 3% and 1% of the human proteome, respectively (Dupont et al., 2006; Waldron et al., 2009)

Table 1: Metal-binding proteins in biology

FUNCTION TYPE	DESCRIPTION	EXAMPLES
Di-atomic molecule transport	Di-atomic molecules such O_2 and NO can bind reversibly to Fe, Cu, or Zn ions.	• Hemoglobin/Myoglobin • Hemocyanins • Hemerythrins • Nitric Oxide Synthase
Electron transfer	The metal center acts as a current carrier without catalyzing a chemical change on the bound substrate	• Fe-S cluster containing proteins • Cytochromes • Blue copper proteins
Structure	Metal coordination plays a role in protein stability, folding and structure, protein-protein, or protein-nucleic acid interactions	• Zn-finger domains • RING-domain • RNA and DNA polymerases
Catalysis	The metal center catalyzes a chemical change on the bound substrate	• EC 1. Oxidoreductases (44%)* • EC 2. Transferases (40%)* • EC 3. Hydrolases (39%)* • EC 4. Lyases (36%)* • EC 5. Isomerases (36%)* • EC 6. Ligases (59%)* **percentage within each class corresponding to metalloenzymes*

1.2. Iron in biology – essential, harmful, and hard to get

Iron is the most abundant element on Earth, accounting for approximately 35% of the mass of the entire planet and constituting 5% of the crust of the Earth. It is a Group 8 and Period 4 transition metal and its atomic number is 26. As for all transition metals, Fe contains partially filled *d*-orbitals permitting the facile gain and loss of electrons, and making it an active participant in oxidation-reduction chemistry. Its two most common oxidation states are Fe^{2+} (ferrous) and Fe^{3+} (ferric), allowing Fe to act as electron acceptor, and thus Fe can be considered a Lewis acid. In addition, Fe acts as central atom in numerous coordination complexes, favoring hexa-coordinate complexes with ligands containing O, N, and S (Bertini et al., 2007; Lippard and Berg, 1994).

Most Fe-containing proteins wield it into prosthetic groups of Fe-S clusters and heme, while others bind mono- and bi-nuclear Fe centers (Table 2)

1.2.1. Iron-Sulfur clusters proteins

Iron -Sulfur [Fe-S] clusters are small inorganic compounds present in all Superkindoms of life. They are thought to be the earliest catalysts in the evolution of biomolecules, and their biosynthesis is indispensable for life (Hansch and Mendel, 2009; Lill and Muhlenhoff, 2008). Iron -Sulfur clusters can exist in rhombic [2Fe-2S] or cubic [4Fe-4S] clusters, although occasionally the cubic form can lose one Fe to form a distorted and elongated [3Fe-4S] cluster (Lill and Muhlenhoff, 2008; Rouault and Tong, 2005). The Fe within clusters can transition between its two oxidation states (+2 and +3), while the S is always in its -2 oxidation state, and reduction potentials of Fe-S clusters can range from +300mV to -500mV. On occasion, two [4Fe-4S] clusters can come together to make large metallo-clusters that often contain other metals such Mo, Ni and V(Lill and Muhlenhoff, 2008). While Fe-S cluster assembly occurs spontaneously under anaerobic conditions *in vitro*, their assembly *in vivo* necessitates a complex assembly machinery conserved from bacteria to humans (Lill and Muhlenhoff, 2008; Rouault and Tong, 2005).

Proteins containing Fe -S clusters participate in a plethora of biochemical processes including enzymatic reactions, respiration, electron transfer, nucleic acid

metabolism, ribosome biogenesis, tRNA modification, co-factor biosynthesis, and regulation of gene expression. Defects in Fe -S cluster formation or mutations in genes encoding specific Fe – S proteins are the etiology of various hematological and neurological diseases, such Friedreich's ataxia, cerebellar ataxia, X-linked sideroblastic anemia, and microcytic anemia, as well as the formation of tumors (Lill and Muhlenhoff, 2008; Rouault and Tong, 2005).

1.2.1. Heme proteins

Heme is a prosthetic group consisting of an Fe atom contained within a tetrapyrrole molecule called porphyrin. The Fe in heme can easily switch between its Fe^{2+} and Fe^{3+} states, although it may be present in the stable Fe^{4+} form in peroxidases. Although there are multiple heme types, heme A, B, C, and O are the most abundant. The remaining heme types (L, M, D, and S) are derivatives of the most common form, heme B, and the differences among heme types are the side chains attached to the porphyrin ring (Bertini et al., 2007; Lippard and Berg, 1994). It is believed that heme appeared in evolution in cyanobacteria for the transfer of electrons even before O_2 became available. However, in modern proteomes heme proteins are mainly involved in the sensing, storage and delivery of O_2, as well as other di-atomic gases such NO and CO. Heme proteins participate in numerous biochemical processes including electron transport, catalysis, signal transduction, and gene regulation. Other examples of processes in which heme proteins participate include free radical scavenging, sterol and

fatty acid metabolism, as well as xenobiotic detoxification (Bertini et al., 2007; Lippard and Berg, 1994).

Porphyrias are disorders in which enzymes of the heme biosynthetic pathway are affected, thus causing the hyperaccumulation of porphyrin or porphyrin precursors. According to the site of porphyrin hyperaccumulation, they are classified into hepatic (acute) porphyrias and erythropoietic (cutaneous) porphyrias. Hepatic or acute porphyrias can severely affect the nervous system causing symptoms such acute neuropathy, seizures, cardiac arrhythmias and metal disturbances, while erythropoietic or cutaneous porphyrias may cause photosensitivity, blisters and skin necrosis (Stipanuk, 2000).

1.2.3. Other Fe-coordinating proteins

Proteins that bind Fe-centers that are different from Fe-S clusters and heme are ubiquitous to all forms of life. Because these Fe-centers usually bind amino acids directly, they are believed to have evolved early in primeval life, probably even before the emergence of the heme prosthetic group. These proteins can be classified into mononuclear Fe-binding and binuclear Fe-binding. The Fe in mononuclear proteins can be found in both the Fe^{2+} and Fe^{3+}oxidation states, and it can participate in catalytic reactions as either a Lewis acid or base in addition to their role in electron transport reactions. Binuclear proteins contain two Fe ions and are found in three oxidation states: di-ferrous, di-ferric, and a mix of the two, and participate mainly as two-electron

acceptor in enzymatic reactions, in the activation of O_2, and in Fe storage. Table 2 contains a modest list of Fe-binding proteins, and illustrates the wide variety of functions in which these proteins participate, underscoring their importance in biological systems (Bertini et al., 2007; Lippard and Berg, 1994; Stipanuk, 2000).

Table 2: Iron-binding proteins in biology

BIOLOGICAL ROLES OF IRON BINDING PROTEINS

Fe-S cluster proteins

1. *Electron transfer*
   - a. *Mitochondrial electron transport chain*
     - i. Complex I: NADH dehydrogenase
     - ii. Complex II: Succinate dehydrogenase
     - iii. Complex III: Cytochrome *c* reductase
   - b. *Other electron transfer systems*
     - i. Adrenoxin component of cytochrome P450 systems
     - ii. Xanthine oxidase
2. *Non-redox Fe-S cluster proteins*
   - *a. Aconitase*
     - i. Mitochondrial aconitase
     - ii. Cytosolic aconitase/IRE-binding protein
   - ***b.*** *Ferrochelatase*
   - ***c.*** *DNA primase*

Heme proteins

1. *Oxygen carriers*
   - a. Hemoglobin/myoglobin
2. *Nitric Oxide binding*
   - a. Guanylate cyclase
3. *Electron transfer*
   - a. *Mitochondrial electron transport chain*
     - i. Complex II: cytochrome b_{560} in succinate dehydrogenase
     - ii. Complex III: cytochrome b_{562}, b_{566}, and c_1 in the cytochrome *c* reductases complex
     - iii. Cytochrome *c*
     - iv. Complex IV: cytochrome *a* in cytochrome *c* oxidase
   - b. *Other electron transfer systems*
     - i. Cytochrome b_5 in fatty acyl CoA desaturases
     - ii. Cytochrome b_5 in sulfite oxidase
4. *Activation of oxygen or peroxides*
   - *a. Mono-oxygenases, di-oxygenases, and oxidases*
     - i. Cytochrome P450 systems
     - ii. Nitric oxide synthase
     - iii. Sulfite oxidase
   - *b. Peroxidases*
     - i. Catalase
     - ii. Secretory peroxidases
     - iii. Thyroid peroxidase
     - iv. Myeloperoxidase
     - **v.** Prostaglanding H_2 synthase

Other Fe binding proteins

1. *Mono-nuclear Fe*
   - a. *Mono-oxygenases*
     - i. Phenylalanine hydroxylase
     - ii. Tyrosine hydroxylase
     - iii. Tryptophane hydroxylase
   - b. *Di-oxygensaes*
     - i. Prolyl hydroxylases
     - ii. Lysyl hydroxylase
     - iii. Lypoxygenase
2. *Bi-nuclear Fe*
   - **a.** Ribonucleotide reductases

Modified from *Biochemical and physiological aspects of human nutrition*, M.H. Stipanuk (2002).

Ironically, the chemical properties that make Fe a desired co-factor and essential micronutrient also pose two problems to all organisms that require it. First, elevated levels of Fe can have detrimental consequences for the cell. Ferric Fe can react with intracellular superoxide ions, generating the highly unstable Fe^{2+} ion, which in turn can engage in Fenton type chemistry with hydrogen peroxide or lipid peroxides yielding highly reactive hydroxyl radicals. These in turn can indiscriminately damage nucleic acids, lipids and proteins having profound consequences in cell integrity. Moreover, excess Fe can compete for metal-binding sites within non Fe-proteins causing their inactivation. Second, despite its abundance, Fe bioavailability is highly limited at physiological pH (~7) in the presence of oxygen. This is in part because at neutral pH Fe^{2+} is highly unstable and it is rapidly oxidized to Fe^{3+}, which forms very insoluble (10^{-9} M) ferric oxides that precipitate in the presence of H_2O (Ratledge and Dover, 2000). Thus, cells face the dual challenge of having to acquire Fe from an environment where its availability is limited in order to meet their essential needs, while avoiding its hyper-accumulation to prevent Fe-catalyzed cellular damage. As a result, organisms as disparate as bacteria and humans have evolved sophisticated homeostatic mechanisms to ensure appropriate intracellular Fe levels (Dunn et al., 2007; Hentze et al., 2004; Kaplan et al., 2006).

Given the importance of Fe in health and disease, Fe-homeostasis has been under extensive investigation aimed at elucidating the mechanisms of Fe acquisition, distribution and regulation (Escolar et al., 1999; Hentze et al., 2004; Kaplan et al., 2006)

The remarkable conservation of entire cellular pathways among organisms, coupled with the genetic tractability and easy manipulation of model systems such bacteria and yeast have made possible the discovery of many of the molecular intricacies of Fe metabolism and homeostasis in mammals (De Freitas et al., 2003). The continued study of Fe-homeostasis in these model systems will undoubtedly provide invaluable contributions to our understanding of disorders of Fe-imbalance in humans.

1.3. Iron Homeostasis in bacteria

1.3.1. Iron uptake and storage

Iron is an essential micronutrient for all bacteria with the exception of members of the *Lactobacillae* family (Archibald and Duong, 1984) and *Borrelia burgdoferi*, the causing agent of Lyme disease (Posey and Gherardini, 2000). While a concentration of at least 10^{-7} M is required to support bacterial growth, the estimated concentration of free Fe in terrestrial and aquatic environments is only ~10^{-9} M under aerobic conditions at pH:7 (Ratledge and Dover, 2000), and of ~10^{-18} M in biological fluids (Bullen et al., 1978; Wienk et al., 1999). It is not surprising, then, that bacteria have evolved multiple strategies to acquire Fe from their environment, which include ferrous (Fe^{2+}) or ferric

(Fe^{3+}) iron transport systems. Ferrous transport systems predominate among anaerobic and acidophilic bacteria due to the increased solubility of Fe^{2+} under these conditions. However, non-acidophilic bacteria can reduce Fe^{3+} prior to uptake, though little is known about the mechanisms of extracellular Fe^{3+} reduction (Cowart, 2002). Ferrous Fe is transported across the plasma membrane through promiscuous divalent metal transporters such metal-ABC permeases and Nramp-like transporters (Kehres and Maguire, 2002; Zaharik and Finlay, 2004), or by the Fe^{2+} specific transport system, Feo (Cartron et al., 2006). The most common pathways for Fe acquisition in bacteria, however, are those in which Fe is transported in the form of ferric complexes. Outer membrane receptors (Cir, FecA, FepA, FhuA, FhuE and Fiu) recognize ferric citrate, siderophores[1] , or host-proteins such hemoproteins and transferrin[2] -complexes, which are then transported across the outer membrane through the ATP-dependent TonB-ExbB-ExbD complex. Following translocation into the periplasm, ferric complexes are ferried through inner-membrane ABC permeases[3] such the FecBCDE, FepBCDEFG and FhuBCD systems into the cytosol (Masse and Arguin, 2005). The mechanisms by which Fe is released from ferric complexes inside the cell remain to be fully understood, but it likely involves an initial reduction step prior to release and incorporation into Fe-

[1] Siderophores are small organic molecules synthesized by bacteria and most fungi with extraordinarily high affinity for Fe^{3+}, and therefore provide an excellent means for Fe-scavenging.
[2] Transferrin is a blood plasma glycoprotein that binds Fe^{3+} tightly but reversibly and it is involved in the delivery of Fe to peripheral tissues.
[3] ATP-Binding Cassette (ABC-) proteins are transmembrane proteins that utilize the energy from ATP hydrolysis for the transport of substrates across membranes.

utilizing proteins. Excess Fe is stored into heme-bacterioferritin (Bfr) or the non-heme ferritin, FtnA. While these storage proteins are only distantly related, both are composed of 24 identical (or highly similar) 19kDa subunits that form a nearly spherical and hollow structure of approximately 450kDa capable of storing up to 2000 atoms of Fe^{3+} bound to phosphate (Andrews, 1998). In addition, each subunit contains ferroxidase activity that may be important for Fe release.

1.3.2 The ferric uptake repressor, Fur

Due to the inability to excrete excess Fe from the cell, microorganisms must tightly regulate Fe uptake in order to avoid toxicity. The major regulator of Fe homeostasis in bacteria is the Fe^{2+}-dependent ferric uptake repressor, Fur. Fe^{2+} binding by Fur increases its affinity for DNA sequences called Fur boxes located upstream of genes encoding proteins involved in Fe-uptake pathways such siderophore synthesis and metabolism, hindering the access of RNA polymerase and thereby repressing their expression (Escolar et al., 1999; Masse and Arguin, 2005). In addition, studies demonstrated that Fur represses the expression of a sigma transcriptional factor and a small non-coding RNA called RyhB, or SraI. Apo-Fur cannot bind DNA. As a consequence, when intracellular Fe levels decrease, genes under Fur control are de-repressed and transcribed. Fur also appears to regulate the expression of genes involved in acid shock response, oxidative stress, energy metabolism, bioluminescence, and production of toxins and virulence factors (Hall and Foster, 1996; Hantke, 1981; Litwin

and Calderwood, 1993; Masse and Arguin, 2005; Niederhoffer et al., 1990; Stojiljkovic and Hantke, 1994; Tardat and Touati, 1993).

1.3.3 RyhB-mediated response to iron deficiency

RyhB was identified in two genome-wide studies aimed at the identification of non-coding RNAs in *E. coli* (Argaman et al., 2001; Wassarman et al., 2001). Analysis of this 90nt small RNA revealed a Fur box in the promoter region and a high RNA-RNA pairing with sdhCDAB mRNAs, which encode subunits of the succinate dehydrogenase complex. It was later demonstrated that during Fe-deficiency, RyhB pairs with mRNAs near the site of ribosome loading aided by the Hfq RNA chaperone, promoting the recruitment of the RNA degradosome, which in turn degrades both RyhB and the target mRNAs (Masse and Arguin, 2005; Masse and Gottesman, 2002; Masse et al., 2007; Masse et al., 2005). Microarray experiments revealed that RyhB downregulates at least 18 transcripts encoding a total of 56 proteins that are involved in Fe-metabolism or require Fe for function such aconitase, fumarase, bacterioferritin, ferritin, and Fe-SOD (superoxide dismutase). Interestingly, these experiments also revealed that RyhB only targets for degradation mRNAs encoding non-essential Fe-requiring proteins, whereas mRNAs encoding Fe-utilizing proteins with essential functions such ribonucleotide reductase remain unaffected by RyhB activity (Masse et al., 2005).

1.4. Iron homeostasis in baker's yeast

1.4.1. Iron uptake and storage

Despite its abundance, Fe is poorly available in the presence of oxygen at physiological pH. As a consequence, organisms have evolved sophisticated strategies to acquire Fe from their environment in order to survive. *Saccharomyces cerevisiae* employs two mechanisms of Fe acquisition: divalent Fe-transport systems and a siderophore transport system (Van Ho et al., 2002).

Uptake of divalent Fe in yeast requires the initial reduction of Fe^{3+} from ferric salts or from siderophores by plasma membrane metalloreductases encoded by the *FRE* genes (Figure 1). Fre1 and Fre2 are flavocytochrome reductases that account for up to 98% of the plasma membrane reducing activity of ferric salts (Anderson et al., 1992; Dancis, 1998; Georgatsou et al., 1992), while Fre3 and Fre4 catalyze the reduction of Fe^{3+} bound to siderophores, lowering its affinity and causing its release. Divalent Fe can subsequently be transported across the plasma membrane into the cell through the low affinity divalent metal transporters Fet4 and Smf1[4] , or through a high affinity Fe-selective transport system comprised of the multicopper oxidase Fet3[5] and the Fe-permease Ftr1 (Philpott and Protchenko, 2008; Van Ho et al., 2002)(Figure 1). Iron availability inversely regulates the expression of low and high affinity transport systems.

[4] Yeast Smf1 and Smf2 belong to the Nramp family (natural resistant-associated macrophage proteins) of divalent metal transporters to which mammalian DMT-1 (Nramp2) and Nramp1 belong.
[5] Fet3 is a multi-copper ferroxidase that converts Fe^{2+} back to Fe^{3+} for transport by the interacting permease Ftr1. Fet3 is homologous to mammalian hephaestin and ceruloplasmin.

In addition to divalent Fe acquisition, yeast can obtain Fe^{3+} from siderophore chelates. Yeast does not produce siderophores, but it can utilize siderophores secreted by other microorganisms in a process that is thought to involve their initial capture by the cell wall mannoproteins Fit1-3. While it is unclear how siderophore-Fe complexes are ferried across the periplasmic space, subsequent transport of intact siderophore-Fe chelates across the plasma membrane is mediated by a group of proteins belonging to the major facilitator superfamily of transporters, Arn1-4. Each Arn transporter exhibits specificity for different types of bacterial and/or fungal siderophores, and much remains to be understood as to how the bound Fe dissociates and is mobilized for later cellular use (Philpott et al., 2002; Van Ho et al., 2002).

Most of the Fe taken up by the cell is imported into the mitochondria for incorporation into heme and Fe-S clusters. Not surprisingly, most of the cellular Fe is contained within these organelles. Much remains to be understood about the mechanism of Fe import into mitochondria, but studies have demonstrated that transport is dependent on mitochondrial membrane potential, and it is somehow facilitated by the inner membrane transporters Mrs3 and Mrs4. Assembly of mitochondrial Fe-S proteins takes place *in situ*, while incorporation of Fe-S clusters into non-mitochondrial proteins

takes place in the cytosol and requires Fe-S cluster export from the mitochondria through the Atm1[6] transporter (Figure 1)(Lill and Muhlenhoff, 2008).

Excess cytosolic Fe can have detrimental effects on cellular integrity. Consequently, Fe that is not imported into the mitochondria for Fe-S clusters and heme synthesis or used by other Fe-binding proteins is transported to the vacuole through the vacuolar Fe-transporter Ccc1 for safe storage. The stored Fe can be mobilized back from the vacuole into the cytosol by the low affinity transporter Smf3, or the high affinity transport system Fet5/Fth1, which work in conjunction with the vacuolar reductase Fre6. These systems are analogous to the plasma membrane Smf1, Fet3/Ftr1 and Fre1-4, respectively (Figure 1)(Van Ho et al., 2002).

[6] Atm1 is a yeast ABC-transporter located to the inner mitochondrial membrane important for Fe-S cluster biosynthesis; homologous to human ABC7.

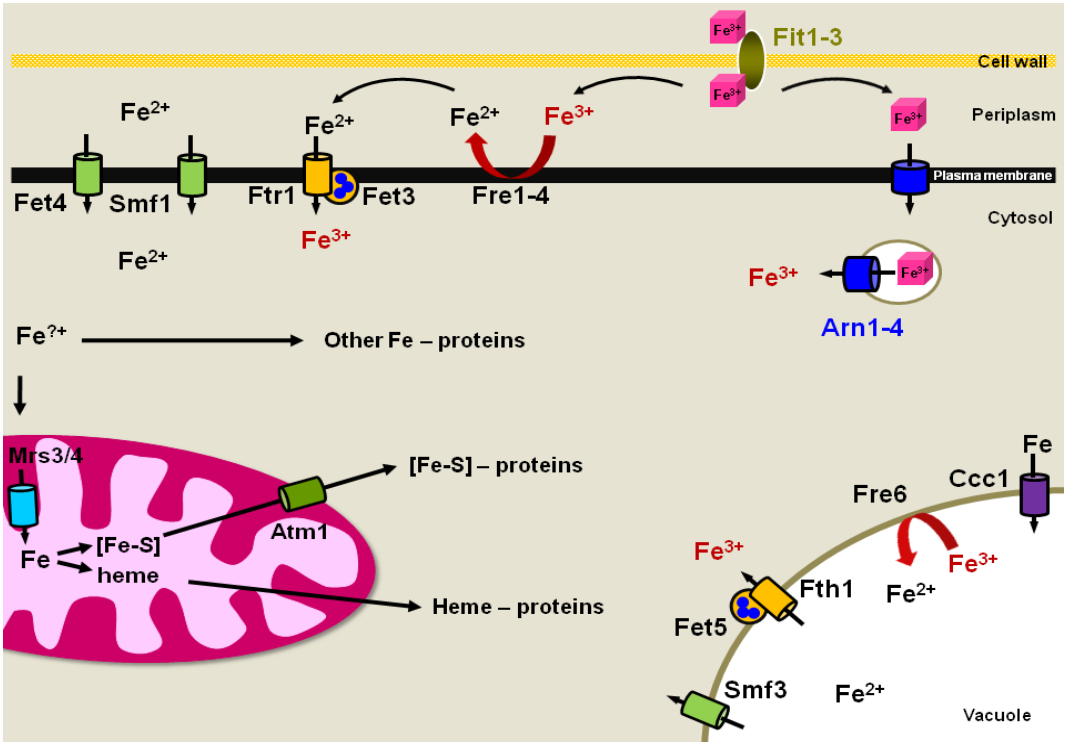

Figure 1. Iron homeostasis in yeast.

Iron can be acquired by yeast as inorganic Fe or in siderophores-chelates. Uptake of inorganic Fe requires the initial reduction of Fe^{3+} to Fe^{2+} by the plasma membrane reductases Fre1-4, and subsequently transported across the plasma membrane by low affinity (Fet4 and Smf1) or high affinity (Fet3/Ftr1) transport systems. Capture of siderophore-chelates is mediated by the cell wall mannoproteins Fit1-3. The Fe in siderophore-chelates can be either reduced at the plasma membrane for transport as inorganic Fe, or the entire siderophore-chelate may be transported via specialized transporters, Arn1-4. Cytosolic Fe is mainly transported to the mitochondrial matrix in a process that requires the activity of the inner mitochondrial transporters, Mrs3 and Mrs4, for incorporation into Fe-S clusters and heme. Export of Fe-S clusters to the cytosol is mediated by the ABC-transporter Atm1. Iron is also used in non Fe-S clusters and non-heme coordinating proteins in the cytosol, and excess Fe is transported into the vacuole through the Ccc1 transporter for safe storage. Vacuolar Fe can be mobilized back to the cytosol after a reduction step carried out by Fre6, and transported through Smf3 or Fet5/Fth1.

1.4.2. Transcriptional regulation of iron homeostasis

Iron sensing in yeast is mediated by the transcription factors Aft1 and Aft2, which activate the expression of a group of genes collectively referred to as the Fe-

regulon under conditions of Fe-limitation (Table 3)(Courel et al., 2005; Rutherford et al., 2003; Shakoury-Elizeh et al., 2004). The Fe-regulon includes genes whose products are involved in the reduction of Fe at the plasma membrane (*FRE1-4*), low and high-affinity Fe uptake (*FET4*, *FET3* and *FTR1*), siderophore recognition and transport (*FIT1-3* and *ARN1-4*), and redistribution of intracellular Fe-stores (*FRE6, SMF3, FET5* and *FTH1*) (Section 1.4.1 and Figure 1). In addition, Aft1 and Aft2 activate the expression of genes whose functions promote cellular changes that lead to a metabolism better suited for growth under Fe-limitation. These genes include a H^+-biotin symporter (*VHT1*), a heme oxygenase (*HMX1*), and the genes *CTH1* and *CTH2* (also called *TIS11*) (Table 3). Much remains to be understood about the exact mechanism of Fe-sensing. However, studies have demonstrated that activation of the Fe-regulon by Aft1, the most extensively studied Fe-responsive transcription factor, occurs in response to a deficit in mitochondrial Fe-S cluster synthesis and not in response to cytosolic Fe levels (Chen et al., 2004). While expression of Aft1 occurs under conditions of both high and low Fe, its subcellular localization is regulated by Fe-levels (Yamaguchi-Iwai et al., 2002). Studies demonstrated that Aft1 is a nucleocytoplasmic shuttling protein, whose nuclear import is Fe-independent. However, nuclear export of Aft1 requires Fe and therefore, under conditions of Fe-limitation Aft1 is retained in the nucleus, thereby inducing the activation of genes in the Fe-regulon (Ueta et al., 2007). Interestingly, conditions other than Fe-limitation such glucose depletion during diauxic shift and exposure to high

concentrations of Co also cause the activation of the Fe-regulon. However, the mechanisms of Aft1 activation or the function of the Fe-regulon under these conditions is currently unknown (Haurie et al., 2003; Stadler and Schweyen, 2002)

Table 3. The Fe-regulon

GENES ACTIVATED BY AFT1 AND AFT2 DURING IRON DEFICIENCY	
Gene	**Function**
IRON UPTAKE	
FRE1 and *FRE2*	Major plasma membrane metalloreductases
FRE3 and *FRE4*	Plasma membrane metalloreductases involved in reduction of siderophore-bound Fe^{3+}
FET3	Plasma membrane multicopper oxidase
FTR1	Plasma membrane Fe^{2+} permease
FET4	Plasma membrane low affinity divalent metal transporter
FIT1-3	Cell wall mannoproteins involved in siderophore capture
ARN1-4	Plasma membrane siderophore transporters
IRON MOBILIZATION FROM VACUOLE	
FRE6	Vacuolar metalloreductase
SMF3	Low affinity vacuolar Fe-effluxer
FET5	Vacuolar multicopper oxidase
FTH1	Vacuolar Fe^{2+} permease
METABOLIC ADAPTATION	
VHT1	Biotin transporter
HMX1	Heme oxygenase homologue
CTH1	mRNA-destabilizing protein
CTH2 (TIS11)	mRNA-destabilizing protein

Iron transport into the vacuole is mediated by the divalent metal transporter Ccc1 for safe storage. Under conditions of limited Fe, the *CCC1* mRNA is destabilized Cth2 to prevent storage of the already limited cellular Fe (see section 1.4.3). Conversely, in the presence of elevated Fe concentrations Ccc1 expression increases as a protective

mechanism from Fe-induced cellular damage (Li et al., 2005). A recent study identified Yap5 as responsible for the Fe-dependent transcriptional activation of the *CCC1* gene (Li et al., 2008). Yap5 belongs to the family of basic-region leucine zipper (bZIP) transcription factors (similar to mammalian AP-1) involved in the response to environmental stresses such oxidative stress and Cd exposure (Fernandes et al., 1997). Yap5 recognizes the Yap consensus TTCACGA sequence located in the promoter region of the *CCC1* gene independently of Fe levels. However, elevated Fe concentrations appear to catalyze modifications of thiol groups in a highly conserved cysteine-rich motif within Yap5, which in turn leads to transcriptional activation of the *CCC1* gene (Li et al., 2008).

The presence of multiple transcription factors responsive to varying Fe-concentrations underscores the importance of maintaining cellular Fe balance. Aft1/2 sense low Fe and activate genes involved in Fe acquisition systems, while Yap5 senses high Fe and activates the vacuolar Fe storage system. It remains to be determined whether Yap5 also activates the expression of other genes whose functions may be the protection against Fe-induced cellular damage.

1.4.3. Post-transcriptional regulation of iron homeostasis

Concomitant with transcription of the Fe-regulon, key components of Fe-dependent metabolic pathways such the tricarboxylic acid (TCA) cycle, the electron transport chain, Fe-S cluster and heme biosynthesis, as well as proteins involved in Fe-

storage and the biosynthesis of glutamate, branched amino acids, and fatty acids are coordinately down-regulated under conditions of Fe-limitation. The proteins Cth1 and Cth2, whose genes are under the control of Aft1/2 and thus are *bona fide* members of the Fe-regulon, negatively regulate the stability of a large percentage of these mRNAs (Lesuisse et al., 2003; Puig et al., 2005; Puig et al., 2008; Vergara and Thiele, 2008). Cth1 and Cth2 belong to a family of RNA-binding proteins conserved from yeast to humans, characterized by the presence of two tandem zinc-fingers of the CCCH-type which constitute an mRNA-binding domain that recognizes specific AU-rich sequences (AREs) within the 3'unstranslated region (3'-UTR) of select mRNAs. An interaction between these proteins and an ARE-containing mRNA causes the destabilization of the bound transcript (Blackshear, 2002; Thompson et al., 1996).

Interestingly, a large percentage of the mRNAs whose steady state levels are decreased under conditions of Fe-deficiency harbor AREs within their 3'UTRs. Thus, under Fe-deficiency Cth1 and Cth2 are expressed and bind the AREs in the 3'UTRs of specific mRNAs involved in Fe-dependent processes, thereby promoting their accelerated degradation (Puig et al., 2005; Puig et al., 2008; Vergara and Thiele, 2008). Moreover, their combined activity results in dramatic changes in glucose metabolism including the elevated expression of genes involved in glucose metabolism and increased glycogen storage (see Chapter 2 of this dissertation).

Interestingly, Cth1 and Cth2 appear to only be partially redundant. Cth1 preferentially targets mRNAs encoding mitochondrial proteins, while Cth2 promotes the degradation of most of Cth1 targets as well as other mRNAs encoding proteins involved mitochondrial and non-mitochondrial Fe-requiring processes (Puig et al., 2008). While Cth1 is transiently expressed reaching maximum levels soon after Fe-deficient conditions are imposed, Cth2 expression gradually increases during Fe-deficiency over time, remaining at its highest levels even after 6 or 8 hrs of Fe-deficiency. These observations have lead to the hypothesis that Cth1 and Cth2 act as a molecular rheostat allowing metabolic adaptation to varying degrees of Fe-limitation, whereby Cth1 activity is sufficient for adaptation to transient or modest Fe-deficiency by targeting mitochondrial functions. However, if the deficiency is not remedied, Cth2 is strongly induced providing a means for a more generalized shift from a highly Fe-dependent to a less Fe-dependent metabolism as a cellular strategy to prioritize Fe-allocation (Puig et al., 2008).

Excess cellular Fe can catalyze the formation of highly reactive hydroxyl radicals that can damage membranes, proteins and nucleic acids having profound consequences on cellular integrity. To date, no efflux mechanisms for Fe detoxification have been identified (Li et al., 2008). Therefore, Fe-homeostasis must be tightly regulated at the level of uptake, allocation and storage. In particular, mechanisms to rapidly down-regulate Fe-regulon functions, whose purpose is to increase cellular Fe-levels, must exist

in order to avoid toxicity in the face of acute increases of extracellular Fe. Regulation would be especially important if a sudden elevation in Fe-levels occurs following a period of severe starvation, in which metabolism has been modified for lower Fe demand. The rapid nuclear export of Aft1 in the presence of increased intracellular Fe is one mechanism by which the cell avoids the futile expression of the Fe-acquisition genes. Moreover, exposure to high Fe concentrations (1mM $FeSO_4$) promotes the rapid internalization and ubiquitin-dependent degradation of the high affinity Fe-transport system, while as little as 10μM $FeSO_4$ causes a dramatic reduction of the *FET3* mRNA (Felice et al., 2005). In addition, the RNA endonuclease Rnt1 contributes to the rapid degradation of mRNAs encoded by the Fe-regulon genes (Lee et al., 2005). Rnt1 is the lone member of the RNase III family of double-stranded RNA endonucleases in yeast, which specifically cleaves RNA hairpins capped with AGNN tetraloop structures. The resulting cleavage intermediates are consequently degraded by 5′→3′ exonucleases. Strains in which the *RNT1* gene has been deleted ectopically express members of the Fe-regulon and are hypersensitive to Fe toxicity. Theoretical RNA folding models predict that the secondary structures of mRNAs corresponding to several members of the Fe-regulon, including mRNAs encoding two reductases, the high affinity Fe-transport and siderophore transport systems form imperfect stem-loop structures capped by AGNN-type tetraloops. These observations suggest that Rnt1 post-transcriptionally limits the

expression of members of the Fe-regulon to reduce the potentially toxic effects of high Fe-conditions (Lee et al., 2005).

1.4.4. Metabolic regulation of iron homeostasis

Studies in yeast indicate that cells growing under Fe-limited conditions not only increase the expression of Fe-uptake and mobilization systems but also re-adjust their metabolism in order to more efficiently utilize the scarce Fe, suggesting a hierarchical order of Fe-utilization whereby Fe is spared for essential processes and away from non-essential ones (Puig et al., 2008; Shakoury-Elizeh et al., 2004; Vergara and Thiele, 2008).

Generally speaking, cellular energy production can be divided into three major steps: (1) breakdown of macromolecules into their building blocks (proteins into amino acids, fats into fatty acids, and polysaccharides into simple sugars); (2) breakdown of amino acids, fatty acids and simple sugars into acetyl-CoA with the production of limited ATP and NADH; and (3) complete oxidation of acetyl-CoA through the TCA cycle and electron transport chain accompanied by the production of large amounts of ATP in the mitochondrion. The TCA cycle and the electron transport chain are heavily Fe-utilizing processes that are dispensable for yeast growth (Dickinson and Schweizer, 2004). However, their repression leads to secondary consequences on energy metabolism as the alternative glycolytic pathway to produce ATP is much less efficient. Yeast cells grown under Fe-limiting conditions have elevated levels of mRNAs encoding proteins involved in the high affinity uptake of glucose, glycolysis, reserve carbohydrate

metabolism, and mRNAs whose expression is activated by glucose-starvation. In addition, Fe-deficiency leads to the phosphorylation of the AMP-activated kinase Snf1, a key player in the adaptation to low-glucose conditions, and Fe-starved cells hyperaccumulate glycogen in a Cth1/Cth2-dependent manner (Puig et al., 2008). Thus, Fe-deficient cells undergo a metabolic switch away from a highly Fe-dependent mechanism of ATP generation toward glycolytic metabolism (Fe-independent), which leads to an increase in glucose demand due to its reduced efficiency at generating ATP (Puig et al., 2008; Shakoury-Elizeh et al., 2004).

Another example of a metabolic regulatory change that takes place in response to Fe is the switch from biotin biosynthesis (highly Fe-dependent) to biotin import (Fe-independent) during Fe-deficient conditions. Biotin synthesis takes place in mitochondria in a process that requires the activity of three crucial enzymes: DAPA[7] -aminotransferase (Bio3), dethiobiotin synthase (Bio4) and biotin synthase (Bio2), a homodimeric protein that coordinates a [2Fe-2S] and a [4Fe-4S] cluster per monomer. Alternatively to its biosynthesis, biotin can be acquired from the environment and transported across the plasma membrane through the high affinity H+-biotin symporter, Vht1. In response to Fe limitation the *BIO3, BIO4,* and *BIO2* mRNAs are down-regulated while the *VHT1* gene is highly up regulated by Aft1 (Shakoury-Elizeh et al., 2004). In addition to expression of the biotin transporter, Aft1 also activates the expression of the

[7] Di-amino-pelargonic acid

HMX1 gene, which encodes a protein with 21% identity with human heme oxygenase (Protchenko and Philpott, 2003). While it remains unclear whether Hmx1 is a bona fide heme oxygenase, studies have shown that its activity does contribute to the degradation of heme, and it has been proposed that its main function is to allow the recycling of intracellular heme-Fe during conditions of Fe-limitation.

1.5. Iron homeostasis in mammals

1.5.1. Iron uptake and storage

Iron obtained from dietary sources comes in the form of heme and inorganic non-heme Fe. Heme-Fe is obtained mainly from hemoglobin and myoglobin in red meats and it is the best dietary source of Fe. Inorganic non-heme Fe is acquired from grains and vegetables. Heme-Fe is more highly bioavailable because at the alkaline pH of the small intestine, heme polymerization is reduced, and solubility and absorption are not affected by other dietary components. Contrarily, under these conditions inorganic Fe is present mainly in its Fe^{3+} state, which forms highly stable complexes not readily absorbed. In addition, inorganic Fe absorption is highly influenced by other dietary components such phytates (found in legumes, grains and rice), polyphenols (some fruits and vegetables, and soy protein), and tannins (found in coffee and tea), which chelate Fe making it unavailable for absorption. A few reductants such ascorbate and other organic acids, however, can improve non-heme Fe absorption (West and Oates, 2008).

Due to the absence of excretory Fe mechanisms, Fe balance is highly controlled at the level of uptake and nearly all of the available systemic Fe is recycled from senescent red blood cells (RBCs). The only forms of Fe loss in humans are through the desquamation of enterocytes and skin cells, and in women through menstruation and child bearing. Dietary Fe absorbed by the enterocytes of the duodenum and upper jejunum is deposited in the blood plasma and rapidly bound to transferrin for delivery to the bone marrow, liver and other organs. In the bone marrow Fe is used in the production of RBCs, which account for the largest pool of Fe in the body. Senescent RBCs are phagocytosed by macrophages which recycle the Fe by either storing or depositing the Fe back into the blood plasma. Excess Fe can also be stored in parenchymal tissues such as the liver (Figure 2), which can be re-deposited in the blood plasma upon need (De Domenico et al., 2008; Hentze et al., 2004).

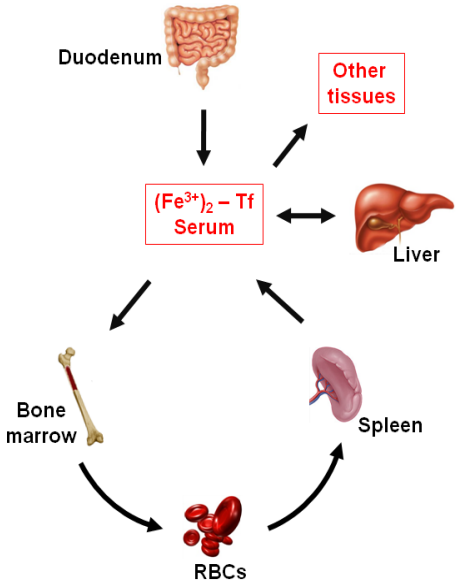

Figure 2. Systemic iron uptake and storage in mammals

Iron in food is present primarily as heme or inorganic Fe^{3+}. There is evidence supporting a role for a heme-transporter, but it remains to be identified. Figure 3 describes our current understanding on inorganic Fe^{3+} absorption. Inorganic Fe^{3+} is first solubilized to Fe^{2+} by the Dcytb reductase. Subsequent transport of ferrous Fe across the apical membrane of the enterocyte is mediated by the divalent metal transporter DMT-1[8], which also transports other divalent metals such Mn^{2+} and Zn^{2+}. Once inside the cell, Fe can be stored into ferritin, or exported to the blood plasma through the Fe-exporter ferroportin. Ferrous Fe transported by ferroportin is quickly re-oxided to Fe^{3+} by the

[8] Divalent metal transporter 1; belongs to the same Nramp family of solute carriers as yeast Smf1 and Smf2.

multicopper oxidase hephaestin[9] , and is rapidly bound by the Fe^{3+}-protein carrier, transferrin (Tf). The Tf-Fe^{3+} chelates in blood plasma are delivered to erythroid precursors and peripheral tissues, where they translocate into cells through Tf-receptors expressed at the plasma membrane. Tf-Fe^{3+}/Tf-Receptor complexes are rapidly internalized by receptor mediated endocytosis through clathrin-coated pits that get acidified, promoting a conformational change in both Tf-Fe^{3+} and the Tf-receptor consequently releasing the bound Fe^{3+}. Endosomes express the reductase STEAP-3[10] , as well as DMT-1. Thus, endosomal Fe^{3+} released from the Tf/Tf-receptor complex is reduced to Fe^{2+} by the reductase STEAP3 and transported through DMT-1 into the cytosol for cellular use (De Domenico et al., 2008; Hentze et al., 2004).

Most of the Fe in mammals is found in the form of heme within RBCs which have a life span of approximately 120 days in humans. Senescent and damaged RBCs are phagocytosed by macrophages and degraded within lysosomes (Figure 3). The heme recovered from RBCs digestion is then degraded by heme oxygenase causing the release of the bound Fe, which can be either stored into ferritin, or exported from the macrophages to the blood plasma through ferroportin. Ferrous Fe exported by ferroportin in macrophages requires re-oxidation by the GPI-linked multicopper oxidase ceruloplasmin prior to reloading into circulating transferrin. When Fe absorption or recycling exceeds metabolic demands, Tf-bound Fe^{3+} can be stored in the hepatocytes or

[9] Hephaestin is a multi-copper oxidase ferroxidase homologous to ceruloplasmin and yeast Fet3.
[10] STEAP3 is a metalloreductase homologous to the yeast family of FRE metalloreductases.

retained by macrophages and released back into blood plasma upon need (De Domenico et al., 2008; Hentze et al., 2004).

1.5.2. Systemic regulation of iron balance – hepcidin

Regulation of systemic Fe homeostasis is mediated by the cysteine-rich peptide hormone hepcidin. This 25-amino-acid circulating hormone is secreted by the liver and it is derived from an 84-amino-acid precursor encoded by the *HAMP* gene (Hentze et al., 2004). Hepcidin is a member of the family of *defensins*, a group of antimicrobial peptides present in insects, plants and mammals, with a high level of conservation between mouse and human. Hepcidin negatively regulates Fe entry into circulating plasma by promoting ubiquitin-dependent degradation of ferroportin in intestinal epithelial cells and macrophages (Figure 3). As a consequence, Fe export from these cells is inhibited leading to increased cytosolic Fe-levels, which are stored into ferritin (De Domenico et al., 2007). Hepcidin expression increases in response to high levels of circulatory Fe as well as in response to inflammation and infection, and it decreases in response to hypoxia and anemia. Thus, hepcidin expression is inversely proportional to Fe-needs and it provides a molecular means of communication between Fe-utilizing tissues and cells involved in uptake and storage of Fe (De Domenico et al., 2008; Hentze et al., 2004).

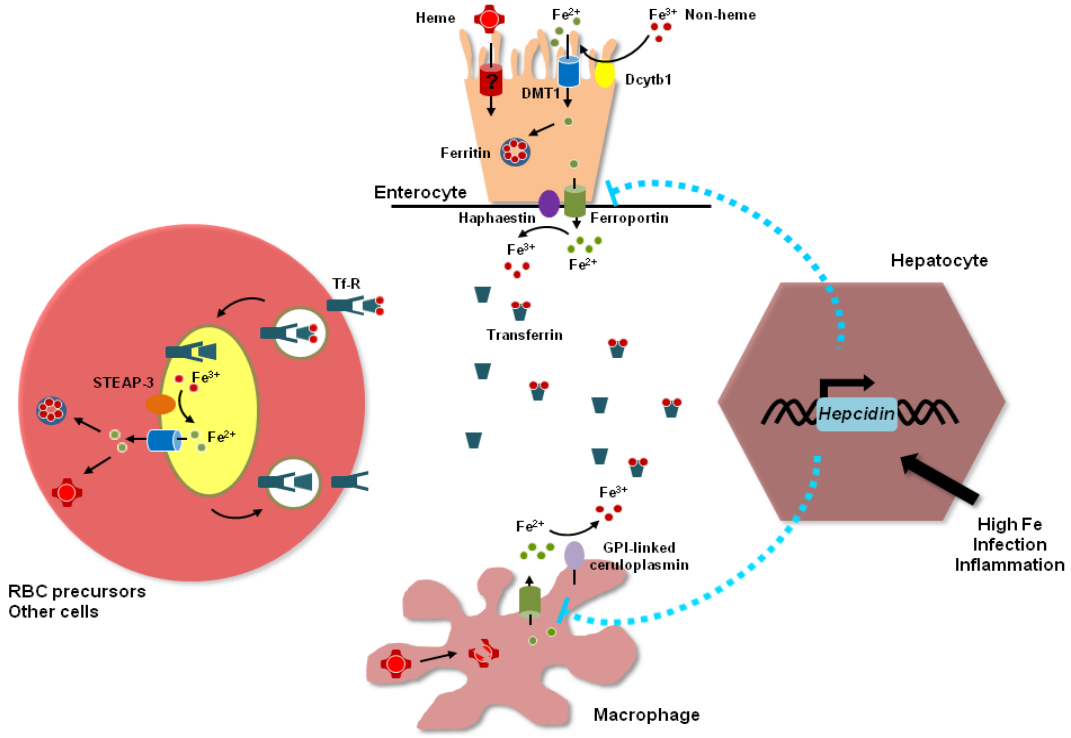

Figure 3. Cellular iron uptake and storage

1.5.3. Cellular regulation of iron balance – the IRE/IRP system

Post-transcriptional regulation of mRNAs encoding proteins involved in Fe uptake, storage and utilization by Iron Regulatory Proteins (IRP1 and IRP2) is central to cellular Fe homeostasis. IRP1 and IRP2 bind to hairpin structures named Iron Responsive Elements, or IREs, containing a six nucleotide sequence 5′-CAGUGN-3′ that forms an apical loop on a stem of five paired bases preceded by an unpaired cytosine on the 5′ strand. The rest of the stem may be of variable length. The 5′UTRs of mRNAs encoding ferritin heavy and light chains, erythroid 5-aminolevulinic acid synthase

(eALAS, the first enzyme in heme synthesis), mitochondrial aconitase (TCA cycle enzyme), and ferroportin contain single IRE hairpins that are bound by IRP1/IRP2. This interaction results in translation inhibition and thus, a decrease in the expression of the encoded proteins. In contrast, the mRNAs encoding Transferrin Receptor 1 (TfR1) and DMT-1 contain IREs within their 3'UTRs and their interaction with IRP1/2 stabilizes the transcripts and consequently increased protein expression. Therefore, when Fe is low the IRP/IRE system ensures limited Fe storage, export, and utilization, while increasing cellular Fe import. Labile Fe pools regulate the interaction between IRP1/2 with IREs through different mechanisms. During Fe-sufficient conditions a cubane [4Fe-4S] cluster assembles within the IRE-binding pocket of IRP1 converting it into a cytosolic aconitase, therefore preventing its interaction with IREs. In contrast, IRP2 does not bind [Fe-S] clusters and under Fe-replete conditions it is targeted for proteasomal degradation (Hentze et al., 2004; Rouault, 2006). IRP1/2 are regulated by other effectors such H_2O_2, which leads to disassembly of the [4Fe-4S] cluster within IRP1, and NO and hypoxia which activate both IRP1 and IRP2 (Hentze et al., 2004; Rouault, 2006).

1.5.4. Disorders of iron of balance

Deregulated Fe homeostasis, either overload or deficiency, is the underlying cause of numerous human diseases. One of the most common genetic disorders of Fe-overload is Hereditary Hemochromatosis (HH), an autosomal recessive disorder that affects mainly men of Eastern European descent. HH is caused by mutations in genes

whose products are involved in hepcidin regulation (including the *HAMP* gene itself; see section 1.5.2), resulting in inadequate hepcidin production leading to the uncontrolled absorption of Fe from the intestines and decreased export from storage cells. As a consequence, Fe hyper-accumulates in the liver, heart, and pancreas causing clinical complications such diabetes, arthritis, heart failure, liver cirrhosis and cancer. The mechanisms of Fe-induced organ damage are not understood, but it appears that lipid peroxidation and fibrogenesis are key factors in disease progression. The most efficacious treatment to date is the removal of circulatory Fe by phlebotomy therapy (Hentze et al., 2004; Stipanuk, 2000)

While HH arises from disruption of systemic regulation of Fe-balance, other Fe-overload disorders such as Friedreich's Ataxia (FRDA) develop as a result of disruption of cellular Fe-homeostasis. FRDA, the most common form of hereditary ataxia, results as a consequence of a mutations in the FXN gene (usually GAA triplet expansions or point mutations) encoding the frataxin protein (homologous to yeast Yfh1). Frataxin is a small protein expressed in the mitochondrial matrix, and while its function is not fully understood it appears to serve as Fe donor for the biogenesis of Fe-S clusters in mitochondria. Frataxin deficiency leads to a decrease in Fe-S cluster production, and consequently to a decrease in Fe-S cluster proteins in the cytosol. Absence of cytosolic Fe-S clusters causes the constitutive IRE-binding activity of IRP1, which results in increased transferrin receptor expression and decreased ferritin (see section 1.5.3). As a

consequence, cells hyperaccumulate Fe in the mitochondria in an attempt to compensate for the loss of cytosolic Fe-S clusters. FRDA symptoms vary from difficulty walking (ataxia) and speech difficulties to heart failure. Damage to the nervous system presumably occurs due to oxidative damage of mitochondria (Hentze et al., 2004; Lill and Muhlenhoff, 2008; Rouault, 2006).

While genetic disorders associated with Fe-deficiency have not been identified, Fe-deficiency can occur as a consequence of chronic bleeding, malabsorption syndromes, or inadequate Fe intake, particularly in persons whose diets are rich in plant-derived foods, which contain low Fe in addition to phytate, a potent Fe-chelator. Experimentation in animal models has demonstrated that Fe-deficiency in early life causes irreversible changes in the brain related to defects in myelination of neurons and dopaminergic function (Beard, 2001). Other effects of Fe-deficiency include defects in immune response to infection, including reduction of bactericidal activity of macrophages and a decrease of Fe-containing proteins involved in the generation of oxygen radicals for the killing of intracellular pathogens. At present, Fe-deficiency represents the number one nutritional disorder in the world. It affects approximately 30% of the world's population (Baynes and Bothwell, 1990a), and in 2005 it was estimated that worldwide 48% of pregnant women, and 46% of children between ages 5 and 12 were anemic (Arredondo and Nunez, 2005). Unlike most other public health problems, Fe-deficiency affects both developed and developing countries, mainly

women and children. The consequences of Fe-deficiency include anemia, difficulty maintaining body thermoregulation, increased susceptibility to infection, slow growth and cognitive development, weakness and fatigue, and decreased school and work performance. In fact, Fe-deficiency has an enormous impact on the economy of entire nations. It is estimated that in South Asia alone $4.2 billion are lost annually due to decreased physical productivity as a consequence of Fe-deficiency (Horton and Ross, 2003).

A common form of Fe-deficiency anemia is referred to as anemia of inflammation or anemia of chronic disease (Cartwright et al., 1946). Inflammatory stimuli such those following bacterial infection cause an acute reduction in circulating Fe by activating the antimicrobial peptide hepcidin (see section 1.5.2), which promotes Fe retention in intestinal mucosa and in macrophages, presumably in an attempt to limit bacterial growth (Schaible and Kaufmann, 2004). In anemia of inflammation, these inflammatory stimuli persist leading to a prolonged hypoferremia that eventually leads to Fe-limited erythropoiesis (De Domenico et al., 2008).

1.6. Post-transcriptional regulation of mRNA stability by ARE-binding proteins

1.6.1. Molecular mechanisms of mRNA decay

Messenger RNA turnover plays an important role in the regulation of gene expression by setting transcript steady-state levels, clearing aberrant mRNAs, and

degrading specific mRNAs in response to environmental stimuli. Many of the key players in mRNA decay have been identified in yeast and it is clear that the mechanisms of turnover are highly conserved from yeast to metazoans. In fact, the nomenclature of mRNA turnover participant proteins has been adopted by investigators using different model organisms (Garneau et al., 2007; Parker and Song, 2004; Wilusz et al., 2001). Unless otherwise noted, the gene and protein names described in this section are the same in yeast and higher eukaryotic systems.

Eukaryotic mRNAs are characterized by a 5′ 7-methylguanosine cap and a 3′ poly-adenine (poly-A) tail, which are incorporated into the nascent mRNA co-transcriptionally. Both structures protect the integrity of the mRNA from exonucleases by interacting with the cytoplasmic cap binding protein, eIF4E, and the poly-(A)-binding protein (Pab1 in yeast, and PABP in mammals)(Garneau et al., 2007; Parker and Song, 2004; Wilusz et al., 2001). There are two general mechanisms of mRNA turnover, both of which require an initial deadenylation step – removal of the poly-(A) tail. Following deadenylation, the cap structure can be removed and the mRNA degraded in the 5′→3′ direction, or it can be degraded in the 3′→5′. Figure 4 summarizes the two pathways of mRNA decay.

The first step in mRNA decay in yeast and higher eukaryotes is the removal of the poly-(A) tail (Figure 4). There are three well characterized deadenylases: the Pan2/Pan3 complex, the Ccr4-Not-Pop2 complex, and the PARN complex (Garneau et

al., 2007; Parker and Song, 2004; Wilusz et al., 2001). The Pan2/Pan3 complex mediates trimming of the poly-(A) tail of nascent transcripts to a standard length of approximately 60 to 80 nucleotides, and its deadenylase activity is thought to be Pab1-dependent (Parker and Song, 2004). The Ccr4-Not-Pop2 deadenylase complex is composed of nine proteins, but only Ccr4 and Pop2 are thought to have nuclease activity. The Ccr4-Not-Pop2 complex is the main deadenylase in yeast, and in contrast to the Pan2/Pan3 complex, it is inhibited by Pab1. While Ccr4-Not-Pop2 has some deadenylase activity in mammals, the main poly-(A) nuclease in mammals is constituted by the PARN complex. PARN deadenylase activity is cap-dependent, and it is strongly inhibited by cap-binding proteins. There appears to be no PARN homologues in yeast (Garneau et al., 2007; Parker and Song, 2004; Wilusz et al., 2001). Once the mRNA has been deadenylated, 3′→5′degradation of the transcript is catalyzed by a group about 10 to 12 exonucleases collectively known as the Exosome. Once digestion of the entire mRNA has taken place, the remaining 5′-7-methylguanosine cap is metabolized by the scavenger decapping protein, DcpS (Figure 4)(Parker and Song, 2004).

Removal of the poly-(A) tail also primes mRNA for decapping. Deadenylated mRNAs are bound at their 3′-end by the Lsm1-7 complex, which promotes the enzymatic activity of the Dcp1/Dcp2 decapping complex (Figure 4). Other decapping associated factors include the DExD/H-box RNA helicase Dhh1 (p54/RCK in mammals) and the enhancers of decapping Edc1-3 (Fillman and Lykke-Andersen, 2005). In

addition, the yeast specific proteins Pat1 and Pbp1, as well as mammalian specific Hedls and RAP55 proteins, also stimulate decapping activity. The body of the mRNA is then degraded in the 5′→3′ direction by the cytosolic exonuclease Xrn1 following decapping. Proteins involved in decapping and the Xrn1 exonuclease are concentrated in cytoplasmic foci referred to as Processing Bodies (P-bodies, or PBs)(Sheth and Parker, 2003). Thus, PBs are considered the site for 5′→3′ mRNA degradation by Xrn1, although it has recently been suggested that PBs in addition serve as mRNA storage units as members of the translation initiation machinery also localize to these structures. Therefore, deadenylated mRNAs may escape degradation to re-enter translation (Brengues et al., 2005). Visualization of PBs under normal growth conditions is difficult, but they become abundant and easy to visualize upon exposure to different stresses or disruption of the activity of decapping proteins, or the Xrn1 nuclease. Furthermore, disruption of transcription, translation elongation, or deadenylation compromises the number and size of PBs observed (Teixeira and Parker, 2007).

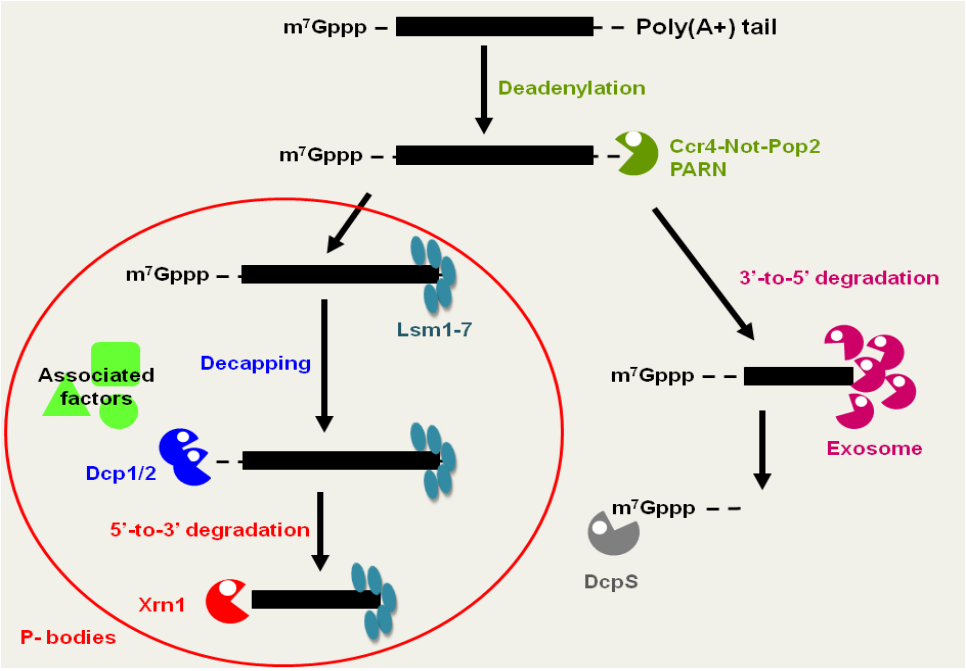

Figure 4. Mechanism of mRNA degradation

1.6.2. AU-rich elements (AREs)

The regulation of gene expression at the level of mRNA stability allows the cell to rapidly adjust to varying intracellular and extracellular stimuli (Wilusz et al., 2001). The best understood instability element is the AU-rich element or ARE. As the name implies, AREs are sequences rich in adenosine and uridine, initially identified by their ability to induce the rapid destabilization of mRNAs encoding proto-oncogenes and cytokines (Chen and Shyu, 1995). However, recent studies suggest that between 5-8% of all human transcripts harbor AREs, underscoring the importance of these regulatory sequences in the control of gene expression (Bakheet et al., 2001). While AREs are

primarily located in the 3′-untranslated region (3′UTRs) of mRNAs, they have also been found in 5′UTRs and within coding sequences (Chen et al., 1995), and they can be classified into three groups based on the distribution of the pentameric sequence 5′-AUUUA-3′ (Table 4). It should be noted however, that the presence of the 5′-AUUUA-3′ motif alone does not always confer instability to a heterologous mRNA; it appears that the context in where AREs are found is important for their function as mRNA destabilizing elements. Class I AREs contain several dispersed copies of the 5′-AUUUA-3′ motif usually between long U-rich regions. Class II AREs usually contain two or more of the nonameric sequence 5′-UUAUUUAUU-3′ and they represent the best understood class of AREs. Lastly, Class III AREs are not as clearly defined, but they are usually U-rich regions that do not contain the pentamer 5′-AUUUA-3′ motif (Chen and Shyu, 1995). Examples of mRNAs harboring sequences belonging to each of the ARE classes are listed in Table 4.

1.6.3. ARE-binding proteins (AUBPs)

Most ARE-containing mRNAs encode proteins involved in the regulation of cell growth and proteins involved in inflammatory response. Not surprisingly, defects in ARE-dependent regulation of gene expression are associated with pathologies such cancers, chronic inflammation and auto-immune disorders (Chen and Shyu, 1995; Chen et al., 1995). As a consequence much effort has been devoted to the identification and functional understanding of ARE-binding proteins (AUBPs) with respect to mRNA

stability and in some cases translation regulation. Binding of AUBPs to ARE-mRNAs can have dramatically different effects on the stability of the bound transcript. For instance, while some AUBPs promote the rapid deadenylation-dependent degradation of ARE-mRNAs (e.g. TTP, Brf1, KSRP), others promote a dramatic increase in the stabilization of the same transcript (HuR, Hel-N1). Even more, a single AUBP can exert both destabilization and stabilization of a transcript under different conditions or in different cell types (e.g. AUF1). In addition, binding of AUBPs can also affect translational efficiency (e.g. HuR, Hel-N1 and TIA-1).Three of the best understood AUBPs identified to date are TTP, AUF1 and HuR (Blackshear, 2002; Garneau et al., 2007; Peng et al., 1998; Wilusz et al., 2001). Table 4 lists a few of the ARE-mRNAs to which they bind as well as the outcome of the interaction. However, only TTP is described in detail.

Table 4. AU-rich element classification and ARE-binding proteins

AU-Rich Elements (AREs) and AU-Rich Element Binding Proteins (AUBPs)		
ARE classification	**Examples**	
Class I: 5′-AUUUA-3′ within U-rich region	*c-fos, c-myc,* PTH, IF-γ, PAI-2, cyclin A, cyclin B1, cyclin D1	
Class II: 5′-UUAUUUAU(U/A)-3′ within a U-rich region	TNF-α, GM-CSF, IF-α, IF-β, Cox-2, IL-2, IL-3, bcl-2, VEGF	
Class III: U-rich region, non-AUUUA	*c-jun,* GLUT1, p53	
AUBPs and their effect on mRNA stability	**Stabilization**	**Destabilization**
HuR	**Class I:** *c-fos*, cyclin A, cyclin B1, cyclin D1 **Class II:** TNF-α, GM-CSF, Cox-2, IL-3, VEGF	
AUF1	**Class I:** *c-fos*, *c-myc*, PTH **Class II:** TNF-α, GM-CSF	**Class I:** *c-fos*, *c-myc*, cyclin D1 **Class II:** GM-CSF, IL-3
TTP		**Class II:** TNF-α, GM-CSF, Cox-2, IL-2, IL-3

Classification based on Chen and Shyu (1995). Bakheet et al. (2003) further classify Class II into five groups.

1.6.3.1. $CX_8CX_5CX_3H$-proteins in mammals

Tristetraprolin (TTP, also known as Tis11, ZFP36, and NUP475) is the founding member of a family of proteins characterized by a 63 amino-acid domain containing two identical zinc fingers of the $CX_8CX_5CX_3H$ type located in tandem and separated by an 18-residue linker region. In addition, each zinc finger is preceded by a lead-in sequence YKTEL. Its name however, Tristetraprolin, was given due to the presence of three Pro-Pro-Pro-Pro motifs (Blackshear, 2002; Carballo et al., 1998). The function of these tetraprolin domains, if any, remains unknown. Other members of this family include mammalian Brf1 (ZFP36L1 or Tis11b) and Brf2 (ZFP36L2 or Tis11d), and homologues

have been identified in many organisms from yeast to plants, although the conservation appears to be restricted to the region containing the CCCH-tandem zinc finger domain (TZF) (Baou et al., 2009; Blackshear, 2002).

TTP was originally recognized in a screen aimed the identification of immediate-early response genes by exposure to insulin, phorbol esters, LPS and serum. The rapid but transient increase in mRNA steady state levels and the presence of two zinc fingers in the predicted protein led to the original hypothesis that TTP might be a transcription factor. Moreover, localization experiments demonstrated that TTP localized mostly to the nucleus of resting fibroblasts, but relocalized to the cytosol within five minutes of serum exposure further suggesting that TTP was a transcriptional activator whose activity was regulated by changes in subcellular localization (Baou et al., 2009; Blackshear, 2002; Phillips et al., 2002; Taylor et al., 1996a; Taylor et al., 1996b). Its actual function did not become clear until a TTP($^{-/-}$) mouse was developed. Though apparently normal at birth, TTP($^{-/-}$) mice developed phenotypes characteristic of inflammatory syndromes soon thereafter. In addition to slow growth, some of the phenotypes included erosive polyarticular arthritis, alopecia, dermatitis, conjunctivitis, cachexia, hunched posture, and symmetrical arthritis of the paw joints. Because these phenotypes highly resembled those observed in mouse models of inflammatory syndromes of TNF-α excess, TTP($^{-/-}$) mice were treated with antibodies against TNF-α. The anti- TNF-α therapy essentially suppressed all the phenotypes associated with ablation of the TTP

gene. Continued studies in macrophages demonstrated that TTP functioned as a negative regulator of TNF-α mRNA stability (Blackshear, 2002; Carballo et al., 1998; Taylor et al., 1996a). This observation coupled with the previous identification of an ARE instability element within the TNF-α 3'UTR lead to the discovery that TTP was indeed an ARE-binding protein, that the CCCH-tandem zinc finger domain constituted an mRNA recognition motif, and that binding of TTP to the TNF-α ARE promoted the rapid destabilization of the transcript. Furthermore, it was clear that integrity of the CCCH-zinc fingers as well as the integrity of the ARE-sequences within the mRNA is essential for targeted transcript destabilization. Binding of TTP promotes deadenylation and rapid degradation of mRNAs in a process referred to as ARE-Mediated mRNA Decay, or AMD (Section 1.6.4) (Barreau et al., 2005; Brennan and Steitz, 2001; Lai et al., 1999; Lykke-Andersen and Wagner, 2005).

Many efforts have been dedicated to the identification and prediction of TTP cognate mRNAs. As the list of putative targets continues to grow, it has become evident that TTP binds mainly sequences within the so-called class II AREs (Table 4), which are usually one or more 5'-UUAUUUAUU-3' nonameric sequences that may overlap forming long AU-rich stretches (Bakheet et al., 2001; Chen and Shyu, 1995). A recent NMR structure of the TZF of Brf2 (Tis11d) bound to an RNA 5'-$U_1U_2A_3U_4U_5U_6A_7U_8U_9$-3' oligonucleotide provided insights into the interaction between the TZF and AREs (Hudson et al., 2004). In addition to demonstrating that the nonameric sequence is a

linear molecule that lacks any secondary structure, the NMR also revealed that both zinc fingers form almost identical structures each one binding a one half 5′-UAUU-3′ sequence of the RNA oligonucleotide through electrostatic and hydrogen-bonding interactions. The first zinc finger interacts with the second 5′-$U_6A_7U_8U_9$-3′ half, and the second finger with the first 5′-$U_2A_3U_4U_5$-3′ half. The TZF:ARE interaction is further strengthened by stacking of aromatic residues with the RNA bases, in particular with A_3 and A_7 supporting previous observations that mutations in these residues abolishes mRNA binding. Lastly, the 5′-most U (U_1) of the nonamer does not interact with the TZF, suggesting tolerance for nucleotide substitutions at this position (Hudson et al., 2004).

Early experiments by the Blackshear Lab demonstrated that as TTP abundance increased upon stimulation with LPS, its apparent molecular mass also increased over time as evidenced by changes in electrophoretic mobility of TTP in SDS/PAGE gels. This increase in molecular mass was demonstrated to correspond to phosphorylation of TTP, and later studies showed that complete dephosphorylation of TTP increased binding affinity for ARE-containing probes (Blackshear, 2002). Several signaling pathways have been implicated in the regulation of cytokine expression including the p38/MAPK-MK2, JNK, and PI3K (Chen et al., 1998; Ming et al., 1998; Winzen et al., 1999). Recent studies have demonstrated that MK2 directly phosphorylates TTP at Ser^{52} and Ser^{178} (of mouse TTP) in LPS stimulated microphages. Phosphorylation of TTP at Ser^{52} and Ser^{178}

coincides with increased cytosolic TTP levels, and phoshphorylation appears to confer protection of TTP from degradation by the proteasome. Despite increased cytosolic levels, however, phosphorylation of TTP renders it inactive resulting in high levels of TNF-α mRNA. Phosphorylation of Ser^{52} and Ser^{178} promotes an interaction with 14-3-3 adaptor proteins, which in turn regulate the subcellular localization of TTP; binding of 14-3-3- causes TTP accumulation in the cytosol, but it is excluded from P-bodies(Johnson et al., 2002; Stoecklin et al., 2004). In contrast, the non-MK2 phosphorylatable Ser^{52}Ala and Ser^{178}Ala mutant allele of TTP is constitutively active, cannot bind 14-3-3 proteins and it is constitutively localized to P-bodies. Phosphorylation of TTP by MK2 is countered by the action of the protein phosphatase 2A, PP2A. Thus, the interplay between phosphorylation and dephosphorylation appears to be an important factor in TTP regulation (Sandler and Stoecklin, 2008).

1.6.4. ARE-mediated mRNA decay – AMD

Due to the critical role that AMD plays in the regulation of several pro-inflammatory cytokines and proto-oncogenes, the mechanisms by which TTP and related proteins promote AMD have been under intensive investigation (Garneau et al., 2007; Lykke-Andersen and Wagner, 2005; Parker and Song, 2004; Wilusz et al., 2001). Cytosolic mRNA degradation in eukaryotes generally involves the shortening of the poly-(A) tail, followed by removal of the 5′-cap, and finally exonucleolytic degradation in the 5′→3′ direction, which takes place in cytosolic foci known as Processing Bodies (P-

bodies, or PBs). Alternatively, a deadenylated transcript can be degraded from the 3′→5′ by the cytosolic exosome (Figure 4)(Parker and Song, 2004).

Investigations on TTP-dependent AMD have revealed that TTP promotes the rapid removal of the poly-(A) tail of ARE-containing transcripts by interacting with cytosolic deadenylases (Lai et al., 1999; Lai et al., 2003), and there is growing evidence suggesting that both mechanisms of degradation, the 5′→3′ and the 3′→5′, contribute to TTP-dependent AMD. First, TTP interacts with the Dcp1/2-decaping complex, activates in vitro decapping of ARE-containing transcripts, and disruption of the 5′→3′ exonuclease Xrn1 causes defects in AMD, as well as the retention of TTP in PBs. Second, in vitro mRNA decay assays suggest that members of the exosome can promote the degradation of ARE-containing transcripts, and the exosome protein PM-Scl75 has been found to interact with both TTP, as well as with ARE sequences within target transcripts (Chen et al., 2001; Garneau et al., 2007; Lykke-Andersen and Wagner, 2005; Wilusz et al., 2001). Thus, it appears that TTP promotes the accelerated decay of target transcripts by activating deadenylation and both cytosolic pathways of mRNA turnover. However, despite our increasing understanding in the mechanisms of TTP-dependent AMD, little is known about where TTP first comes in contact with target mRNAs, or how TTP and related proteins can discriminate *bona fide* ARE-containing transcripts from any other ARE-containing mRNA.

1.7. $CX_8CX_5CX_3H$ proteins in yeast – Cth1 and Cth2

The yeast genome encodes two members of the $CX_8CX_5CX_3H$-family of mRNA binding proteins, which arose from the whole genome duplication event (Wolfe and Shields, 1997). Early work by the Herschman and Blackshear labs aimed at the cloning and characterization of these genes in an attempt to uncover the elusive function of this presumed family of transcription factors (Ma and Herschman, 1995; Thompson et al., 1996). The cloned genes were named *CTH1* and *CTH2* based on the two $CX_8CX_5CX_3H$ sequences characteristic of this family of proteins (Cysteine-Three-Histidine 1 and 2, corresponding to the *YDR151C* and *YLR136C* loci, respectively) (Thompson et al., 1996). The absence of any overt phenotypes in *cth1Δ* and *cth2Δ* strains made the identification of their function impossible at the time. However, these studies determined that expression of the *CTH1* mRNA was constitutive (Thompson et al., 1996), while the *CTH2* transcript was almost undetectable in cells grown in 2% glucose and robustly expressed in cells grown in medium containing acetate as sole carbon source (Ma and Herschman, 1995). A switch from acetate-containing medium to glucose-containing medium caused rapid (30 min) repression of *CTH2* mRNA expression. In addition, deletion of *CTH1* or mutations within its tandem zinc fingers caused a 5.1 and 3.8 fold higher expression of *CTH2* mRNA in cells grown in 2% glucose (Thompson et al., 1996). While no clear phenotype was identified for the *cth2Δ* strain, Ma and Herschman hypothesized that Cth2 might be involved in some aspect of metabolism, because the absence of *CTH2*

caused pH changes of the growth medium as evidenced by a color change on plates containing bromothymol blue as pH indicator. Moreover, the Blackshear lab demonstrated that over-expression of Cth1 and mouse TTP caused roughly a 50% growth inhibition compared to wild-type cells, while Cth2 caused a mere 15% growth inhibition. Removal of the tandem zinc fingers within Cth1, Cth2 and TTP suppressed the toxicity associated with their over-expression, suggesting that cytotoxicity is associated with their cellular function (Thompson et al., 1996). Most importantly, these data indicated that mouse TTP is functional in yeast, and as such yeast can be used as a surrogate system to elucidate the molecular mechanisms of $CX_8CX_5CX_3H$-family members.

The *CTH1* gene is 978-nt long and it encodes a basic (pI:8.8) 325 amino-acid peptide of approximate molecular weight 36.7 kDa. The *CTH2* gene is shorter (858-nt) and the encoded 285 amino-acid protein is slightly more basic than Cth1; pI: 9.4. The molecular weight of Cth2 is approximately 32.3 kDa (Saccharomyces Genome Database). Cth1 shares 46% overall identity, and 59% overall similarity with Cth2, but 78% identity and 87% similarity within the 68 amino-acid long region containing the tandem zinc fingers. Cth1 and Cth2 homology to TTP and family members is restricted to the tandem zinc finger domain sharing 52% identity. However, the YKTEL lead-in sequence that precedes each zinc finger, is variant in the second zinc finger within Cth1 and Cth2 (YRTKP and FRTKP, respectively)(Ma and Herschman, 1995; Thompson et al., 1996).

The generation of a TTP($^{-/-}$) mouse model (Taylor et al., 1996a) and the studies that followed demonstrated that this family of proteins were a novel type of mRNA binding proteins that recognize specific AU-rich sequences within the 3'UTRs of select transcripts through an interaction with the $CX_8CX_5CX_3H$-domain of the protein. This interaction promotes the accelerated turnover of the bound transcript (see section 1.6.3.1). In yeast, expression of the *CTH1* and *CTH2* genes is activated by the Fe-responsive transcription factors Aft1 and Aft2 under conditions of Fe-starvation, and the function of Cth1 and Cth2 proteins is to cooperatively promote a post-transcriptional reprogramming of metabolism that allows the cellular adaptation to growth under Fe-limiting conditions. Cth1 is expressed rapidly and transiently after Fe-limitation conditions are imposed, whereas expression of Cth2 occurs later in a more graded fashion over time during Fe-deficiency (Puig et al., 2008). This difference in protein expression may be partially explained by differences in promoter occupancy of the Aft1 transcription factor. While occupancy of the *CTH2* promoter by Aft1 is Fe deficiency-induced, Aft1 occupancy of the *CTH1* promoter seems to be constitutive, perhaps accounting for its rapid induction during Fe-limitation (Puig et al., 2008). Preliminary observations also suggest that the *CTH1* and *CTH2* mRNAs harbor AREs within their 3'UTRs, and biochemical experiments indicate that both mRNAs are themselves subject to ARE-mediated regulation by the Cth1 and Cth2 proteins. Thus, it is likely that the pattern of expression of Cth1 and Cth2 are the result of both transcriptional and post-

transcriptional regulation. While the importance of maintaining this pattern of expression is not fully understood, it should be noted that over-expression of Cth1 is highly toxic while Cth2 over-expression only causes mild reductions in cell growth (Thompson et al., 1996).

Recent studies have begun to uncover the mechanism by which Cth2 promotes ARE-mediated mRNA degradation (AMD) of target transcripts. It has been demonstrated that during Fe-deficiency Cth2 promotes AMD of the well-characterized *SDH4* target mRNA via the 5′→3′ pathway. First, Cth2 interacts with the DEAD-box Dhh1 helicase – an activator of decapping and core component of PBs, and *dhh1Δ* strains accumulate higher levels of the *SDH4* transcript during Fe-deficiency than wild type cells. Second, examination of decay intermediates trapped by the insertion of a poly(G) tract in the 3′UTR of the *SDH4* mRNA revealed the accumulation of a 5′→ poly(G)-intermediate in *cth2Δ* cells, but not in wild type cells during Fe-deficiency. Lastly, Cth2 accumulates in PBs in strains defective in 5′→3′ mRNA turnover, such the *dcp1Δ*, *dcp2Δ*, or *xrn1Δ* strains (Pedro-Segura et al., 2008). While a role for the exosome in Cth2-dependent AMD has not been identified to date, degradation of another ARE-containing target of Cth2, *ISA1*, is partially independent of Dhh1 (Pedro-Segura et al., 2008). Thus, it would be interesting to ascertain whether the exosome can also degrade mRNAs destined for AMD in yeast.

2. Cooperation of two mRNA-binding proteins drives metabolic adaptation to iron deficiency

2.1 Introduction

The ability of iron (Fe) to engage in redox reactions makes it is a widely utilized co-factor in many central biochemical processes including oxygen delivery and storage, mitochondrial oxidative phosphorylation, DNA replication and repair, lipid metabolism, and chromatin modification. Abnormal Fe accumulation, either in excess or insufficient levels, underlies several human diseases including hereditary hemochromatosis, Friedreich's ataxia, aceruloplasminemia and Fe-deficiency anemia (Dunn et al., 2007; Hentze et al., 2004). Indeed, Fe-deficiency represents the most common nutritional deficiency, estimated to affect more than two billion people worldwide (Baynes and Bothwell, 1990b).

Given the importance of Fe in health and disease, Fe-homeostasis has been under intensive investigation aimed at elucidating the mechanisms of Fe acquisition, distribution and regulation (Escolar et al., 1999; Hentze et al., 2004; Kaplan et al., 2006). One regulatory mechanism for Fe-homeostasis in mammals involves the iron-regulatory proteins IRP1/IRP2, which post-transcriptionally modulate the expression of specific mRNAs in response to intracellular Fe (Hentze et al., 2004; Rouault, 2006). When cellular Fe is low, IRP1 and IRP2 bind to stem-loop structures, known as iron-responsive elements (IREs), within the 5'-untranslated region (UTR) of transcripts including those encoding the iron storage protein ferritin, mitochondrial aconitase, the heme

biosynthetic enzyme eALAS, and the Fe efflux transporter ferroportin, thereby inhibiting their translation. Concurrently, IRP1 and IRP2 also bind IRE sequences within the 3'-UTR of the transferrin receptor mRNA, stabilizing the transcript and thus increasing its translational efficiency. As a consequence, there is a decrease in sequestration of Fe by ferritin and an increase in the capacity to mobilize transferrin-bound Fe. Once Fe levels are adequate, IRP1 acquires a [4Fe-4S] cluster, inter-converting to a cytoplasmic aconitase, and IRP2 is degraded (Hentze et al., 2004; Rouault, 2006). A post-transcriptional mechanism that controls cellular Fe homeostasis has also been described in bacteria. During Fe-starvation a small non-coding RNA from *Escherichia coli*, RyhB, is synthesized and promotes the degradation of mRNAs encoding proteins involved in Fe homeostasis, Fe-dependent metabolism and Fe storage. Once Fe levels are adequate, expression of RyhB ceases due to its transcriptional repression by the ferric uptake regulator, Fur (Masse et al., 2007).

Previous studies have demonstrated that under Fe-limiting conditions *S. cerevisiae* utilizes two Fe-responsive transcription factors, Aft1 and Aft2, to activate expression of genes collectively known as the Fe-regulon (Courel et al., 2005; Rutherford et al., 2003; Shakoury-Elizeh et al., 2004). Additional mechanisms of Fe induced gene transcription occur in an Aft1/2-independent manner (Shakoury-Elizeh et al., 2004; Li et al., 2007). Genes in the Fe-regulon encode proteins involved in Fe-uptake, redistribution of intracellular Fe-stores, Fe-S biogenesis, and heme-utilization.

Concomitant with transcription of the Fe-regulon under conditions of Fe deficiency, the steady state levels of mRNAs encoding enzymes involved in many Fe-dependent metabolic processes including the tricarboxylic acid (TCA) cycle, mitochondrial respiration, heme biosynthesis and fatty acid synthesis, as well as that coding for the Ccc1 Fe storage protein, are markedly reduced (Lesuisse et al., 2003; Puig et al., 2005; Shakoury-Elizeh et al., 2004). A member of the Fe-regulon, Cth2, belongs to a family of mRNA-binding proteins conserved from yeast to humans, that is characterized by the presence of two tandem zinc-fingers of the $CX_8CX_5CX_3H$ type (CCCH) that constitute an mRNA-binding domain (Blackshear, 2002). Members of this family of proteins promote the rapid degradation of select mRNA molecules, by recruiting RNA decay enzymes to AU-rich Element (ARE)-containing mRNAs (Lykke-Andersen and Wagner, 2005). Cth2 protein binds AREs within the 3'-untranslated region (3'-UTR) of many mRNAs encoding proteins involved in Fe homeostasis and Fe-dependent metabolic processes, thereby promoting mRNA degradation (Puig et al., 2005). Consistent with a role for Cth2 in orchestrating genome-wide changes in metabolism in response to Fe deficiency, *cth2Δ* cells exhibit a growth defect on low Fe medium. Furthermore, the growth defect of *cth2Δ* cells is exacerbated by a mutation in the *CTH1* gene, encoding a putative homologue of Cth2, whose function has not been previously described.

Here we demonstrate that the *CTH1* gene is a direct target of the Aft1/2 transcription factors that is activated rapidly and transiently in response to Fe deficiency. Microarray analyses revealed that, while Cth2 predominantly stimulates the degradation mRNAs encoding general Fe homeostasis and Fe utilizing proteins that function in metabolism, Cth1 preferentially targets mRNAs encoding components of the mitochondrial oxidative phosphorylation machinery and other known or predicted mitochondrial functions. Moreover, we demonstrate that Cth1 and Cth2-stimulated mRNA decay results in the elevated expression of genes that are involved in the transport, metabolism, and storage of glucose. Consistent with this regulation, Fe starvation results in elevated glycogen levels and activation of Snf1 protein kinase, a central regulator of cellular carbon metabolism. Taken together, the *S. cerevisiae* Cth1 and Cth2 mRNA binding proteins play critical roles in targeting specific functional classes of mRNAs for degradation in response to Fe deficiency. Moreover, the coordinated activities of these two proteins impart changes in cellular metabolism consistent with a shift away from oxidative phosphorylation and toward carbohydrate utilization.

2.2 Materials and Methods

Yeast strains and growth conditions

The AFT1-TAP strain was obtained from the TAP-tag collection (Ghaemmaghami et al., 2003) and verified by PCR and immunoblotting. The snf1Δ strain used was DTY434 (Matα ade2-101 trp1Δ1 lys2-801 ura3-52 snf1Δ). All other yeast strains

used in this study have been previously described (Puig et al., 2005). For spot assays, cells were grown in synthetic complete medium (SC) minus specified nutrients to mid-exponential phase and spotted in 10-fold serial dilutions starting at A_{600} = 0.1 on SC or SC plus 750 μM of the membrane permeable Fe-chelator, ferrozine, to impose Fe-starvation. For liquid cultures, 100μM of the Fe-specific chelator BathoPhenanthroline diSulfonate (BPS) was used to impose Fe-deficiency, and 300μM Ferrous Ammonium Sulfate (FAS) was used to create Fe-replete conditions (cultures grown under these conditions for 6 to 8 hrs reach an OD_{600} = ~0.4 to 0.6). Thus, all conditions described as Fe- and Fe+ refer to the supplementation of either BPS or FAS in liquid cultures. Yeast three hybrid experiments were carried out as previously described (Puig et al., 2005)

Plasmids

The overlap extension method was used to create the *CTH2 : CTH1* fusion and to create gene, promoter and 3'-UTR mutations. The coding sequences from wild type *CTH2* and *CTH1* were cloned into the p416TEF vector using standard cloning methods. Wild-type *CTH1* and the *CTH1*-C225R alleles were fused to the Gal4 activation domain in the pACT2 vector and used for the yeast three-hybrid assay. Other plasmids used in this work have been previously described (Puig et al., 2005). Both the 2x*FLAG-CTH1* and the *CTH2* genes are under the regulation of their endogenous promoter and 3'UTRs. All plasmid inserts were verified by sequencing. Plasmid pSNF1-316 was a gift from Dr. Martin Schmidt at the University of Pittsburg.

Chromatin Immunoprecipitation

Overnight cultures of *AFT1-TAP* cells (Ghaemmaghami et al., 2003) were re-inoculated to A_{600} = 0.1 in 50 mL SC medium supplemented with either 300 μM FAS (Fe+) or 100 μM BPS (Fe-), and grown for 8 hours at 30°C. Formaldehyde crosslinking and ChIP using 500 μg of total protein was carried out as described (Keller et al., 2005) in three independent experiments. Promoter occupancy by Aft1 was ascertained by PCR using primers annealing at the promoter region of *CTH1.* Primers for *FET3* and *CTH2* promoters were used as positive controls, and *CMD1* as negative controls. PCR products were visualized on 2% agarose gels using ethidium bromide.

Messenger RNA half-life determinations

Cells were grown overnight in SC-Ura-Leu-Raffinose (2% raffinose; no glucose) and re-inoculated in SC-Ura-Leu-Galactose (2% galactose; no glucose) supplemented with 100 μM BPS until exponential growth phase (OD_{600} = ~0.4 – 0.6). Glucose was added to a final concentration of 4% to extinguish transcription of the *GAL1-SDH4* fusions and aliquots were taken after glucose addition, total RNA extracted and analyzed by RNA blotting using *SDH4* and *ACT1* probes. *SDH4* levels were quantified using a STORM 840 phosphoImager (Amersham) and normalized to *ACT1* levels. The mRNA half-life was determined from at least three independent experiments.

Protein analyses

cth1Δcth2Δ cells were co-transformed with pRS415-*CTH2* and pRS416-*2xFLAG-*

CTH1. Overnight cultures were re-inoculated to A_{600} = 0.05 in SC-Ura-Leu and allowed to grow to A_{600} = 0.10, at which point 100μM BPS was added, and began time course at the indicated times. Total protein was extracted using the Triton-X 100/glass bead method, and 50 μg of total protein were resolved in a 10% SDS-PAGE and transferred onto a nitrocellulose membrane. Flag-Cth1 fusion protein was detected using an HRP-conjugated α-Flag anti-body from Sigma. An α-Pgk1 antibody was used as loading control. Two chemiluminescence substrates were used for the detection of the HRP-conjugated anti-body, Pico and Fempto (Pierce). To detect Snf1-phosphorylation, DTY434 cells (*snf1Δ*) were transformed with plasmid pSNF1-316 (SNF1-3HA) or vector alone, and grown in SC-ura overnight. Overnight cultures were re-inoculated to A_{600} = 0.2 in SC-Ura medium supplemented with either 300 μM FAS or 100 μM BPS and grown for 6 hrs at 30°C. Protein extractions were done using ice-cold RIPA buffer and glass beads supplemented with protease inhibitors (Roche mini-tablet) and phosphatase inhibitors (30mM $Na_4P_20_7$, 50mM NaF, 100uM Na_3VO_4, 25mM β-glycerolphosphate). 500ug of total protein were used to immunoprecipitate Snf1-HA using 20μL of monoclonal anti-HA agarose conjugate beads (Sigma), using a standard IP protocol. Immunoprecipitated samples were fractionated in 10% SDS-PAGE gels, transferred onto nitrocellulose membranes, and phosphospecific anti-bodies against Snf1 were used (anti-PT210 (M. Schmidt) or anti-P-AMPKalpha (Cell Signaling)) as well as anti-Snf1 (yK-16 Santa Cruz) as loading control. For positive and negative controls of Snf1

phosphorylation, additional cultures were grown in SC-ura medium containing either 4% or 0.05% glucose, respectively.

Microarray analyses

cth1Δcth2Δ cells independently transformed with pRS416, pRS416-*CTH1* or pRS416-*CTH2* were grown in triplicate in SC-Ura containing 100 μM BPS until exponential growth phase, RNA was extracted, labeled and hybridized to Yeast Genome S98 Afffymetrix arrays. For further information about sample preparation, synthesis of labeled cDNA, hybridization, scanning and data acquisition, and quality control steps, visit the Duke Microarray Core Facility at http://www.genome.duke.edu/cores/microarray/. All data were analyzed using GeneSpring 6.1 (Silicon Genetics), using volcano plot with minimum of 1.5 fold change and a p-value < 0.05. Microarray data have been deposited in NCBI's Gene Expression Omnibus (GEO, http://www.ncbi.nlm.nih.gov/geo/) and are accessible through GEO Series accession number GSE11236.

Glycogen measurements

cth1Δch2Δ mutants were transformed with vectors (pRS416 + pRS415) or with both *CTH* (pRS416-*CTH1* + pRS415-*CTH2*), inoculated at OD=0.1 in SC-ura-leu and grown for 8 hours in medium containing either 300μM FAS or 100μM BPS. Extraction and glycogen determination was performed as described in Parrou and Francoise (1997).

2.3 Results

2.3.1 Cth1 function in response to Fe-deficiency

The yeast genome harbors a gene encoding a protein structurally related to Cth2, Cth1, which shares an overall 46% identity and 56% similarity with Cth2, as well as 79% identity within the tandem zinc finger (TZF) domains (Figure 5A). The TZF region of Cth2, and other TZF protein family members, is essential for binding to ARE-sequences within the 3'-UTR of their target mRNAs (Puig et al., 2005) We previously demonstrated that *cth2Δ* cells grow poorly on Fe-limited media and exhibit defects in the degradation of a specific set of ARE-containing mRNAs (Puig et al., 2005). Furthermore, deletion of the *CTH1* gene exacerbates the growth and mRNA degradation defects of *cth2Δ* cells under Fe-limiting conditions (Puig et al., 2005). To evaluate the function of Cth1 during Fe deficiency, Cth1 was expressed under conditions of Fe-deficiency by fusing the *CTH2* promoter region to the *CTH1* coding sequence (*CTH2:CTH1*). The *CTH2:CTH1* plasmid conferred an Fe-regulated pattern of expression to *CTH1* similar to *CTH2* mRNA, as ascertained by RNA blotting experiments (data not shown). Cells (*cth1Δ cth2Δ*) harboring the empty vector, or containing the *CTH1*, *CTH2* or *CTH2:CTH1* plasmid were evaluated for cell growth under conditions of Fe limitation and for steady state levels of mRNAs known to be degraded in a Cth2-dependent manner. As shown in Figure 5B, the growth defect of *cth1Δcth2Δ* cells on Fe-chelated medium was only partially suppressed by native *CTH1* expression levels, but more significantly rescued in cells harboring the

CTH2, or *CTH2:CTH1* plasmid. The steady-state levels of two Cth2 target mRNAs, *SDH4* and *CCP1*, was examined by RNA blotting. Both *SDH4* and *CCP1* encode mitochondrial Fe-dependent enzymes – a subunit of the succinate dehydrogenase complex and cytochrome c peroxidase, respectively. As previously observed (Puig et al., 2005) and shown in Figure 5C, both *CCP1* and *SDH4* mRNA levels were greatly reduced as a consequence of Fe-limitation in wild-type cells, but not in *cth1Δcth2Δ* cells carrying an empty vector. In contrast, there is a significant decrease in both *CCP1* and *SDH4* mRNA steady state levels in *cth1Δcth2Δ* cells expressing *CTH2*, *CTH1* or *CTH2:CTH1*. Taken together these results indicate that Cth1 can promote a decrease in steady state levels of two Cth2 mRNA targets under Fe deprivation conditions.

Although both Cth1 and Cth2 negatively regulate *SDH4* and *CCP1* mRNA levels under conditions of Fe deficiency, it is not clear if Fe deficiency is needed for their function. We ascertained whether Cth1 or Cth2 could promote a decrease in *SDH4* mRNA levels under Fe sufficiency conditions. The *CTH1* and *CTH2* genes were expressed independently in *cth1Δcth2Δ* cells using the constitutive yeast *TEF1* promoter. Cells expressing either the *TEF1:CTH1* or *TEF1:CTH2* genes, but not vector alone, exhibited decreased steady-state levels of the *SDH4* transcript, under Fe-deficiency or Fe-replete conditions (Figure 5D). These observations demonstrate that both Cth1 and Cth2, when constitutively expressed, are able to promote a decrease in *SDH4* steady-state mRNA levels irrespective of Fe availability. These results suggest that their activity

is not regulated post-translationally by Fe, but rather they are regulated predominantly at the level of gene expression.

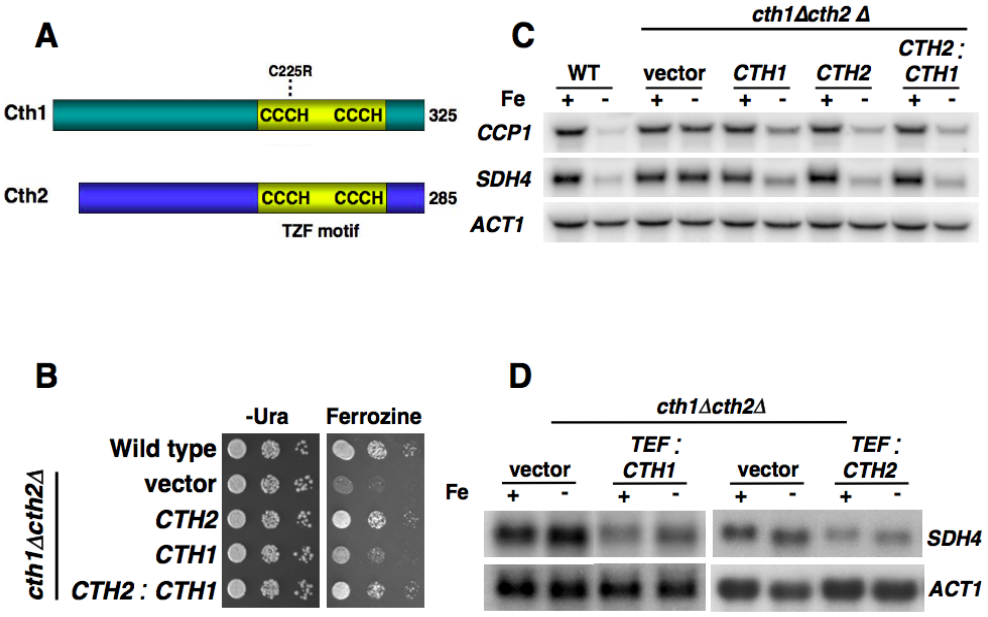

Figure 5: Over-expression of *CTH1* partially rescues *cth2Δ* phenotypes

A. Representation of the Cth1 and Cth2 proteins. The mutation within the tandem zinc-fingers (TZF) of Cth1 is indicated. **B**. Over-expression of *CTH1* partially suppresses the growth defect of *cth1Δcth2Δ* cells on Fe-depleted medium. BY4741 cells transformed with pRS416 (Wild-type), and *cth1Δcth2Δ* cells transformed with pRS416 (vector), pRS416-*CTH2*, pRS416-*CTH1*, or pRS416-*CTH2:CTH1* were spotted on SC-Ura or SC-Ura + 750 µM Ferrozine to induce Fe-deprived conditions. **C**. Over-expression of *CTH1* promotes down-regulation of Cth2 mRNA targets. *cth1Δcth2Δ* cells transformed with pRS416, pRS416-*CTH1*, pRS416-*CTH2*, or pRS416-*CTH2:CTH1* were grown in medium containing either 300 µM Ferrous Ammonium Sulfate (FAS; Fe +) or 100 µM Bathophenanthroline disulfonate (BPS; Fe -) and steady-state levels of *SDH4* and *CCP1* were analyzed by RNA blotting. *ACT1* was used as a loading control. **D**. Cth1 and Cth2 promote down-regulation of the *SDH4* transcript independently of Fe-levels. *cth1Δcth2Δ* cells transformed with p416*TEF1*, p416*TEF1-CTH1*, or p416*TEF1-CTH2* were grown and assayed as in panel C.

2.3.2 Aft1 and Aft2 regulate *CTH1* transcription

While Cth1 contributes to growth and *SDH4* mRNA degradation under conditions of Fe deficiency, previous studies demonstrate that *CTH2,* but not *CTH1* mRNA levels are elevated in response to long-term Fe-deficiency (Shakoury-Elizeh et al., 2004; Puig et al. 2005). Visual inspection of the *CTH1* promoter region revealed two putative Aft1/Aft2-binding sites starting at nucleotide positions -286 (5′-GCACCCAA-3′) and -94 (5′-TCACCCAA-3′) from the *CTH1* translation initiation codon (Figure 6A). Furthermore, a genome-wide localization analysis of transcription factors in the *S. cerevisiae* revealed occupancy of the *CTH1* promoter by the Aft1 transcription factor (Lee et al., 2002). To ascertain if Aft1 directly activates *CTH1*, Aft1 recruitment to the *CTH1* promoter was assessed by chromatin immuno-precipitation (ChIP) experiments using a strain harboring a functional TAP-tagged *AFT1* allele. While there is a low level of Aft1-TAP occupancy on the *FET3* and *CTH2* promoters in cells grown under Fe-supplemented conditions, Aft1-TAP is enriched in cells grown under Fe-starvation conditions, as expected (Figure 6B). Moreover, we detect occupancy by Aft1-TAP on the *CTH1* promoter under both Fe-supplemented and Fe-deprived conditions (Figure 6B). No Aft1-TAP occupancy was detected on the *CMD1* promoter, a gene not responsive to Fe levels, under either condition (Figure 6B). To ascertain whether Aft1 recruitment to the *CTH1* promoter results in transcriptional activation, the *CTH1* promoter region was fused to the coding sequence of a *lacZ* reporter gene (Figure 6A, top) and β-galactosidase

activity was measured. As shown in Figure 6C, the wild type *CTH1* promoter strongly induced expression of the *lacZ* reporter gene under Fe-limitation conditions in wild-type cells. This activity was decreased by ~80% in the *aft1Δ* strain and the remaining β-galactosidase activity was further reduced in the *aft1Δaft2Δ* strain to levels approximating those detected under high Fe conditions in all three strains (Figure 6C). To ascertain the potential role of the putative Aft1/Aft2-binding sites within the *CTH1* promoter on transcriptional activation, both Aft1/2 consensus sites within the *CTH1*:*lacZ* fusion were mutated at nucleotide residues previously demonstrated to be required for activation via Aft1/2 (Yamaguchi-Iwai et al., 1996; Puig et al. 2005) (Figure 6A, M2 mutant). The wild type and M2 reporter genes were assayed for β-galactosidase activity in response to Fe-deprivation in wild-type cells. As shown in Figure 6D, mutagenesis of both Aft1-Aft2 consensus promoter elements severely compromised activation of the *CTH1:lacZ* fusion gene in response to Fe-deprivation. Immunoblotting experiments from cells grown under Fe-limitation demonstrate that a Flag-Cth1 fusion protein is detectable within 0.5hr of the imposed Fe-limitation, reaching the highest steady state levels of expression by 2hr (Figure 6E). These data demonstrate that the *CTH1* promoter is transcriptionally activated in response to Fe-deficiency in a manner that is dependent on the Fe-responsive transcription factors, Aft1 and Aft2. In addition, these data suggest that the expression of Cth1 occurs early and transiently in the response to Fe-limitation.

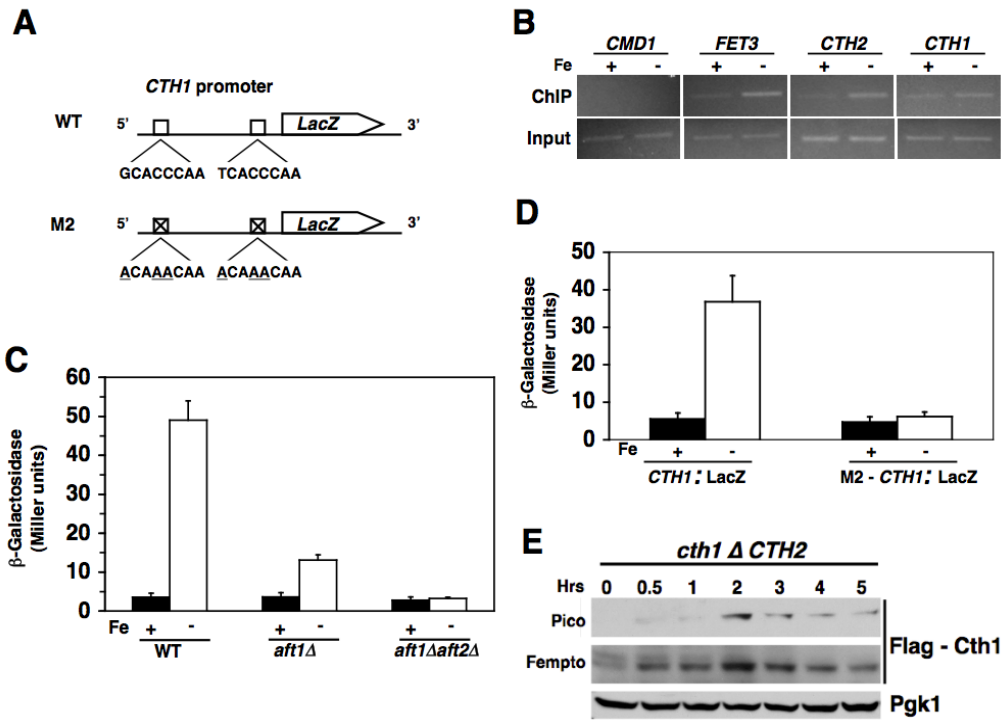

Figure 6: *CTH1* is rapidly and transiently activated by Aft1 and Aft2 during iron-limiting conditions

A. Representation of the promoter region of *CTH1* and the two putative Aft1-Aft2 binding sites, and the *CTH1:lacZ* fusion used for β-galactosidase assays. **B.** Aft1 occupancy of the *CTH1* promoter was tested by chromatin immunoprecipitation (ChIP) from cells grown in medium containing either 300 μM FAS (Fe +) or 100 μM BPS (Fe -) to exponential phase. ChIP performed as described under Materials and Methods. *CMD1* was used as a negative control, and *FET3* and *CTH2* as positive controls. **C.** Aft1 and Aft2 transcription factors are required for the *CTH1:lacZ* reporter activation upon Fe-deficiency. Wild-type, *aft1Δ* and *aft1Δaft2Δ* cells expressing a *CTH1:lacZ* fusion were grown under Fe+ or Fe- conditions and β-galactosidase activity was assayed. Results from four independent experiments are shown. **D.** Mutations in the putative Aft1-Aft2 binding sites in the *CTH1* promoter region compromise Fe deficiency-dependent activation of the *CTH1:lacZ* reporter in wild-type cells. Wild-type cells expressing either *CTH1:lacZ* or *M2-CTH1:lacZ* fusion were assayed as in panel **C. E**. Expression of the Flag-Cth1 fusion protein. Described under Materials and Methods.

2.3.3 Cth1 stimulates mRNA turnover

The mRNA destabilizing activity of Cth2 requires the integrity of the two $CX_8CX_5CX_3H$ tandem zinc fingers (TZFs), which constitute critical Zn-coordinating elements within the mRNA-binding domain, as well as the integrity of AU-rich elements (AREs) within the 3′-UTR of target mRNAs (Puig et al., 2005). Given that Cth1 over-expression can partially rescue the *cth1Δcth2Δ*-associated Fe-deficiency phenotypes, including the *SDH4* mRNA turnover deficit, we investigated the mechanisms by which Cth1 mediates *SDH4* mRNA down-regulation. We assayed the ability of Cth1 to interact with ARE-containing mRNAs using the yeast three-hybrid method (SenGupta et al., 1996). Wild type and mutated DNA fragments encoding ARE-containing RNA from the *SDH4* and *ACO1* 3′-UTRs (Figure 7A) were fused to bacteriophage MS2 RNA (Puig et al., 2005) and co-expressed in a reporter yeast strain with a Cth1-Gal4 trans-activation domain fusion protein. Interactions between Cth1 and the fusion RNAs were monitored by growth on medium lacking histidine (-His) and by measuring reporter gene-driven β-galactosidase activity. As shown in Figure 7B (right panel), cells co-transformed with plasmids expressing the wild type *SDH4* or *ACO1* 3′-UTR RNA fragments fused to MS2 RNA and the Cth1-Gal4 fusion protein can grow on medium lacking histidine, indicative of an interaction between Cth1 protein and the 3′-UTR of the *SDH4* and *ACO1* mRNAs. This interaction is not observed when *SDH4* and *ACO1* mRNAs are co-expressed with a mutant form of the Cth1-Gal4 fusion protein in which cysteine residue

225 within the TZF of Cth1 has been replaced with an arginine residue (C225R mutant, Figure 5A), suggesting that the integrity of the TZFs is required for Cth1 to interact with the mRNAs (Figure 7B). To further evaluate specific binding to *SDH4* mRNA, we assayed Cth1 binding to *SDH4* mutant alleles in which one patch (*mt1*) or all ARE consensus sequences (*mt2*) within the *SDH4* 3′-UTR mRNA were mutagenized (Figure 7A). As shown in Figure 7B, cells co-expressing the Cth1-Gal4 fusion protein and *SDH4-mt1* fusion RNA grow poorly in the absence of histidine as compared to cell expressing wild-type *SDH4* RNA. Furthermore, mutation of all AREs within the *SDH4* 3′-UTR (*SDH4-mt2* allele) completely abrogates growth on medium lacking histidine, without altering growth on synthetic complete medium (Figure 7B). As an independent means to assess the Cth1-*SDH4* ARE interaction, β-galactosidase activity driven by the Gal4-dependent reporter gene was measured (Figure 7C). Cells co-expressing the wild-type Cth1-Gal4 protein and *SDH4* RNA fusions exhibited abundant β-galactosidase activity. However, this activity was decreased by ~40% in cells expressing the *SDH4-mt1* fusion RNA and by ~90% in cells expressing the *SDH4-mt2 fusion* RNA (Figure 7C). Very low β-galactosidase activity was detected from cells co-expressing the wild-type *SDH4* fusion RNA with the Cth1 TZF mutant (Cth1 C225R-Gal4) fusion protein. These results strongly suggest that, like Cth2 (Puig et al., 2005), Cth1 specifically binds, within the 3′-UTR of the *SDH4* and *ACO1* mRNAs in a manner that is dependent on the integrity of the AREs and theTZF RNA binding domain.

Expression of Cth2 decreases the half-life of *SDH4* mRNA from ~14 to ~7 min in cells grown in low Fe (Puig et al., 2005). To ascertain if Cth1 also stimulates the turnover of *SDH4* mRNA, *SDH4* was conditionally expressed using the galactose-inducible and glucose-repressible *GAL1* promoter in *cth1Δcth2Δsdh4Δ* yeast cells and co-expressed with either the *CTH2:CTH1* plasmid or vector alone (Figure 7D). Cells were grown in galactose and 100 μM of the Fe-specific chelator, BPS, to induce the expression of both the *GAL1-SDH4-3'-UTR* and the *CTH2:CTH1* transcription units, respectively. Transcription of the *SDH4* gene was shut-off by addition of glucose and steady state mRNA levels were detected and quantitated over time by RNA blotting. As shown in Figure 7D, *SDH4* mRNA half-life decreased from 15.5 ± 1.6 minutes to 9.1 ± 1.7 minutes when Cth1 was expressed. In contrast, there was no decrease in *SDH4* mRNA half-life when the *CTH1-C225R* mutant allele was expressed, nor was the *SDH4* mRNA half-life decreased in the presence of wild type Cth1 when all *SDH4* ARE sequences were mutated (*SDH4*-mt2) (Figure 7D). Taken together, these data demonstrate that Cth1, like Cth2, can promote the accelerated turnover of mRNAs in a manner that is dependent upon a functional Cth1 TZF RNA binding domain and ARE sequences within the 3'-UTR of the target mRNA.

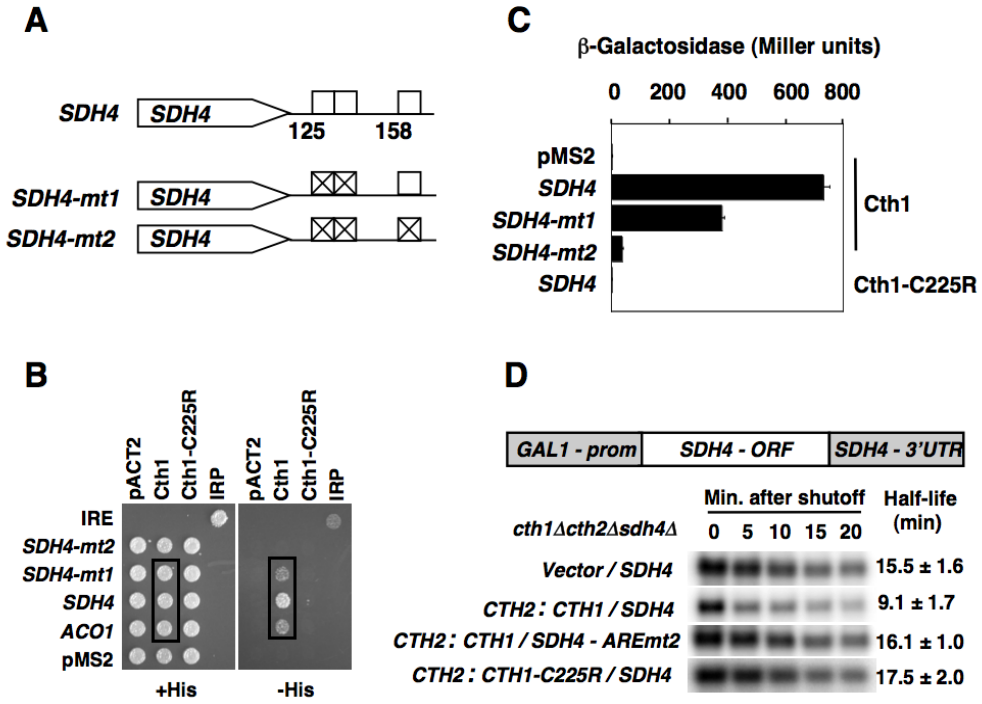

Figure 7: Cth1 accelerates the decay of *SDH4* mRNA

A. Representation of the *SDH4* transcript, the location of the AREs within its 3'-UTR, and the mutations introduced in the ARE clusters (mt1 and mt2; previously described in (Puig et al., 2005)). **B.** Yeast three-hybrid assay used to monitor *in vivo* interactions between Cth1 protein and the ARE-containing fragment of the *SDH4* 3'-UTR mRNA. L40-coat cells were co-transformed with (1) pIIIA/MS2-1 vector alone or containing the 3'-UTR of *SDH4*, *SDH4-mt1*, *SDH4-mt2*, *ACO1*, and the iron-responsive element (IRE) as positive control, and (2) pACT2 vector alone or fused to *CTH1*, *CTH1-C225R*, and the iron regulatory protein (IRP) as a positive control. Cells were grown on SC-Ura-Leu (+His) and SC-Ura-Leu-His (-His) plates for 7 to 10 days at 30°C. Positive interactions are indicated in the box. **C.** Quantitation of the three hybrid results. L40-coat cells co-transformed with (1) pACT2-*CTH1* and (2) pIIIA/MS-1 alone or fused to the 3'-UTR of *SDH4*, *SDH4-mt1*, *SDH4-mt2* were grown on SC-Ura-Leu and assayed for β-galactosidase activity. Cells were also co-transformed with (1) pACT2-*CTH1-C225R* and (2) the 3'-UTR *SDH4* and β-galactosidase activity was assayed. **D.** Cth1 accelerates the rate of decay of the *SDH4* mRNA. *cth1Δcth2Δsdh4Δ* cells were co-transformed with either p415*GAL1:SDH4* and pRS416 (vector), pRS416-*CTH2:CTH1* and pRS416-*CTH2:CTH1-C225R*, or p415*GAL1:SDH4-mt2* and pRS416-*CTH2:CTH1*. Cells were grown in medium containing galactose and100 μM BPS. Glucose was added to stop *SDH4* transcription and RNA analyzed by RNA blotting. *SDH4* levels were normalized to *ACT1* and mRNA half-lives determined from three independent experiments.

2.3.4 Cth1 targets mRNAs mostly encoding mitochondrial proteins

In response to Fe-limiting conditions Cth2 promotes the degradation of many mRNAs that encode proteins involved in Fe-homeostasis and Fe-dependent metabolism, thereby mediating a global remodeling of metabolism that optimizes growth in the presence of limited available Fe (Puig et al., 2005). Results presented here (Figure 5) suggest that Cth1 is able to partially compensate for loss of Cth2, suggesting that Cth1 and Cth2 might play at least partially overlapping roles under Fe-deficiency. The inability of Cth1 to completely rescue *cth2Δ* phenotypes could be due to differences in expression levels of both proteins or to functional differences.

To begin to dissect the individual contribution of Cth1 and Cth2 in the response to Fe-deficiency, we compared the genome-wide expression patterns of *cth1Δcth2Δ* cells expressing physiological levels of *CTH1*, *CTH2*, or vector alone. Figure 8 shows a schematic representation of the results of these experiments from triplicate Affymetrix DNA microarray studies. A total of 60 messenger RNAs were down-regulated by at least 1.5 fold in the presence of *CTH1.* Twenty of the 60 mRNAs down-regulated in cells expressing Cth1 harbor putative 3'-UTR ARE-sequences (Table 5 and Figure 8). Among the 20 ARE-containing transcripts that are down-regulated by Cth1, we identified 13 that encode mitochondrial proteins, including 7 proteins involved in respiration, 3 in amino acid biosynthesis, and 3 proteins of uncharacterized function that have been localized to mitochondria. The remaining 7 ARE-containing transcripts include 2 encoding proteins

involved in rRNA biosynthesis and 5 of diverse function. Down-regulation of the remaining 40 non-ARE containing mRNAs in the presence of Cth1 may be an indirect effect of Cth1 function or Cth1 binding to a non-canonical ARE. It is interesting to note that roughly 25% of these mRNAs (11 out of 40) encode proteins that have been identified as localized to the mitochondria. These results suggest that in response to Fe-deprivation Cth1 promotes the preferential down-regulation of mRNAs involved in critical Fe-dependent mitochondrial processes including respiration and amino acid biosynthesis.

The microarray results from Cth2-expressing cells confirm our previous observations (Puig et al., 2005) and increases the number of mRNAs likely to be direct Cth2 targets (Table 6). A total of 223 mRNAs were down-regulated in Cth2-containing cells under Fe-limiting conditions when compared to cells harboring an empty vector (Table 6 and Figure 8). Ninety-four of these transcripts are potentially direct targets of Cth2, as they harbor either 5′-UAUUUAUU-3′ or 5′UUAUUUAU-3′ ARE consensus sequences within their 3′-UTR. Twenty-two of the 94 ARE-containing mRNAs encode proteins involved in respiration, 9 in amino acid metabolism, 6 in heme/Fe-S cluster biosynthesis, 7 in fatty acid metabolism, 6 mitochondrial proteins and 3 encoding proteins involved in Fe homeostasis. The remaining ARE-containing mRNAs encode proteins involved in distinct cellular processes including stress responses, transport, nucleic acid metabolism and other processes (Table 6 and Figure 8). Down-regulation of

the remaining 128 non-ARE containing mRNAs could be due to secondary effects of Cth2 activity, or Cth2 binding to non-consensus AREs. Taken together, these mRNA expression data indicate that 13 of the 20 target mRNAs of Cth1 are contained within the set of mRNAs targeted by Cth2 (Figure 8 and Table 7). Interestingly, this overlapping subset of 13 ARE-containing mRNAs, down-regulated by both Cth1 and Cth2, primarily encodes proteins involved in mitochondrial functions, including oxidative phosphorylation and amino acid biosynthesis.

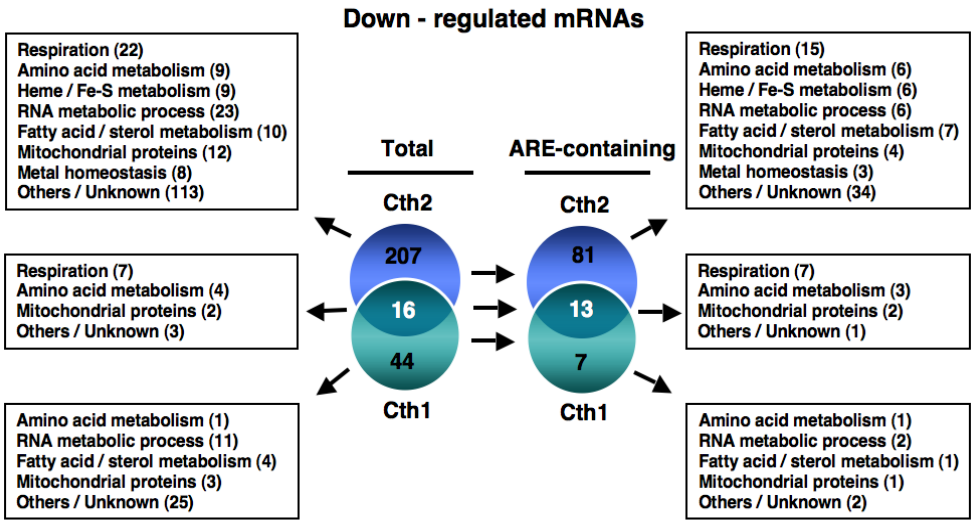

Figure 8: Cth1 and Cth2 have non-identical mRNA targets

(Left) Representation of the total number of mRNAs down-regulated in cells expressing either Cth1 or Cth2, as well as the functional categories of their encoded proteins. mRNAs corresponding to 223 genes were down-regulated by at least 1.5 fold in Cth2-expressing cells and a total of 60 mRNAs in Cth1-expressing cells. The intersect shows that mRNAs from 16 genes exhibited lower steady-state levels in both Cth1- and Cth2-expressing cells. The overlapping set of genes primarily encodes mitochondrial proteins involved in respiration and amino acid biosynthesis. *(Right)* Representation of the subset of ARE-bearing mRNAs down-regulated in Cth1- and Cth2-expressing cells. Ninety-five mRNAs that showed decreased expression levels in the presence of Cth2 harbor ARE-sequences as well as 20 of the mRNAs down-regulated in Cth1-containing cells. Thirteen of the 16 overlapping genes contain 3′-UTR ARE-sequences.

Table 5: Putative targets of Cth1

Genes whose mRNA steady-state levels were lower in *cth1Δcth2Δ* cells transformed with plasmid-borne *CTH1* compared to cells transformed with empty plasmid

ORF	Gene	Fold	Function	Putative 3'-AREs
RESPIRATION (7)				
TCA cycle and electron transport chain				
YJL166W	*QCR8*	2.4	Subunit 8 of ubiquinol cytochrome-c reductase complex	97, 114
YJR048W	*CYC1*	2.0	Cytochrome c, isoform 1	123, 162
YDR529C	*QCR7*	1.8	Subunit VII of the ubiquinol cytochrome-c reductase complex	151, 239
YNL052W	*COX5A*	1.6	Subunit Va of cytochrome c oxidase	188
YLL041C	*SDH2*	2.5	Fe-S protein subunit of succinate dehydrogenase	163, 309, 328
YKL148C	*SDH1*	2.3	Flavoprotein subunit of succinate dehydrogenase	153, 165, 180, 188, 196, 204
YKR066C	*CCP1*	2.8	Mitochondrial cytochrome-c peroxidase	19, 50, 59
AMINO ACID AND NITROGEN METABOLISM (5)				
YOR202W	*HIS3*	1.7	Imidazoleglycerol-phosphate dehydratase	
YJR016C	*ILV3*	1.7	Dihydroxyacid dehydratase	98
YLR355C	*ILV5*	2.0	Acetohydroxyacid reductoisomerase	182
YDR007W	*TRP1*	2.0	Phosphoribosylanthranilate isomerase	16
YDL171C	*GLT1*	1.7	NAD(+)-dependent glutamate synthase (GOGAT)	15, 37, 45, 53, 61, 69, 77
MITOCHONDRIAL PROTEINS (5)				
YOR356W		1.8	Mitochondrial protein with similarity to flavoprotein-type oxidoreductases	14, 38, 82
YLR193C	*UPS1*	1.9	Mitochondrial protein that regulates processing and sorting of Mgm1	141
YER182W	*FMP10*	1.6	Protein of unknown function found in mitochondria	15, 23
YCL057c-a		2.8	Protein of unknown function found in mitochondria	
YLR390W	*ECM19*	1.9	Protein of unknown function found in mitochondria	
RNA METABOLIC PROCESS (11)				
rRNA trancription and processing				
YOR341W	*RPA190*	1.6	Largest subunit of RNA polymerase I	276
YLR196W	*PWP1*	1.6	WD-40 protein involved in rRNA processing; similar to beta-transducin superfamily	
YMR285C	*NGL2*	1.6	Protein involved in 5.8S rRNA processing	252

SNR75	*SNR75*	1.7	C/D box snoRNA involved in 2'-O-methylation of LSU rRNA	
SNR72	*SNR72*	2.8	C/D box snoRNA involved in 2'-O-methylation of LSU rRNA	
Translation				
YMR286W	*MRPL33*	2.6	Mitochondrial ribosomal protein of the large subunit	
YLR406C	*RPL31B*	1.6	Protein component of the large (60S) ribosomal subunit	
YGR271W	*SLH1*	1.7	RNA helicase related to Ski2p	
Other				
YNL245C	*CWC25*	1.5	Component of a complex containing Cef1p, involved in pre-mRNA splicing	
YNL138w-a	*YSF3*	1.5	Component of the U2 snRNP	
YDL112W	*TRM3*	1.9	2'-O-ribose methyltransferase involved in tRNA methylation	
FATTY ACID BIOSYNTHESIS AND STEROL ACQUISITION (4)				
YPL231W	*FAS2*	1.9	Alpha subunit of fatty acid synthetase	
YKL182W	*FAS1*	2.2	Beta subunit of fatty acid synthetase	
YOR011W	*AUS1*	1.8	Transporter of the ATP-binding cassette family involved in uptake of sterols	
YNL111C	*CYB5*	1.6	Cytochrome b5	69
TRANSPORT (5)				
Nutrient transport				
YPL274W	*SAM3*	1.5	High-affinity S-adenosylmethionine permease	
YJL198W	*PHO90*	1.6	Low-affinity phosphate transporter	
Vesicle-mediated transport				
YJR005W	*APL1*	1.6	Beta-adaptin, large subunit of the clathrin AP-2	
YDR100W	*TVP15*	1.5	Integral membrane protein localized to late Golgi vesicles	206
YJL222W	*VTH2*	2.2	Putative membrane glycoprotein similar to Vth1p and Pep1p/Vps10p	
OTHER FUNCTIONS (17)				
Ras-protein signal transduction				
YJL005W	*CYR1*	1.5	Adenylate cyclase, required for cAMP-dependent protein kinase signaling	
YOL081W	*IRA2*	4.0	GTPase-activating protein that negatively regulates RAS	
Protein degradation				
YJL197W	*UBP12*	1.5	Ubiquitin-specific protease	
YMR314W	*PRE5*	1.6	20S proteasome alpha-type subunit	
YDR457W	*TOM1*	1.9	E3 ubiquitin ligase of the hect-domain class	

Nucleotide metabolic process				
YDL125C	*HNT1*	1.7	Adenosine 5'-monophosphoramidase	
YML056C	*IMD4*	1.8	Inosine monophosphate dehydrogenase involved in GMP biosynthesis	
Subtelomeric region genes				
YJL225C		1.5	Putative helicase encoded by the Y' element of subtelomeric regions	
YKL219W	*COS9*	1.8	Protein of unknown function encoded in subtelomeric region	261
Cell wall organization and biogenesis				
YLR342W	*FKS1*	2.0	Catalytic subunit of 1,3-beta-D-glucan synthase	
YMR306W	*FKS3*	1.6	Protein similar to 1,3-beta-D-glucan synthase catalytic subunit Fks1p	
Miscellaneous				
YMR222C	*FSH2*	1.7	Serine hydrolase similar to Fsh1 and Fsh3	
YNL279W	*PRM1*	1.8	Pheromone-regulated multispanning membrane protein involved in mating	
YKR102W	*FLO10*	1.8	Lectin-like protein with similarity to Flo1p	71
YPR030W	*CSR2*	2.0	Nuclear protein with involved in utilization of galactose and nonfermentable carbon sources	
YNL271C	*BNI1*	1.8	Formin. Involved in nucleation of linear actin filaments,	
YBR136W	*MEC1*	3.9	DNA checkpoint protein and PI kinase superfamily member	
HYPOTHETICAL/DUBIOUS ORFs (6)				
YMR245W		1.6	Hypothetical protein	
YMR074C		1.9	Hypothetical protein	
YMR073C		2.1	Hypothetical protein	
YMR007W		2.1	Dubious open reading frame unlikely to encode a protein	
YAR061W		2.6	Pseudogene/Hypothetical protein	
YKR103W	*NFT1*	2.9	Putative transporter of the multidrug resistance-associated protein subfamily	

Table 6: Putative targets of Cth2

Genes whose mRNA steady-state levels were lower in *cth1Δcth2Δ* cells transformed with plasmid-borne *CTH2* compared to cells transformed with empty plasmid

ORF	Gene	Fold	Function	Putative 3'-AREs
RESPIRATION (29)				
TCA cycle				
YGL062W	*PYC1*	1.6	Pyruvate carboxylase	43
YLR304C	*ACO1*	3.1	Mitochondrial aconitase also required for mtDNA maintenance	33, 151, 178
YIL125W	*KGD1*	2.3	Mitochondrial alpha-ketoglutarate dehydrogenase complex	193, 230
YKL148C	*SDH1*	2.4	Flavoprotein subunit of succinate dehydrogenase	153, 165, 180, 188, 196, 204
YLL041C	*SDH2*	3.3	Iron-sulfur protein subunit of succinate dehydrogenase	163, 309, 328
YKL141W	*SDH3*	2.2	Cytochrome b subunit of succinate dehydrogenase	91
YOR136W	*IDH2*	1.7	Subunit of mitochondrial NAD(+)-dependent isocitrate dehydrogenase	237
Electron Transport Chain				
YMR145C	*NDE1*	1.6	Mitochondrial external NADH dehydrogenase	
YBL030C	*PET9*	1.6	Major ADP/ATP carrier of the mitochondrial inner membrane	
Ubiquinol cytochrome c reductase				
YFR033C	*QCR6*	2.2	Subunit VI of the ubiquinol cytochrome-c reductase complex	31
YDR529C	*QCR7*	2.2	Subunit VII of the ubiquinol cytochrome-c reductase complex	151, 239
YJL166W	*QCR8*	2.0	Subunit VIII of ubiquinol cytochrome-c reductase complex	97, 114
YGR183C	*QCR9*	1.6	Subunit IX of the ubiquinol cytochrome-c reductase complex	73
YEL024W	*RIP1*	2.1	Rieske iron-sulfur of ubiquinol-cytochrome-c reductase	293, 355
YPL215W	*CBP3*	1.9	Protein required for assembly of ubiquinol cytochrome-c reductase complex	39
YGR174C	*CBP4*	1.7	Protein required for assembly of ubiquinol cytochrome-c reductase complex	81
YJR048W	*CYC1*	1.6	Cytochrome c, isoform 1	123, 162
Cytochrome c oxidase				
YML129C	*COX14*	1.5	Protein required for assembly of cytochrome c oxidase	
YGL187C	*COX4*	2.1	Subunit IV of cytochrome c oxidase	53
YNL052W	*COX5A*	2.1	Subunit Va of cytochrome c oxidase	188
YHR051W	*COX6*	2.6	Subunit VI of cytochrome c oxidase	88
YLR395C	*COX8*	1.8	Subunit VIII of cytochrome c oxidase	105
YDL067C	*COX9*	2.5	Subunit VIIa of cytochrome c oxidase	44
YOR065W	*CYT1*	2.2	Cytochrome c1	203, 453, 462, 471
YDR079W	*PET100*	1.9	Chaperone that facilitates the assembly of cytochrome c oxidase	55
YLL009C	*COX17*	2.2	Cu-metallochaperone that transfers copper to Sco1 and Cox11	

ATP synthesis coupled proton transport

YNL315C	*ATP11*	1.9	Molecular chaperone required for the assembly of F1 sector of mitochondrial F1/F0 ATP synthase	
YML081c-a	*ATP18*	1.5	Subunit of the mitochondrial F1F0 ATP synthase	
YBR039W	*ATP3*	1.7	Gamma subunit of the F1 sector of mitochondrial F1F0 ATP synthase	

AMINO ACID METABOLISM (14)

YDR035W	*ARO3*	2.0	3-deoxy-D-arabino-heptulosonate-7-phosphate (DAHP) synthase	80
YDL171C	*GLT1*	2.1	NAD(+)-dependent glutamate synthase (GOGAT)	15, 37, 45, 53, 61, 69, 77
YOR202W	*HIS3*	2.5	Imidazoleglycerol-phosphate dehydratase	
YJR016C	*ILV3*	2.2	Dihydroxyacid dehydratase, involved in synthesis of branched-chain amino acids	98
YNL104C	*LEU4*	1.8	Alpha-isopropylmalate synthase (2-isopropylmalate synthase)	34, 50
YDR234W	*LYS4*	2.0	Homoaconitase, which is a step in the lysine biosynthesis Pathway	38, 51
YOR241W	*MET7*	1.6	Folylpolyglutamate synthetase	54, 165
YGL184C	*STR3*	1.9	Cystathionine beta-lyase, converts cystathionine into homocysteine	
YDR007W	*TRP1*	1.6	Phosphoribosylanthranilate isomerase	16
YBR166C	*TYR1*	1.6	Prephenate dehydrogenase	
YFL021W	*GAT1*	1.6	Transcriptional activator of genes involved in nitrogen catabolite repression	107
YNL183C	*NPR1*	1.5	Protein kinase that stabilizes several plasma membrane amino acid transporters	403
YPL180W	*TCO89*	1.6	Subunit of TORC1	
YBR035C	*PDX3*	1.6	Pyridoxine (pyridoxamine) phosphate oxidase	

HEME/Fe-S METABOLISM (9)

YPL172C	*COX10*	1.7	Protoheme IX farnesyltransferase	
YER141W	*COX15*	1.6	Protein required for the hydroxylation of heme O to form heme A	168
YDR232W	*HEM1*	2.1	5-aminolevulinate synthase	103, 141
YOR176W	*HEM15*	2.7	Ferrochelatase; catalyzes the insertion of ferrous iron into protoporphyrin IX	44, 100
YOR278W	*HEM4*	1.7	Uroporphyrinogen III synthase	30
YLR205C	*HMX1*	2.0	Heme-binding peroxidase involved in the degradation of heme	
YLL027W	*ISA1*	1.8	Mitochondrial protein involved in biogenesis of the Fe-S clusters	47, 63
YKL040C	*NFU1*	2.5	Involved in Fe-metabolism in mitochondria; similar to NifU	192, 204
YPL252C	*YAH1*	1.7	Ferredoxin required for formation of cellular iron-sulfur proteins	

RNA METABOLIC PROCESS (23)

Transcription

YOR110W	*TFC7*	1.7	Subunit of TFIIIC that binds BoxA promoter sites of tRNA	
YOR116C	*RPO31*	1.7	RNA polymerase III subunit C160	
YPL086C	*ELP3*	1.7	Histone acetyltransferase of the Elongator complex of RNA pol II	
YOR337W	*TEA1*	1.6	Activator required for full Ty enhancer-mediated transcription	
YPL016W	*SWI1*	1.7	Subunit of the SWI/SNF chromatin remodeling complex	
YOR140W	*SFL1*	1.6	Transcription repressor negatively regulated by cAMP-dependent Tpk2	137
YOL051W	*GAL11*	1.6	Component of the Mediator complex; interacts with RNA polII	
YBL066C	*SEF1*	2.0	Putative transcription factor, has homolog in *K. lactis*	340, 409, 473, 488
Translation				
YDR091C	*RLI1*	2.4	Essential Fe-S protein required for ribosome biogenesis and translation initiation	280, 291
RDN25-1	*RDN25*	2.5	25S ribosomal RNA, component of the large (60S) ribosomal subunit	
YNL040W		1.9	Putative alanyl-tRNA synthase	
YBR167C	*POP7*	1.6	Subunit of RNase MRP and nuclear RNase P, involved in rRNA and tRNA maturation	
YER049W	*TPA1*	1.6	Putative protein involved termination efficiency, mRNA poly(A) tail length and mRNA stability	
YKL191W	*DPH2*	2.1	Protein required for synthesis of diphthamide of translation elongation factor 2	
Mitochondrial translation				
YMR012W	*CLU1*	1.5	eIF3 component of unknown function	24
YPL013C	*MRPS16*	1.8	Mitochondrial ribosomal protein of the small subunit	
YKR085C	*MRPL20*	1.6	Mitochondrial ribosomal protein of the large subunit	
YML091C	*RPM2*	2.5	Component of mt RNase P, which is involved in tRNA maturation and translation of mitochondrial mRNAs	20
YOL023W	*IFM1*	1.7	Mitochondrial translation initiation factor 2	
YPL183w-a		1.6	Putative mitochondrial ribosomal protein coded in the nuclear genome	
Other				
YNL124W	*NAF1*	1.5	Protein required for the assembly of box H/ACA snoRNPs and for pre-rRNA processing	
YNL138w-a	*YSF3*	1.6	Member of the U2 snRNP, associated with the SF3b complex	
YBR163W	*DEM1*	1.7	Unknown function similarity to RNA-processing protein Pta1p	18
FATTY ACID METABOLISM (10)				
YPL170W	*DAP1*	2.0	Heme-binding protein involved in regulation of Erg11	19, 148
YGR175C	*ERG1*	1.9	Squalene epoxidase essential for ergosterol-biosynthesis	122, 133
YHR007C	*ERG11*	1.8	Lanosterol 14-alpha-demethylase, involved in ergosterol biosynthesis	174, 203, 273
YMR208W	*ERG12*	1.8	Mevalonate kinase, acts in the biosynthesis of isoprenoids and sterols	20
YML126C	*ERG13*	1.5	3-hydroxy-3-methylglutaryl-CoA (HMG-CoA) synthase	

YBR041W	*FAT1*	1.6	Fatty acid transporter and very long-chain fatty acyl-CoA synthetase	
YMR272C	*SCS7*	2.3	Sphingolipid alpha-hydroxylase	89, 105
YJR019C	*TES1*	2.0	Peroxisomal acyl-CoA thioesterase likely to be involved in fatty acid oxidation	63
YBR058c-a	*TSC3*	1.5	Protein involved in sphingolipid biosynthesis	
YPR113W	*PIS1*	1.9	Phosphatidylinositol synthase, required for biosynthesis of phosphatidylinositol	48, 65

MITOCHONDRIAL PROTEINS (16)

YOR045W	*TOM6*	1.8	Component of the TOM (translocase of outer membrane) complex	
YEL052W	*AFG1*	2.0	Putative mitochondrial ATPase of the CDC48/PAS1/SEC18 (AAA) family	36
YER017C	*AFG3*	1.5	Component of the mitochondrial inner membrane m-AAA protease and is also required for correct assembly of mitochondrial enzyme complexes	21
YBR234C	*ARC40*	1.6	Essential subunit of the ARP2/3 complex, which is required for mitochondrial inheritance	
YNR017W	*MAS6*	1.5	Essential component of the mitochondrial import system	
YPR083W	*MDM36*	1.5	Required for normal mitochondrial morphology and inheritance	
YLR190W	*MMR1*	1.8	Phosphoprotein that localizes only to mitochondria of the bud	
YOR356W		2.2	Mitochondrial protein with similarity to flavoprotein-type oxidoreductases	14, 38, 82

Putative mitochondrial proteins

YER182W	*FMP10*	2	Found in mitochondrial proteome	15, 23, 30
YDR070C	*FMP16*	1.8	Found in mitochondrial proteome	138
YBR047W	*FMP23*	1.6	Found in mitochondrial proteome	
YMR157C	*FMP39*	1.8	Found in mitochondrial proteome	
YMR221C	*FMP42*	2.1	Found in mitochondrial proteome	28, 70, 260
YKR049C	*FMP46*	1.6	Putative redox protein containing a thioredoxin fold	

METAL HOMEOSTASIS (8)

YDR534C	*FIT1*	3.0	Cell wall mannoprotein involved in siderophore uptake	264
YOR079C	*ATX2*	1.8	Golgi membrane protein involved in manganese homeostasis	
YLR220W	*CCC1*	2.2	Putative vacuolar Fe2+/Mn2+ transporter	24, 144
YGR146C		1.6	Induced by Aft2p; multicopy suppressor of a ts mutant hsf1	
YKR052C	*MRS4*	2.0	Mitochondrial iron transporter	
YBR207W	*FTH1*	1.5	Member of the high affinity vacuolar Fe-transport system, Fet5/Fth1	
YBR295W	*PCA1*	1.9	P-type cadmium-transporting ATPase	77
YOL158C	*ARN4*	1.7	Endosomal ferric enterobactin transporter	

RESPONSE TO STRESS (15)

YGR088W	*CTT1*	1.7	Cytosolic catalase T, involve in protection from oxidative damage by H_2O_2	9, 47

YOR010C	*TIR2*	1.6	Putative cell wall mannoprotein, induced by cold shock and anaerobiosis	
YBR001C	*NTH2*	1.6	Putative neutral trehalase, required for thermotolerance	
YML028W	*TSA1*	1.8	Ubiquitous thioredoxin peroxidase	
YBL064C	*PRX1*	1.5	Mitochondrial peroxiredoxin (1-Cys Prx) with thioredoxin peroxidase activity, induced during respiratory growth and under conditions of oxidative stress	
YOR208W	*PTP2*	2.1	Phosphotyrosine-specific protein phosphatase involved in the inactivation of MAPK	
YLR337C	*VRP1*	1.7	Proline-rich, actin-associated protein involved in cytoskeletal organization	94
YHR008C	*SOD2*	1.9	Manganese-superoxide dismutase; protects cells against oxygen toxicity	
YOL05c-a	*DDR2*	1.5	Multistress response protein	
YFR034C	*PHO4*	1.6	Basic helix-loop-helix (bHLH) transcription factor	
YOR020C	*HSP10*	1.6	Mitochondrial matrix co-chaperonin that inhibits the ATPase activity of Hsp60p	
YDR423C	*YAP2*	1.9	AP-1-like bZIP transcriptional activator involved in multiple stress responses, iron metabolism, and pleiotropic drug resistance	
YFL031W	*HAC1*	1.8	bZIP transcription factor (ATF/CREB1 homolog) that regulates the UPR	
YKL109W	*HAP4*	1.7	Heme activator protein	275, 304
YNL064C	*YDJ1*	1.7	Protein chaperone involved in regulation of the HSP90 and HSP70 functions	

TRANSPORT (17)

Nutrient transport

YGR121C	*MEP1*	1.9	Ammonium permease	57
YPR079W	*MRL1*	1.7	Membrane protein similar to mammalian mannose-6-phosphate receptors	
YOR306C	*MCH5*	2.4	Plasma membrane riboflavin transporter; facilitates the uptake of vitamin B2	
YDL247W	*MPH2*	1.6	Alpha-glucoside permease	
YBR068C	*BAP2*	1.5	High-affinity leucine permease	
YHR094C	*HXT1*	1.7	Low-affinity glucose transporter	
YGR065C	*VHT1*	1.6	High-affinity plasma membrane H+-biotin (vitamin H) symporter	

Vesicle-mediated transport

YPL149W	*ATG5*	1.7	Autophagy-related protein	
YLR206W	*ENT2*	1.5	Epsin-like protein required for endocytosis and actin patch assembly	
YGL002W	*ERP6*	1.9	Member of the p24 family involved in ER to Golgi transport	71
YDR229W	*IVY1*	1.6	Phospholipid-binding protein that interacts with both Ypt7p and Vps33p	
YPL145C	*KES1*	1.5	Member of the oxysterol binding protein family	
YPL085W	*SEC16*	1.5	COPII vesicle coat protein required for ER transport vesicle budding	
YDL195W	*SEC31*	1.5	Essential component (p150) of the COPII coat of secretory pathway vesicles	
YAR042W	*SWH1*	1.7	Protein similar to mammalian oxysterol-binding protein	
YDR100W	*TVP15*	1.7	Integral membrane protein localized to late Golgi vesicles	206
YPR087W	*VPS69*	1.7	Dubious ORF; deletion causes vacuolar protein sorting defect	

DNA METABOLIC PROCESS (8)

YOR080W	*DIA2*	1.9	Origin-binding F-box protein;plays a role in DNA replication	

YGL066W	*SGF73*	1.5	73 kDa subunit of SAGA histone acetyltransferase complex	160
YBR073W	*RDH54*	1.5	DNA-dependent ATPase involved repair of double-strand breaks in DNA	
YER070W	*RNR1*	1.5	Ribonucleotide-diphosphate reductase (RNR), large subunit	
YJL026W	*RNR2*	1.8	Ribonucleotide-diphosphate reductase (RNR), small subunit	68
YGR180C	*RNR4*	1.8	Ribonucleotide-diphosphate reductase (RNR), small subunit	38, 125
YLL022C	*HIF1*	1.7	Component of the HAT-B histone acetyltransferase complex	215
YKR091W	*SRL3*	1.8	Overexpression suppressor of rad53 null lethality	

OTHER FUNCTIONS (39)

Cell wall organization and biogenesis

YNL243W	*SLA2*	2.3	Actin-binding protein involved in cytoskeleton assembly	48
YGR032W	*FKS2*	1.7	Catalytic subunit of 1,3-beta-glucan synthase	91
YPL053C	*KTR6*	1.7	Probable mannosylphosphate transferase	59
YDR483W	*KRE2*	1.5	Alpha1,2-mannosyltransferase of the Golgi involved in protein mannosylation	
YBL043W	*ECM13*	1.7	Non-essential protein of unknown function	
YIL146C	*ECM37*	1.8	Non-essential protein of unknown function	

N-glycosylation

YBR243C	*ALG7*	1.7	UDP-N-acetyl-glucosamine-1-P transferase	
YGR227W	*DIE2*	1.5	Dolichyl-phosphoglucose-dependent glucosyltransferase of the ER	52
YPR183W	*DPM1*	1.6	Dolichol phosphate mannose (Dol-P-Man) synthase of the ER membrane	
YPR051W	*MAK3*	2.5	Catalytic subunit of N-terminal acetyltransferase of the NatC type	52
YMR101C	*SRT1*	1.7	Cis-prenyltransferase involved in synthesis of long-chain dolichols	

Cell cycle

YNL116W	*DMA2*	1.6	Protein involved in regulating spindle position and orientation	
YDL101C	*DUN1*	1.6	Ser-Thr kinase required for DNA damage-induced transcription	
YML034W	*SRC1*	1.5	Protein with a putative role in sister chromatid segregation	
YGR049W	*SCM4*	1.9	Potential regulatory effector of CDC4 function, suppresses a ts allele of CDC4	148
YOR230W	*WTM1*	3.0	Transcriptional repressor involved in regulation of meiosis and silencing	145
YPL018W	*CTF19*	1.5	Outer kinetochore protein, required for accurate mitotic chromosome segregation	
YGL056C	*SDS23*	1.6	Homolog of the Schizosaccharomyces pombe Sds23 protein	
YPL250C	*ICY2*	2.1	Protein involved in chromatin organization and nuclear transport	
YPL137C	*GIP3*	1.5	Glc7-interacting protein whose overexpression relocalizes Glc7p from the nucleus	96

Protein degradation

YHR113W		2.2	Cytoplasmic aspartyl aminopeptidase	33
YKL103C	*LAP4*	1.8	Vacuolar aminopeptidase	478
YMR184W	*ADD37*	1.6	Protein of unknown function involved in ER-associated protein degradation	
YPL154C	*PEP4*	2.0	Vacuolar aspartyl protease (proteinase A)	

Degradation of Fructose-1,6-bisphosphatase				
YDR255C	*RMD5*	1.8	Required for ubiquitination of fructose-1,6-bisphosphatase	175
YBR105C	*VID24*	1.8	Involved in proteasome-dependent catabolite degradation of FBPase	
Response to pheromone				
YPL156C	*PRM4*	2.2	Pheromone-regulated protein	
YDL039C	*PRM7*	2.1	Pheromone-regulated protein	
Alcohol metabolism				
YLR251W	*SYM1*	1.7	Protein required for ethanol metabolism; induced by heat shock	
YGL256W	*ADH4*	1.5	Alcohol dehydrogenase type IV, induced in response to zinc deficiency	43, 77
Metabolite biosynthesis				
YBL033C	*RIB1*	1.6	GTP cyclohydrolase II; involved in riboflavin biosynthesis	138, 163
YOR196C	*LIP5*	2.0	Protein involved in biosynthesis of the coenzyme lipoic acid	71, 93, 124
YMR113W	*FOL3*	1.5	Dihydrofolate synthetase, involved in folic acid biosynthesis;	
YML004C	*GLO1*	1.8	Monomeric glyoxalase I, catalyzes the detoxification of methylglyoxal	79
YOL164W	*BDS1*	1.8	Bacterially-derived sulfatase required for use of alkyl- and aryl-sulfates as sulfur sources	
Seripauperin family				
YHL046C	*PAU13*	1.5	Part of 23-member seripauperin multigene family encoded mainly in subtelomeric regions; activated by anaerobiosis and repressed by Heme	
YNR076W	*PAU6*	1.6	Part of 23-member seripauperin multigene family encoded mainly in subtelomeric regions; activated by anaerobiosis and repressed by Heme	
YFL020C	*PAU5*	3.0	Part of 23-member seripauperin multigene family encoded mainly in subtelomeric regions; activated by anaerobiosis and repressed by Heme	
YOL161C	*PAU20*	1.6	Part of 23-member seripauperin multigene family encoded mainly in subtelomeric regions; activated by anaerobiosis and repressed by Heme	

PROTEIN OF UNKNOWN FUNCTION (37)

YBL059W		1.7	Putative mitochondrial protein	
YBL096C		1.5	Hypothetical protein	
YBR007C	*DSF2*	1.6	Deletion Suppressor of mptFive/pufFive mutation	
YBR238C		1.8	Transcription up-regulated by TOR and deletion increases life span	
YBR271W		1.7	Putative S-adenosylmethionine-dependent methyltransferase	
YDL012C		1.5	Putative plasma membrane protein	
YDL037C	*BSC1*	2.1	Protein of unconfirmed function, similar to cell surface flocculin Muc1p	
YDL038C		2.1	Protein of unknown function	
YDL237W		1.7	Protein of unknown function	
YER113C		1.5	Hypothetical protein	
YER156C		2.1	Hypothetical protein	59
YGR197C	*SNG1*	1.6	Protein involved in nitrosoguanidine (MNNG) resistance	50, 303
YHR009C		2.1	Protein of unknown function	62

YIL005W	*ESP1*	1.6	Disulfide isomerase-related protein involved in retention of ER proteins	
YJL079C	*PRY1*	1.7	Related to the plant PR-1 class of pathogen related proteins	
YKR103W	*NFT1*	2.9	Putative transporter of the multidrug resistance-associated protein (MRP) subfamily	
YKR104W	*NFT1*	3.3	Putative transporter of the multidrug resistance-associated protein (MRP) subfamily	
YLL029W		1.8	Protein of unknown function	38
YLR073C		1.8	Protein of unknown function	
YLR187W	*SKG3*	2.0	Protein of unknown function	112
YLR252W		1.6	Hypothetical protein	
YML020W		1.6	Hypothetical protein	133, 136, 141, 153
YMR034C		2.2	protein of unknown function	
YMR122w-a		1.7	Protein of unknown function	
YMR317 W		2.5	Protein of unknown function	
YNL152W		1.5	Protein required for cell viability	
YNL217W		1.5	Hypothetical protein	
YOL083W		2.4	Hypothetical protein	52
YOL092W		1.6	Hypothetical protein	15
YOR015W		1.6	Hypothetical protein	
YOR051C		1.6	Nuclear protein that inhibits replication of Brome mosaic virus in S. cerevisiae	109
YOR203W		1.6	Dubious ORF	
YOR389W		1.5	Hypothetical protein	
YPL277C		1.7	Hypothetical protein	
YPR077C		1.5	Hypothetical protein	
YPR114W		1.8	Hypothetical protein	
YPR174C		1.8	Protein of unknown function	37, 57

Table 7: Common targets of Cth1 and Cth2

Genes whose mRNA steady-state levels were lower in *cth1Δcth2Δ* cells transformed with plasmid-borne *CTH1* or with *CTH2* compared to cells transformed with empty plasmid. (Putative common targets of Cth1 and Cth2)

		Fold			
ORF	**Gene**	***CTH1***	***CTH2***	**Function**	**Putative 3'-AREs**
RESPIRATION (7)					
YJL166W	*QCR8*	2.4	2	Subunit 8 of ubiquinol cytochrome-c reductase complex	97, 114
YJR048W	*CYC1*	2.0	1.6	Cytochrome c, isoform 1	123
YDR529C	*QCR7*	1.8	2.2	Subunit VII of the ubiquinol cytochrome-c reductase complex	151, 239
YNL052W	*COX5a*	1.6	2	Subunit Va of cytochrome c oxidase	188
YLL041C	*SDH2*	2.5	3.3	Fe-S protein subunit of succinate dehydrogenase	163, 309, 328
YKL148C	*SDH1*	2.3	2.4	Flavoprotein subunit of succinate dehydrogenase	153, 165, 180, 188, 196, 204
YKR066C	*CCP1*	2.8	*	Mitochondrial cytochrome-c peroxidase	19, 50, 59
AMINO ACID BIOSYNTHESIS AND NITROGEN METABOLISM (3)					
YJR016C	*ILV3*	1.7	2.2	Dihydroxyacid dehydratase	98
YDR007W	*TRP1*	2.0	1.6	Phosphoribosylanthranilate isomerase	16
YDL171C	*GLT1*	1.7	2.1	NAD(+)-dependent glutamate synthase (GOGAT)	15, 37, 45, 53, 61, 69, 77
OTHER (3)					
YER182W	*FMP10*	1.6	2	Protein of unknown function found in mitochondria	15, 23
YOR356W		1.8	2.2	Mitochondrial protein with similarity to flavoprotein-type oxidoreductases	14, 38, 82
YDR100W	*TVP15*	1.5	1.7	Integral membrane protein localized to late golgi vesicles	206

2.3.5 Cth1/Cth2-dependent changes in carbohydrate metabolism

As a facultative anaerobe, *S. cerevisiae* generates ATP through both glycolysis and mitochondrial oxidative phosphorylation. Consistent with important roles for Fe in cellular metabolism, a common functional category for 11 of 13 mRNAs targeted for degradation by both Cth1 and Cth2, and which harbor consensus AREs, are established or proposed to encode proteins that play key roles in mitochondrial respiration or in other pivotal mitochondrial functions. Based on these results, Fe deprivation could lead to rapid loss of mitochondrial function via Cth1 and Cth2-stimulated mRNA degradation. Moreover, we observed that the steady state level of 17 mRNAs in *CTH1*-expressing cells, and approximately 40 distinct mRNAs in *CTH2* wild type cells is elevated, but not in *cth1Δ cth2Δ* cells, in response to Fe deficiency (Figure 9A and Tables 8 and 9). Among these mRNAs are those that encode proteins involved in glucose uptake (*HXT5, HXT6* and *HXT7*, medium and high affinity glucose transporters), glycolysis (*HXK1,* hexokinase), reserve carbohydrate metabolism (*GPH1* glycogen phosphorylase, *GSY1* glycogen synthase, *PGM2* phosphoglucomutase, *SOL4* 6-phosphogluconolactonase, *YMR090W* dTDP-glucose 4, 6 dehydratase), anaerobic metabolism (*COX5b* subunit 5b of cytochrome oxidase expressed anaerobically, *ALD3* aldehyde dehydrogenase) and other functions proposed to be required for adaptation to low glucose conditions (Saccharomyces Genome Database). Furthermore, their of the genes identified as up-regulated in these microarrays, such as *HSP12*, are known to be

induced by glucose deprivation. These experiments also identified genes involved in DNA repair and meiosis *(APN1, MMS1, MSC1, REC104, SAE3)*, as well as genes involved in RNA metabolism *(SNR46, SEN1, PPE1)*. These regulatory changes, and their dependency on Cth1 and Cth2, have been confirmed by RNA blotting (Figure 9B). Furthermore, this up-regulation is dependent on both Cth1 and Cth2, as it is not observed in a *cth1Δ cth2Δ* strain (Figure 9B and data not shown). A similar pattern of up-regulation of mRNAs that function in glucose uptake, glycolysis and reserve carbohydrate metabolism is also observed in wild type cells in response to Fe deprivation or in cells defective in Fe-S cluster biogenesis (Puig et al., 2005; Hausmann et al., 2008). Taken together, these results suggest that Cth1/Cth2-mediated down-regulation of Fe-dependent metabolic pathways might lead to a secondary energy limitation due to the degradation of mRNAs encoding key mitochondrial proteins. This may result in the enhanced expression of mRNAs encoding high-affinity glucose transporters, glycolytic enzymes and factors involved in the metabolism of reserve carbohydrates.

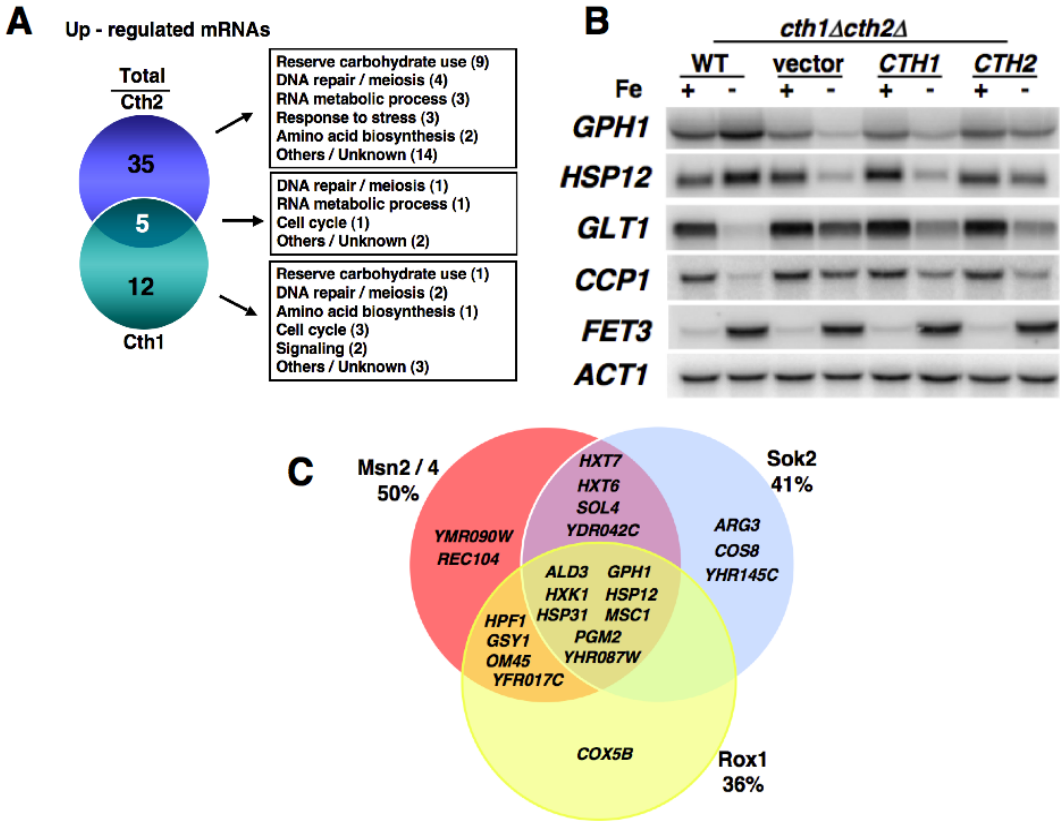

Figure 9: Summary of mRNAs up-regulated in cells expressing either Cth1 or Cth2

A. Forty mRNAs, whose encoded proteins correspond to the indicated functional categories, showed increased levels by at least 1.5 fold in Cth2-expressing cells, and a total of 17 mRNAs in cells transformed with Cth1 during Fe-deficiency when compared to cells harboring an empty vector. The intersect represents the number of common mRNAs up-regulated between Cth1- and Cth2-expressing cells. **B.** Microarray validation. Wild-type and *cth1Δcth2Δ* cells transformed with pRS426, pRS416-*CTH1* or pRS416-*CTH2* were grown in medium containing either 300 μM FAS (Fe+) or 100 μM BPS (Fe-) and analyzed by RNA blotting. *FET3* was used as a control for Fe-deprivation, and *ACT1* as loading control. **C.** Representation of a partial list of genes up-regulated in *CTH2* wild type cells in response to Fe-deficiency grouped by transcription factors experimentally demonstrated to regulate their expression that include Msn2/4, Rox1 and Sok2.

Table 8: mRNAs upregulated in *CTH1*-expressing cells during Fe-deficiency

Genes whose mRNA steady-state levels were higher in *cth1Δcth2Δ* cells transformed with plasmid-borne *CTH1* compared to cells transformed with empty plasmid

ORF	*Gene*	Fold	Function
SIGNALING (2)			
YIL147C	*SLN1*	1.5	Histidine kinase osmosensor that regulates a MAP kinase cascade
YGR070W	*ROM1*	1.9	GDP/GTP exchange protein (GEP) for Rho1p
CHROMATIN REMODELING/DNA REPAIR (3)			
YGR002C	*SWC4*	1.6	Component of the Swr1p complex that incorporates Htz1p into chromatin
YFL049W	*SWP82*	1.6	Member of the SWI/SNF chromatin remodeling complex
YPR164W	*MMS1*	1.7	Protein likely involved in protection against replication-dependent DNA damage
CELL CYCLE (4)			
YNL172W	*APC1*	1.9	Largest subunit of the Anaphase-Promoting Complex/Cyclosome (APC/C)
YMR168C	*CEP3*	1.5	Essential kinetochore protein
YIL101C	*XBP1*	1.5	Transcriptional repressor of CYS3, and SMF2; induced by stress or starvation
YHR017W	*YSC83*	1.6	Mitochondrial protein of unknown function; mRNA induced during meiosis
VARIOUS (8)			
YHR096C	*HXT5*	1.8	Hexose transporter with moderate affinity for glucose, may function in accumulation of reserve carbohydrates during stress
YIL116W	*HIS5*	1.6	Histidinol-phosphate aminotransferase
YCR032W	*BPH1*	1.7	Homologous to the murine beige gene; involved in lysosomal trafficking
YHR075C	*PPE1*	1.6	Carboxyl methyl esterase that may have a role in demethylation of the phosphoprotein phosphatase catalytic subunit
YIL083C		1.6	Putative phosphopantothenoylcysteine synthetase (PPCS) that catalyzes the second step in the biosynthesis of coenzyme A from pantothenate
YFR022W	*ROG3*	1.6	Protein that binds to Rsp5p, which is a hect-type ubiquitin ligase, via its 2 PY motifs
YGL010W		1.7	Hypothetical protein
YIL068w-a		1.9	Dubious open reading frame

Table 9: mRNAs upregulated in *CTH2*-expressing cells during Fe-deficiency

Genes whose mRNA steady-state levels were higher in *cth1Δcth2Δ* cells transformed with plasmid-borne *CTH2* compared to cells transformed with empty plasmid

ORF	Gene	Fold	Function
RESERVE CARBOHYDRATE UTILIZATION (9)			
YFR053C	*HXK1*	1.9	Hexokinase isoenzyme 1; repressed by glucose
YDR343C	*HXT6*	3.2	High-affinity glucose transporter; repressed by glucose
YDR342C	*HXT7*	2.7	High-affinity glucose transporter; repressed by glucose
YPR160W	*GPH1*	3.1	Glycogen phosphorylase; regulated by cAMP and HOG MAP kinase pathway
YFR015C	*GSY1*	2.1	Glycogen synthase; induced by glucose limitation and nitrogen starvation
YMR105C	*PGM2*	1.7	Phosphoglucomutase; functions as the acceptor for a Glc-phosphotransferase
YGR248W	*SOL4*	1.8	6-phosphogluconolactonase with similarity to Sol3p
YMR090W		1.9	Protein of unknown function with similarity to DTDP-glucose 4,6-dehydratases
YIL111W	*COX5B*	1.6	Subunit Vb of cytochrome c oxidase; expressed during anaerobic growth
DNA REPAIR / MEIOSIS (5)			
YKL114C	*APN1*	1.7	Apurinic/apyrimidinic endonuclease, involved in DNA repair
YPR164W	*MMS1*	2.0	Protein likely involved in protection against replication-dependent DNA damage
YML128C	*MSC1*	1.7	Involved directing meiotic recombination events to homologous chromatids
YHR157W	*REC104*	1.6	Involved in early meiotic recombination and crossover
YHR079c-a	*SAE3*	1.6	Meiosis specific protein involved in DMC1-dependent meiotic recombination
RNA METABOLIC PROCESS (4)			
YHR087W		2.0	Protein involved in RNA metabolism
SNR46	*snR46*	2.1	H/ACA box small nucleolar RNA (snoRNA); guides pseudouridylation of large subunit (LSU) rRNA
YLR430W	*SEN1*	3.1	Nuclear helicase required for processing of tRNAs, rRNAs, and small nuclear RNA
YHR075C	*PPE1*	1.7	Carboxyl methyl esterase that may have a role in demethylation of the phosphoprotein phosphatase catalytic subunit
RESPONSE TO STRESS (3)			
YHL048W	*COS8*	1.5	Subtelomerically-encoded protein; potential role in UPR
YFL014W	*HSP12*	1.7	Protects cells from desiccation; induced by heat shock, oxidative stress and glucose depletion. Regulated by the HOG and Ras-Pka pathways
YDR533C	*HSP31*	2.1	Possible chaperone and cysteine protease with similarity to Hsp32p, Hsp33p, and Sno4p

AMINO ACID BIOSYNTHESIS (2)

YMR169C	*ALD3*	1.6	Cytoplasmic aldehyde dehydrogenase, involved in beta-alanine synthesis; repressed by glucose
YJL088W	*ARG3*	1.8	Ornithine carbamoyltransferase; involved in the synthesis of arginine from ornithine

OTHER FUNCTIONS (17)

YHR101C	*BIG1*	1.6	ER protein required for normal content of cell wall beta-1,6-glucan
YCR032W	*BPH1*	2.1	Homologous to the murine beige gene; involved in lysosomal trafficking
YNL172W	*APC1*	2.6	Largest subunit of the Anaphase-Promoting Complex/Cyclosome (APC/C)
YOL155C	*HPF1*	2.5	Haze-protective mannoprotein
YCL024W	*KCC4*	1.7	Protein kinase of the bud neck involved in the septin checkpoint
YIL136W	*OM45*	1.7	Protein of unknown function, constituent of the mitochondrial outer membrane
YDR281C	*PHM6*	1.8	Protein of unknown function, expression is regulated by phosphate levels
YDR112W	*IRC2*	2.2	Hypothetical protein
YLR063W		1.9	Hypothetical protein
YKR012C		1.8	Hypothetical protein
YGR107W		1.8	Dubious ORF
YDR133C		1.8	Dubious ORF
YGL010W		1.7	Hypothetical protein
YHR145C		1.7	Hypothetical protein
YFR017C		1.7	Hypothetical protein
YDR042C		1.6	Hypothetical protein
YER039c-a		1.6	Hypothetical protein

2.3.6 Iron deficiency elicits changes in glucose metabolism

Our results suggest that *S. cerevisiae* cells grown under Fe-limiting conditions have elevated levels of mRNAs encoding proteins involved high-affinity glucose uptake, glycolysis, reserve carbohydrate metabolism, and anaerobic metabolism, as well as mRNAs known to be highly-expressed in response to low glucose conditions (Figure 9A). We found that concomitant with the increased levels of these mRNAs, the *HXT1* mRNA, encoding a low affinity glucose transporter known to be down-regulated during glucose limitation (Ozcan and Johnston, 1999), was down-regulated during Fe-starvation conditions (Table 6). Similarly, *RMD5* and *VID24* mRNAs, encoding two proteins required for the ubiquitination and proteasome-dependent degradation of Fructose 1,6-BisPhophatase (FBPase) during high glucose conditions, were also found to be down-regulated under Fe-starvation conditions (Table 6). Based on these observations, we hypothesized that Fe-deprivation might lead to a secondary glucose starvation. Additionally, a recent report suggests that cells with impaired mitochondrial Fe-S cluster assembly and export systems have increased levels of mRNAs encoding proteins involved in glucose transport (Hausmann et al. 2008).

The serine/threonine protein kinase, Snf1, is a member of the AMP-activated protein kinase family required for the adaptation to glucose starvation in yeast. During glucose limitation Snf1 is phosphorylated, thereby becoming activated and promoting the up-regulation of high affinity glucose transport systems, increased glycolysis and

glycogen biosynthesis, among others activities (Celenza and Carlson, 1986; Wilson et al., 1996; Hardie et al, 1998). We ascertained the phosphorylation status of Snf1 kinase in response to Fe-deprivation by immunobloting using antibodies that specifically recognize the phosphorylated form of Snf1. This experiment revealed that Snf1 from cells grown under Fe-limited, but glucose replete, conditions is more highly phosphorylated than that from cells grown under Fe-supplemented conditions (Figure 10A). This suggests that Fe-limitation could lead to a secondary glucose deficiency, which in turn triggers the phosphorylation-mediated activation of Snf1 kinase. To examine if Fe-deficiency stimulated Snf1 phosphorylation correlates with changes in cellular carbohydrate metabolism, and whether this response is dependent on Cth1 and Cth2, we analyzed glycogen content in wild type and *cth1Δcth2Δ* cells under Fe-sufficient and Fe-deplete conditions. As shown in Figure 10B, *cth1Δcth2Δ* cells, or the same mutant harboring wild type *CTH1* and *CTH2* genes, grown under Fe-supplemented conditions, accumulate similar levels of glycogen. In contrast, under Fe-deficient conditions cells containing the wild type *CTH1* and *CTH2* genes accumulate approximately 7 fold higher levels of glycogen when compared to isogenic *cth1Δcth2Δ* cells. These results suggest that during Fe-deficiency, wild type cells both activate Snf1 kinase and hyper-accumulate glycogen, and this hyper-accumulation is dependent on the presence of Cth1 and Cth2 activity.

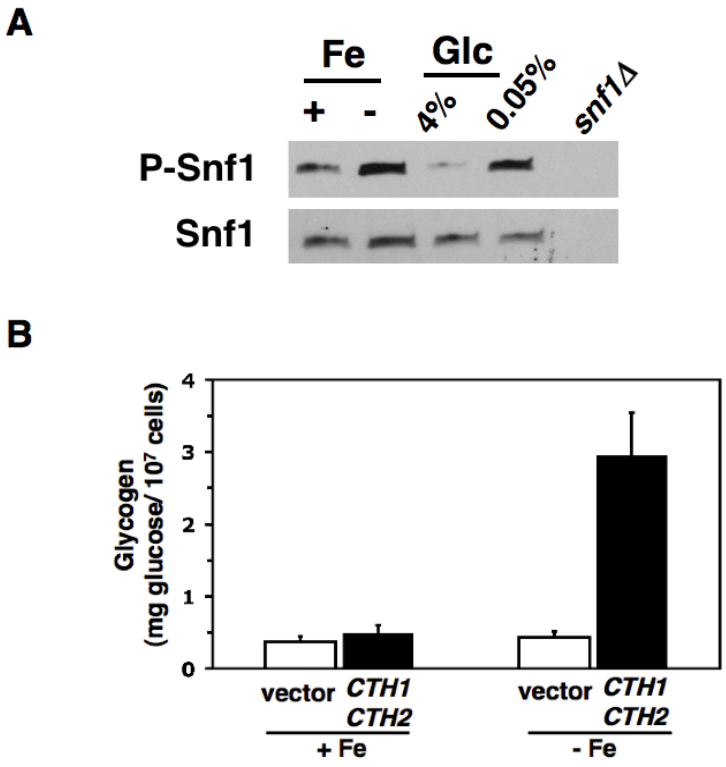

Figure 10: Iron deficiency elicits changes in carbohydrate metabolism

A. Fe deficiency-dependent phosphorylation of Snf1. Snf1-HA was immunoprecipitated from cells grown in 300 μM FAS (Fe +) or 100 μM BPS (Fe -). Immunoprecipitations were analyzed by immublotting using anti-Snf1 and phospho-specific anti-Snf1 antibodies. As negative and positive controls for Snf1-HA phosphorylation, cells were also grown on 4% or 0.05% glucose medium, respectively. **B.** Fe deficiency-induced glycogen hyper-accumulation. Cells were grown in the presence of 300 μM FAS (Fe +) or 100 μM BPS (Fe -) and total glycogen content was analyzed as described by Parrou and Francoise (1997).

2.4 Discussion

Iron functions as a co-factor for a broad range of enzymes that are essential for normal growth, maintenance and development, and organisms must continually adapt to changes in Fe availability. Previous studies have identified regulatory mechanisms in

response to Fe availability at the level of gene transcription, mRNA stability, translation, protein degradation and protein trafficking (Escolar et al., 1999; Hentze et al., 2004; Kaplan et al., 2006). Under conditions of Fe scarcity, *S. cerevisiae* cells induce the expression of the Cth2 mRNA binding protein, which stimulates the turnover of many mRNAs encoding proteins that function in Fe homeostasis, storage and Fe-dependent metabolism. While *cth2Δ* cells exhibit a growth defect under conditions of Fe starvation and defective target mRNA turnover, the additional deletion of the *CTH1* gene, encoding a homologous RNA binding protein, exacerbates these defects.

Observations reported here support a specific role for *CTH1* during Fe deficiency and include the Aft1/2-dependent activation of the *CTH1* promoter in response to Fe deficiency. In addition, a Flag-Cth1 fusion protein is expressed rapidly, but transiently, after cells are deprived of Fe. Preliminary observations suggest that Cth2 can bind to and promote the destabilization of the *CTH1* transcript (Puig, Vergara, and Thiele, unpublished data). While this mechanism has not been explored, it could at least in part account for the decreased steady-state levels of the Cth1 protein after 2hr of Fe-chelation (Figure 7E; unpublished data) and suggests tight regulatory mechanisms for Cth1 expression during Fe-deficiency. Furthermore, this rapid but transient expression of Cth1 would explain why previous experiments, using prolonged Fe deficiency growth conditions, did not identify *CTH1* as an Fe-responsive gene (Rutherford et al., 2003; Shakoury-Elizeh et al., 2004; Puig et al., 2005).

While at present we cannot eliminate the possibility that Cth1 and Cth2 play roles outside of Fe homeostasis, we propose that a primary function for these two proteins, may be to allow rheostatic adaptation to changes in Fe availability. Small fluctuations in Cth1 levels could be sufficient for adaptation to modest or transient Fe deficiency by first targeting mitochondrial functions. If the Fe deficiency is more severe or sustained, Cth2 is strongly induced and provides a means for more widespread metabolic changes that, together, would lead to a shift away from mitochondrial oxidative phosphorylation and toward the down-regulation of Fe storage and other Fe-dependent metabolic activities. Further experiments are required to rigorously test this hypothesis.

While both Cth1 and Cth2 are transcriptionally induced by Aft1/2, bind ARE mRNA sequences to stimulate mRNA turnover and contribute to growth under conditions of Fe deficiency, our results strongly suggest that these proteins have only partial functional overlap in the response to Fe deficiency. Analysis of the mRNA expression pattern of *cth1Δcth2Δ* cells expressing physiological levels of either *CTH1* or *CTH2* indicates that Cth1 and Cth2 share a subset of mRNA targets. Only 13 common mRNAs with recognizable AREs are down-regulated in cells expressing either Cth1 or Cth2. These targets common to both Cth1 and Cth2 include mRNAs encoding proteins involved in mitochondrial respiration and mitochondrial-localized amino acid

metabolism (Table 7). It is currently unclear what determinants give rise to distinct mRNA target specificity for these two similar RNA binding proteins.

Given the critical role that Fe plays in mitochondrial oxidative phosphorylation, the results presented here suggest an additional important role for Cth1 and Cth2 in facilitating a transition between oxidative phosphorylation and glycolytic metabolism in response to Fe deficiency. Wild type cells, but not *cth1Δ cth2Δ* cells, accumulate transcripts encoding proteins involved in glucose uptake, glycolysis and reserve carbohydrate metabolism in concert with the down regulation of those encoding proteins essential for mitochondrial oxidative phosphorylation and other critical mitochondrial processes. To begin to understand the nature of this coordinate up-regulation of these mRNAs, their cognate genes were grouped according to their validated regulation by gene-specific transcription factors. As shown in Figure 9C, of the genes annotated in the Yeastract database (36 of 40), 50% are activated by the Msn2/4 stress-responsive transcription factors, 40% by Sok2 and 36% by Rox1. Notably, Msn2/4 are known induce gene expression in response to glucose deprivation, Sok2 responds to cAMP levels and Rox1 is a heme-dependent repressor of hypoxic genes. Currently, there is no evidence supporting the notion that proteins belonging to the Cth-family can stabilize mRNAs. As such, we hypothesize that Fe deficiency that leads to a Cth1/Cth2-dependent mitochondrial inactivation, through their mRNA-destabilizing activity, would activate each of the signaling pathways that regulate the Msn2/4, Sok2, and Rox1

transcription factors, thus promoting an elevation in the steady state levels of the mRNAs encoding proteins involved in glucose metabolism (Liang-chuan et al., 2005; Ward et al., 1995; Lowry and Zitomer, 1984; Ter Linde and Steensma, 2002).

3. Auto- and trans-regulation of Cth1 and Cth2

3.1. Introduction

The ability of iron (Fe) to easily transition between two valence states makes it a preferred co-factor for innumerable biochemical reactions, ranging from cellular energy production, to oxygen transport, to DNA synthesis and chromatin modification. Hence, Fe is essential for all eukaryotes and virtually all prokaryotes. However, the same chemical properties that make Fe an essential micronutrient also creates two problems; first, Fe is highly insoluble in the presence of oxygen at neutral pH. Thus, despite its abundance, Fe bioavailability is limited; and second, excess Fe is highly toxic as it can engage in Fenton-type chemistry generating highly reactive hydroxyl radicals, which in turn can damage membranes, nucleic acids, and proteins. Excess Fe can also compete with others metals for metal-binding sites within non-Fe metalloproteins (Bertini et al., 2007; Lippard and Berg, 1994). Therefore, cells are faced with the difficult task of acquiring enough Fe to meet essential cellular demands, while avoiding its hyper-accumulation to prevent Fe-catalyzed cellular damage. As a result, organisms have evolved sophisticated homeostatic mechanisms to ensure appropriate intracellular Fe levels (Dunn et al., 2007; Hentze et al., 2004; Kaplan et al., 2006).

In response to Fe-deficiency, the yeast Fe-sensing transcription factors Aft1 and Aft2 activate a group of genes collectively known as the Fe-regulon. Genes in this group encode proteins whose activities increase cellular Fe-concentration and include the high-

affinity plasma membrane Fe-uptake system, siderophore transport systems, Fe-mobilization from intracellular stores and heme re-utilization. In addition, Aft1 and Aft2 activate the *CTH1* and *CTH2* genes whose encoded proteins play an important role in the appropriate allocation of the limited Fe by coordinately promoting the degradation of mRNAs involved non-essential Fe-rich metabolic pathways (De Domenico et al., 2008; Pedro-Segura et al., 2008; Puig et al., 2005; Puig et al., 2008; Rutherford et al., 2001; Rutherford et al., 2003; Shakoury-Elizeh et al., 2004; Vergara and Thiele, 2008).

Cth1 and Cth2 belong to the Tristetraprolin (TTP) family of mRNA destabilizing proteins characterized by an RNA-binding motif consisting of two tandem zinc-fingers of the $CX_8CX_5CX_3H$ type, which bind specific AU-rich elements (AREs) located in the 3'untranslated region (3'UTRs) of select groups of mRNAs, thereby promoting their rapid degradation (Ma and Herschman, 1995; Thompson et al., 1996). In response to Fe-limitation, Cth1 and Cth2 accelerate the rate of decay of groups of mRNAs that encode proteins involved highly Fe-demanding processes by interacting with their AREs. Such Fe-demanding processes include TCA cycle, electron transport chain, heme and Fe-S biosynthesis, sterol and amino acid metabolism, and Fe-storage. As a consequence, the mRNA-destabilizing activity of Cth1 and Cth2 permits the re-allocation of the limited cellular Fe to more essential processes. Interestingly, Cth1 and Cth2 appear to be only partially redundant proteins. While both proteins are capable of binding the same ARE sequences, Cth1 seems to have a predilection for mRNAs encoding Fe-requiring

mitochondrial proteins, while Cth2 promotes the down regulation of a much larger group of mRNAs that encode both mitochondrial and non-mitochondrial Fe-utilizing proteins (Puig et al., 2008). In addition, Cth2 expression gradually and robustly increases during Fe-deficiency over time, while Cth1 is more rapidly and only transiently expressed soon after the Fe-deficient conditions are imposed (Puig et al., 2008). Thus, Cth1 and Cth2 may function as a cellular rheostat in the adaptation to varying changes in Fe-availability. The initial transient expression of Cth1 may be sufficient for adaptation to mild or transient Fe-deficiency by targeting mitochondrial functions. If the Fe-deficiency worsens, Cth2 is robustly expressed providing a means for widespread metabolic reprogramming that would promote a shift from highly Fe-dependent metabolism to Fe-independent alternative pathways. Visual inspection of the *CTH1* and *CTH2* 3'UTRs reveals the presence of putative ARE-sequences, and strains in which the *CTH1* gene has been deleted accumulate elevated steady-state levels of *CTH2* mRNA (Thompson et al., 1996). These observations raise the possibility that the *CTH1* and *CTH2* transcripts may be themselves subject to ARE-dependent regulation by the Cth1 and Cth2 proteins, creating an auto- and trans-regulatory circuit perhaps accounting for differences in their expression. Interestingly, an auto-regulatory mechanism has been described for TTP (Brooks et al., 2004; Tchen et al., 2004); in THP-1 myelocytic cells and in HeLa cells, TTP protein binds ARE-sequences within its own 3'-UTR fused to reporter constructs accelerating their rate of decay. It is noteworthy that

the remaining human $CX_8CX_5CX_3H$-family members, BRF1 and BRF2, also harbor ARE-sequences in their 3'-UTR, perhaps suggesting that this mechanism of auto- and trans-regulation among family members is well conserved across species (Brooks et al., 2004; Tchen et al., 2004).

Excess cellular Fe catalyzes the formation of highly reactive hydroxyl radicals that can irreparably damage macromolecules. To date, no Fe-detoxification mechanisms have been identified in yeast. Consequently, intracellular Fe-concentrations must be tightly regulated at the level of Fe-acquisition, allocation, and storage (Van Ho et al., 2002). In particular, mechanisms must exist to deal with sudden increases in Fe-levels in order to rapidly repress Fe-regulon functions to prevent Fe-induced cellular damage. Regulation would be particularly important if a sudden elevation in Fe-concentration occurs following a period of severe starvation, in which metabolism has been modified for lower Fe demand. Indeed, in response to high Fe conditions yeast activates various molecular strategies to prevent the hyper-accumulation of intracellular Fe and thus protect itself from the damaging effects of elevated Fe concentrations; first, the rapid nuclear export of Aft1 in the presence of increased intracellular Fe prevents ectopic expression of the Fe-regulon; second, the high affinity Fe-transport system Fet3/Ftr1 is targeted for rapid ubiquitin-dependent degradation to prevent Fe uptake (Felice et al., 2005); third, the transcription factor Yap5 activates the expression of the *CCC1* gene, encoding a vacuolar Fe-transporter in order to increase Fe storage (Li et al., 2008); and

fourth, mRNAs encoding several members of the Fe-regulon are cleaved by the RNase III endonuclease Rnt1, followed by their exonucleolytic digestion by 5′→3′ exonucleases (Lee et al., 2005). Moreover, strains expressing a constitutive active Aft1, a deletion in Yap5, or a deletion in Rnt1 are unable to grow in medium containing high concentrations of Fe (Felice et al., 2005; Lee et al., 2005; Li et al., 2008; Philpott et al., 1998).

Here we demonstrate that Cth1 and Cth2 proteins auto- and trans-regulate their expression in an ARE-dependent manner at the level of mRNA stability, and preliminary data suggest a possible role for ARE-dependent regulation of Cth1 and Cth2 translation. Moreover, we hypothesize that Cth1 and Cth2 auto- and trans-regulation are not only important for the transition from high-to-low Fe conditions, but also in the re-adaptation from low-to-high Fe conditions. In addition, our data support an ARE-independent mechanism of regulation of *CTH2* mRNA in response to elevated Fe concentrations.

3.2 Materials and methods

Protein analyses

cth1Δcth2Δ cells were co-transformed with pRS416-*2xFLAG-CTH1* and pRS415-*CTH2*; or, pRS416-*2xFLAG-CTH1* and pRS415; or, pRS416-*2xFLAG-CTH1-AREmutant* and pRS415-*CTH2-AREmutant*. Cells were also co-transformed with pRS415-*2xFLAG-CTH2* and pRS416-*CTH;* or, pRS415-*2xFLAG-CTH2* and pRS416; or, pRS415-*2xFLAG-*

CTH2-AREmutant and pRS416-*CTH1-AREmutant.* Overnight cultures were re-inoculated to A_{600} = 0.05 in SC-Ura-Leu and allowed to grow to A_{600} = 0.10, at which point 100μM BPS (bathophenanthroline disulfonate) was added, and began time course at the indicated times. For re-addition of Fe experiments, cultures were incubated with BPS for 6hr, cells harvested by centrifugation and washed three times with H_2O. Cell pellet re-suspended in 5-mL H_2O and added to medium containing 300μM FAS (Ferrous Ammonium Sulfate) and took samples at the indicated times. Total protein was extracted using the Triton-X 100/glass bead method, and 50 μg of total protein resolved in a 12% SDS-PAGE ReadyGels (BioRad) and transferred onto a nitrocellulose membranes. Flag-Cth1 and Flag-Cth2 fusion proteins were detected using an HRP-conjugated α-Flag anti-body from Sigma. An α-Pgk1 antibody (Molecular Probes) was used as loading control. Chemiluminescence substrates from Pierce were used for the detection of the HRP-conjugated anti-bodies.

RNA Blot Analysis

Cells were grown in SC lacking specific requirements to exponential phase in the presence of either 300 μM FAS (Fe +) or 100 μM BPS (Fe -). Total yeast RNA was extracted by either a modified hot phenol method or the glass-beads method. PCR amplified DNA fragments were gel-purified and radiolabeled with ^{32}P-dCTP using random primers (invitrogen) and used as probes. *ACT1* was always used as loading control. For time course experiments, cells were grown as described under Protein

analyses, and total RNA extraction and RNA blotting analysis as described above.

Yeast strains, yeast three-hybrid, and plasmids

The *cth1Δcth2Δ* strain has been previously described (Puig et al., 2005 and 2008). The Yeast three hybrid experiment was carried out as described in Puig et al., 2005. Plasmids containing the *CTH2* and *CTH2-C190R* constructs have been previously described (Puig et al., 2005). The overlap extension method was used to create the *CTH2p-CTH1* fusion construct, and to mutagenize the Cth1 cysteine residue 225 to arginine. Both *CTH2p-CTH1* and *CTH2p-CTH1-C225R* constructs were cloned into the pRS416 vector. Wild type *CTH1* and the *CTH1*-C225R allele were fused to the Gal4 activation domain in the pACT2 vector. *CTH1*, *CTH2* and *CTH2-AREmt* 3′-UTR sequences shown in Figure 11H were cloned into pIIIA/MS2-1 vector. All plasmids were verified by sequencing.

3.3 Results

3.3.1. Cth1/2 regulate *CTH1* and *CTH2* mRNA levels

Expression of the *CTH1* and *CTH2* genes is activated by the Fe-responsive transcription factors Aft1 and Aft2 in response to Fe-limitation (Puig et al., 2005 and 2008). However, while expression of the Flag-Cth2 fusion increases gradually over time during Fe-deficiency (Figure 11B), Flag-Cth1 is expressed rapidly and transiently after Fe-limitation conditions are imposed (Figure 11A). Previous microarray analyses of isogenic wild-type and *cth2Δ* cells grown under Fe-limiting conditions demonstrated

that *CTH1* mRNA levels are higher in *cth2Δ* mutants than in wild-type cells (Puig et al., 2005). We have validated these results by RNA blotting from *cth2Δ* cells in which wild type *CTH2*, the non-functional allele *CTH2-C190R* or an empty vector have been re-introduced. As shown in Figure 11C, there is no apparent change in steady state *CTH1* mRNA levels in response to low Fe in *cth2Δ* cells expressing the plasmid-borne wild type *CTH2*. However, *CTH1* mRNA levels increase noticeably upon Fe-starvation in cells that harbor the empty vector or in cells that express the non-functional allele *CTH2-C190R*. Early studies also determined that deletion of *CTH1* or mutations within its TZF domain caused a 3-fold average higher expression of *CTH2* mRNA (Thompson et al., 1996). Interestingly, the mRNA steady-state levels from non-functional alleles are elevated in comparison to the corresponding wild-type alleles. As shown in Figure 11D, *cth1Δcth2Δ* cells accumulate elevated levels of mRNA expressed from the non-functional *CTH1-C225R* allele compared to the wild type *CTH1* mRNA. Similarly, mRNA expression of the *CTH2-C190R* allele is elevated compared to *CTH2* wild-type. Visual inspection of the 3'-UTR of *CTH1* region revealed the presence putative ARE sequences starting at nucleotides 53, 80 and 159, and within the *CTH2* 3'-UTR starting at nucleotide 46 after the translation stop (Figure 11F). These observations raised the possibility that *CTH1* and *CTH2* mRNAs might be themselves under the post-transcriptional control of Cth1 and Cth2. To explore this possibility, we used the yeast three-hybrid system (Sengupta et al., 1996) as a surrogate method for RNA binding to test the ability of Cth1

and Cth2 to interact with the *CTH1* and *CTH2* mRNAs. Wild type and mutant DNA fragments corresponding to the ARE-containing 3'UTRs of *CTH1* and *CTH2* were fused to bacteriophage MS2 mRNA and co-expressed in a reporter yeast strain with a Cth1- or Cth2-Gal4 trans-activation domain fusion protein. A positive interaction induces the expression of the *HIS3* reporter gene, and therefore, they are monitored by growth of on medium lacking histide (Figure 11G; Sengupta et al., 1996). As shown in Figure 11H, both Cth1 and Cth2 proteins interact the 3'-UTRs of both the *CTH1* and *CTH2* mRNAs. Mutations in the Cth1 or Cth2 TZFs (Cth1-C225R and Cth2-C190R) abrogated protein-mRNA interactions as evidenced by the inability of the co-transformed cells to grow in the absence of histidine. Furthermore, mutagenesis of the putative ARE-sequence within the *CTH2*-3'-UTR (*CTH2-AREm*) also abrogated interactions with the Cth1 and Cth2 proteins. Co-expression of empty vectors with Cth1/Cth2-Gal4 trans-activators, or 3'UTR-containing constructs were used as negative controls and accordingly showed no growth in the absence of histidine, but grew normally if histidine was supplemented. Similary, cells co-expressing the Iron Responsive Protein (IRP) and Iron Responsive Element (IRE) were used as controls for positive protein-mRNA interaction (Figure 11H). Taken together, these results suggest that Cth1 and Cth2 proteins specifically bind ARE-sequences within 3'-UTRs of *CTH1* and *CTH2* mRNAs in a manner that is dependent on the integrity of the RNA-binding motif and the ARE-sequences found in their respective 3'-UTR sequences.

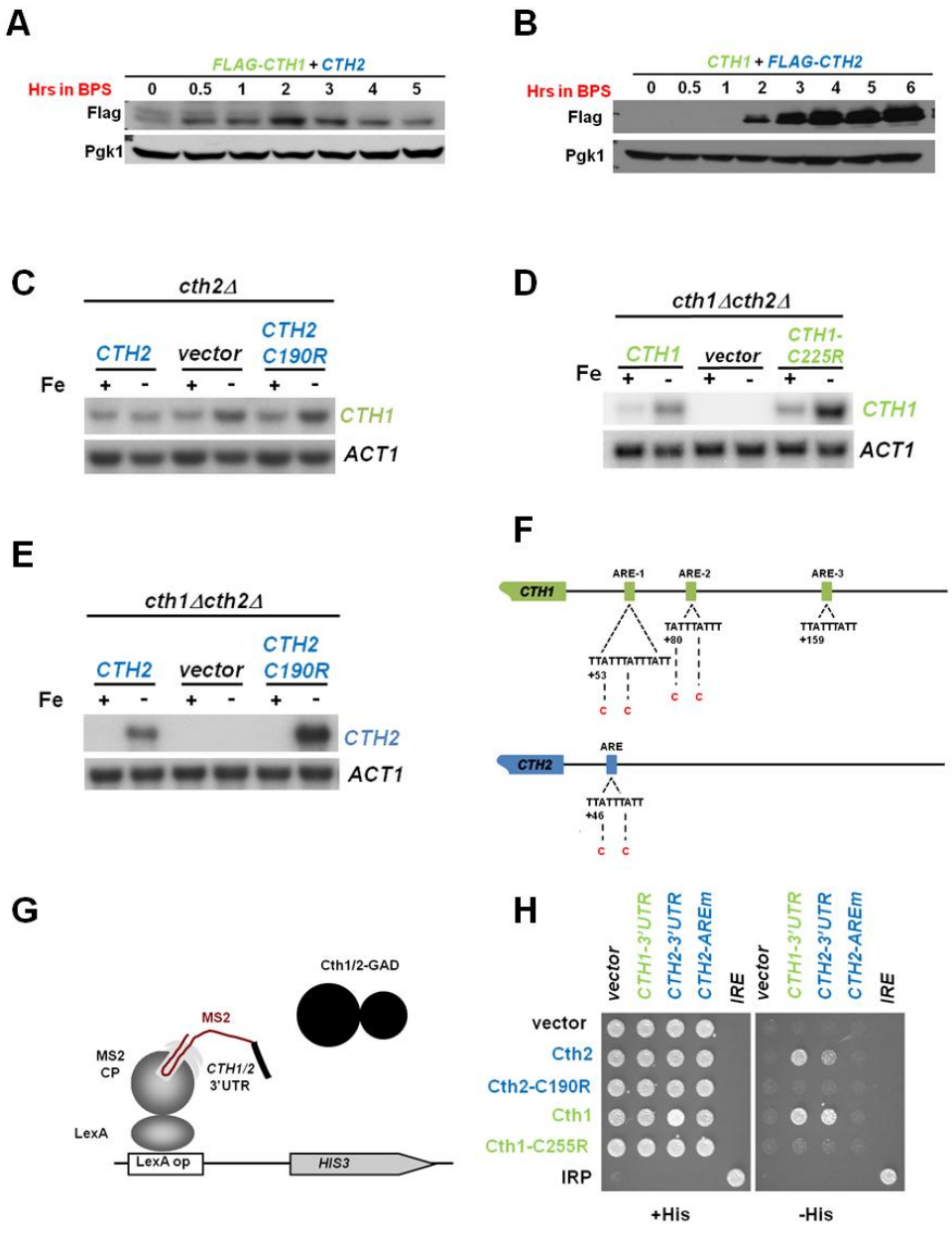

Figure 11. Cth1 and Cth2 proteins affect *CTH1* and *CTH2* mRNAs steady state levels

A. Flag-Cth1 is transiently expressed in response to Fe-deficiency. *cth1Δcth2Δ* cells transformed with pRS416-2*xFLAG-CTH1* and pRS415-*CTH2* were grown in SC-Ura-Leu supplemented with 100μM BPS to induce Fe-deficient conditions. Samples were taken at the indicated times, total protein extracted and

analyzed by immunoblotting using an HRP-conjugated anti-Flag antibody; **B.** Flag-Cth2 expression increases gradually overtime during Fe-deficiency. *cth1Δcth2Δ* cells transformed with pRS415-*2xFLAG-CTH2* and pRS416-*CTH1*were treated as in (**A)**; **C. and E.** *CTH1* and *CTH2* mRNA levels are elevated in the absence of a functional allele of Cth2. *cth2Δ* and c*th1Δcth2Δ* cells transformed with pRS416-*CTH2*, pRS416, or pRS416-*CTH2-C190R* were grown in (Fe +) or (Fe -) conditions to exponential phase, total RNA was extracted and analyzed by RNA blotting using *CTH1* and *CTH2* probes. *ACT1* was used as a loading control; **D.** *CTH1* mRNA levels are elevated in the absence of a functional allele of Cth1. c*th1Δcth2Δ* cells transformed with pRS416-*CTH1*, pRS416, or pRS416-*CTH1-C225R* were treated as in (**C)**; **F.** Representation of the 3′-UTR of *CTH1* and *CTH2*. Putative ARE sequences are shown and point mutations introduced to disrupt the AREs are represented in red; **G.** Schematic representation of the Yeast three-hybrid assay used to monitor *in vivo* interactions between Cth1 and Cth2 proteins with *CTH1* and *CTH2* mRNAs; **H.** L40-coat cells were co-transformed with (1) pIIIA/MS2-1 vector alone or containing the 3′-UTR of *CTH1, CTH2, CTH2-AREmt,* and the iron-responsive element (IRE) as positive control, and (2) pACT2 vector alone or fused to *CTH2*, *CTH2-C190R, CTH1, CTH1-C225R* and the iron responsive protein (IRP) as a positive control. Cells were grown on SC-Ura-Leu (+His) and SC-Ura-Leu-His (-His) plates for 7 to10 days at 30°C

3.3.2. *CTH1/2* -AREs promote instability to a reporter transcript

We ascertained whether the ARE-sequences within the *CTH1* and *CTH2* 3′-UTRs could function as *bona fide* mRNA destabilizing elements. We created chimeric transcripts containing the *GCN4* open reading frame fused to the 3′UTR of *GCN4* as negative control, and the ARE-containing 3′-UTRs of *CTH1, CTH2* or *CTH2* in which two mutations have been introduced within the ARE sequence (*CTH2-AREmt*) (Figure 12A). The chimeric fusions were expressed in *gcn4Δ* cells and their steady-state levels analyzed by RNA blotting hybridized with a *GCN4* DNA probe (Figure 12B). As demonstrated in Figure 12B, the steady-state levels of *GCN4* mRNA did not significantly change in response to Fe-concentrations, while *GCN4-CTH1* and *GCN4-CTH2* mRNA levels were dramatically decreased under Fe-deprivation. Importantly, mutagenesis of the ARE within the *CTH2* 3′-UTR (*CTH2*-mt) abrogated the Fe deficiency-dependent down-regulation of the *GCN4-CTH2mt* chimeric transcript (Figure 12B). In addition, the down-

regulation of both *GCN4-CTH1-3'UTR* and *GCN4-CTH2-3'UTR* transcripts was dependent on the presence of functional Cth1 and Cth2 proteins (Figure 12C and 12D). *cth1Δcth2Δgcn4Δ* cells expressing either *GCN4-CTH1-3'UTR* or *GCN4-CTH2-3'UTR* chimeras were co-transformed with wild type Cth1, vector alone, or the non-functional Cth1-C225R allele as shown in Figure 2C, or with wild-type Cth2, empty vector, or the Cth2-C190R allele (Figure 12D). Iron starvation-dependent degradation of the *GCN4-CTH1-3'UTR* or *GCN4-CTH2-3'UTR* constructs was eliminated in cells co-transformed with empty vectors or with non-functional alleles of Cth1 and Cth2 (Figure 12C and 12D). Together, these data suggest a model where Cth1 and Cth2 can recognize and bind to ARE-sequences within their own mRNAs engaging in a post-transcriptional trans- and auto-regulatory circuit that limits their expression (Figure 13A).

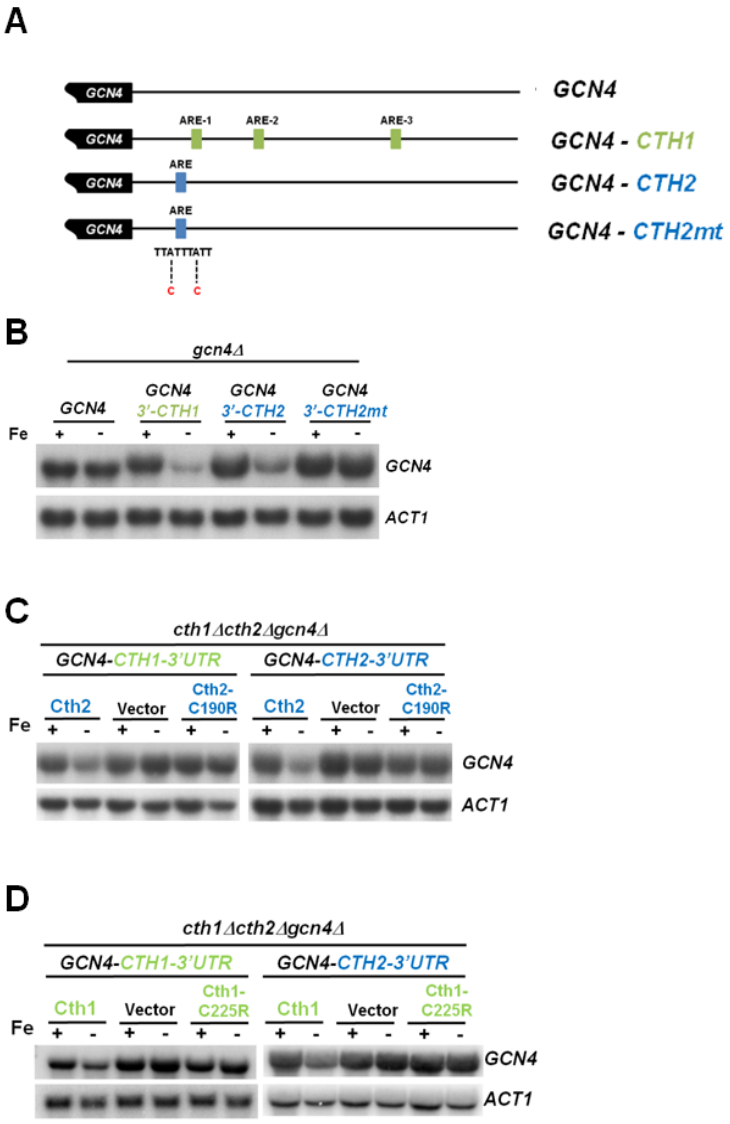

Figure 12. The 3'-UTRs of *CTH2* and *CTH2* confer Fe deficiency-dependent instability to a reporter strain

A. Schematic representation of wild-type *GCN4* and *GCN4* whose 3′-UTR has been replaced by the *CTH1*-3′-UTR (*GCN4-CTH1)*, *CTH2*-3′-UTR (*GCN4-CTH2),* and the mutant *CTH2*-3′-UTRmt (*GCN4-CTH2mt).* Specific mutations are shown in red; **B.** *gcn4Δ* cells expressing *GCN4*, *GCN4-3′-CTH1*, *GCN4-3′-CTH2* and *GCN4-3′-CTH2mt* were grown in (Fe +) or (Fe -), and analyzed by RNA blotting with *GCN4* and *ACT1* probes; **C.** *cth1Δcth2Δgcn4Δ* cells expressing either *GCN4-3′-CTH1* or *GCN4-3′-CTH2* were transformed with pRS416-*CTH2*, pRS416, or pRS416-*CTH2-C190R*. Cells were grown and analyzed as described in (**B**); **D.** *cth1Δcth2Δgcn4Δ* cells expressing either *GCN4-3′-CTH1* or *GCN4-3′-CTH2* were transformed with pRS416-*CTH1*, or pRS416, or pRS416-*CTH1-C225R* constructs under the regulation of the *CTH2* promoter. Cells were grown and analyzed as described in (**B**).

3.3.3. Cth1 and Cth2 auto- and trans-regulation during Fe-deficiency

Immunoblotting experiments from cells grown under Fe-limitation demonstrate that Flag-Cth1 reaches maximum levels of expression approximately 2hr after Fe-deficient conditions are induced, and slowly begin to decline to near basal levels by 5hr (Figure 14A). To establish the role of trans-regulation on Cth1 expression during Fe-limitation, we analyzed the expression of Flag-Cth1 in the absence of Cth2 (Figure 13B), or Flag-Cth1 from a construct containing mutations within its ARE sequences to address the combined auto- and trans-regulatory effects (Figure 13C).

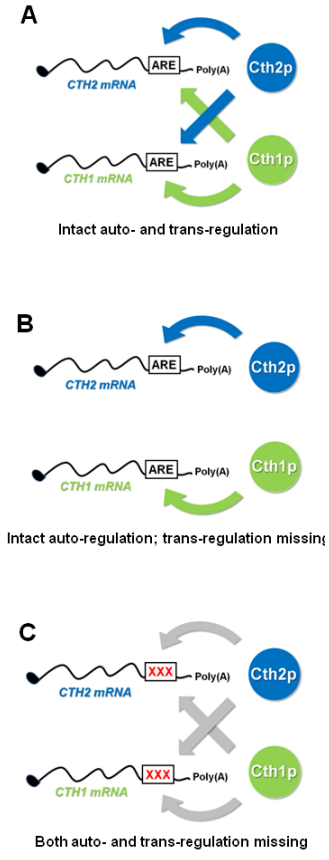

Figure 13. Cth1 and Cth2 auto- and trans-regulate their own expression

A. Cells expressing Cth1 and Cth2 have intact auto- and trans-regulation between them; **B.** Cells expressing only one of the paralogous proteins have intact auto-regulatory capabilities, but lack trans-regulation; **C.** Cells expressing *CTH1* and *CTH2*with mutant ARE sequences experience neither auto- nor trans-regulation. In all three cases, Cth1 and Cth2 proteins are functional.

As observed in Figure 14B, initial steady-state levels of Flag-Cth1 are elevated in the absence of Cth2, and remain highly expressed over the 5hr period of the experiment suggesting a major role for Cth2 trans-regulation of Cth1. In addition, Figure 14C demonstrates that disruption of both auto- and trans-regulation of *FLAG-CTH1* by mutagenesis of its AREs leads to increased levels of Flag-Cth1protein even before Fe-deficient conditions are induced and levels remain elevated after 5hr of growth under Fe-limitation. These observations suggest that auto- and trans-regulation have an additive effect on the control of Flag-Cth1 expression levels even in cells grown in Fe-containing medium. Contraire to Cth1, auto- and trans-regulation appear to have only a small effect on the expression of Flag-Cth2 following the induction of Fe-starvation. As shown in Figure 14E, a slight delay (from 2hr to 3hr) in the detection of Flag-Cth2 is observed in the absence of *CTH1* during Fe-deficiency. A possible explanation for this observation may be that the absence of trans-regulation of the *FLAG-CTH2* mRNA by Cth1 might lead to increased auto-regulation, and therefore a slight delay in Flag-Cth2 expression (Figure 14E). Indeed, no defect in Flag-Cth2 expression is detected from the *FLAG-CTH2-AREm* and *CTH1-ARE12m* co-expressing cells (Figure 14F) suggesting that loss of both auto- and trans-regulation has no major effect on the expression of Flag-Cth2 during Fe-deficiency. Together, these observations indicate that auto- and trans-

regulation controls the transient expression of Cth1, while having little effect on Cth2 expression.

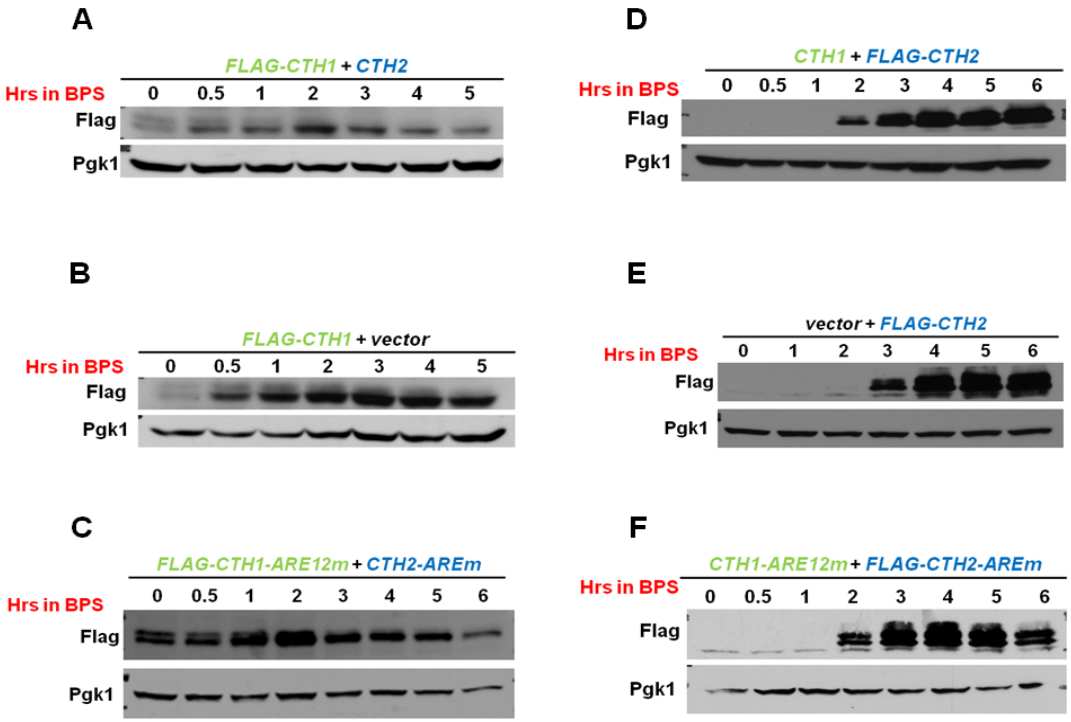

Figure 14. Cth2 strongly trans-regulates Cth1 expression

A – C. *cth1Δcth2Δ* cells were co-transformed with pRS416-2*xFLAG-CTH1* and pRS415-*CTH2* **(A)**; pRS416-2*xFLAG-CTH1* and pRS415 **(B)**; pRS416-2*xFLAG-CTH1-AREmutant* and pRS415-*CTH2-AREmutant* **(C)** and cells were grown and treated as in (**Figure 1A**); **A.** Flag-Cth1 is expressed transiently in response to Fe-deficiency. **B.** Flag-Cth1 steady state levels are higher and transient expression is lost during Fe-deficiency in the absence of *CTH2*. **C.** Mutations within the ARE-sequences causes increased Flag-Cth1 basal levels. **D – F.** Cells were also co-transformed with pRS415-2*xFLAG-CTH2* and pRS416-*CTH* **(D)**; pRS415-2*xFLAG-CTH2* and pRS416 **(E)**; pRS415-2*xFLAG-CTH2-AREmutant* and pRS416-*CTH1-AREmutant* **(F)**. **D.** Expression of Flag-Cth2 increases gradually during Fe-deficiency in the presence of *CTH1*. **E.** In contrast, in the absence of *CTH1*, Flag-Cth2 expression is briefly delayed (~1hr); **F.** Mutations introduced within the ARE-sequences of the mRNA coding for Flag-Cth2 have no effect in protein levels.

3.3.4. Auto- and trans-regulation upon re-exposure to high Fe-levels

Microarray studies demonstrated that while Cth2 has a large set of putative target mRNAs encoding proteins involved in highly Fe-demanding processes, Cth1

appears to preferentially regulate only about 14% of the targets of Cth2, and an even smaller additional group of 7 unique mRNAs (Puig et a., 2008). Thus, Cth2 function is likely to have a greater effect on the metabolic reprogramming of the cell in response to Fe-deficiency compared to Cth1 due the large number of mRNAs it targets for degradation. We hypothesized that severely Fe-starved cells need to rapidly shutoff Cth2 activity if a sudden increase in extracellular Fe occurs in order to restore Fe-dependent pathways and storage mechanisms to avoid Fe-induced damage. To test this hypothesis, *cth1Δcth2Δ* cells co-transformed with *FLAG-CTH2* and *CTH1* were Fe-starved for 6hr and exposed to 300uM Ferrous Ammonium Sulfate (FAS), and samples were collected every five minutes for Immunoblotting analysis of Flag-Cth2. As shown in Figure 15A, Flag-Cth2 levels were dramatically reduced 10m after exposure to Fe, indicating that expression of Flag-Cth2 is rapidly inhibited in response to exogenous Fe. Thus, we ascertained whether auto- and trans-regulation of Cth1 and Cth2 proteins was important for Fe-starved cells to re-adapt to growth under Fe-sufficient conditions. Figure 15B shows that in the absence of the trans-regulatory activity of Cth1, the Flag-Cth2 fusion is still detectable 15m post-exposure to exogenous Fe, and Flag-Cth2 expressed from the *FLAG-CTH2-AREm* construct is detected as late as 25m after Fe re-addition (Figure 15C) indicating that both auto- and trans-regulation contribute to the rapid decrease in Flag-Cth2 expression in response to high Fe. Whether high-Fe conditions induce any changes in the expression of Cth1 has yet to be determined.

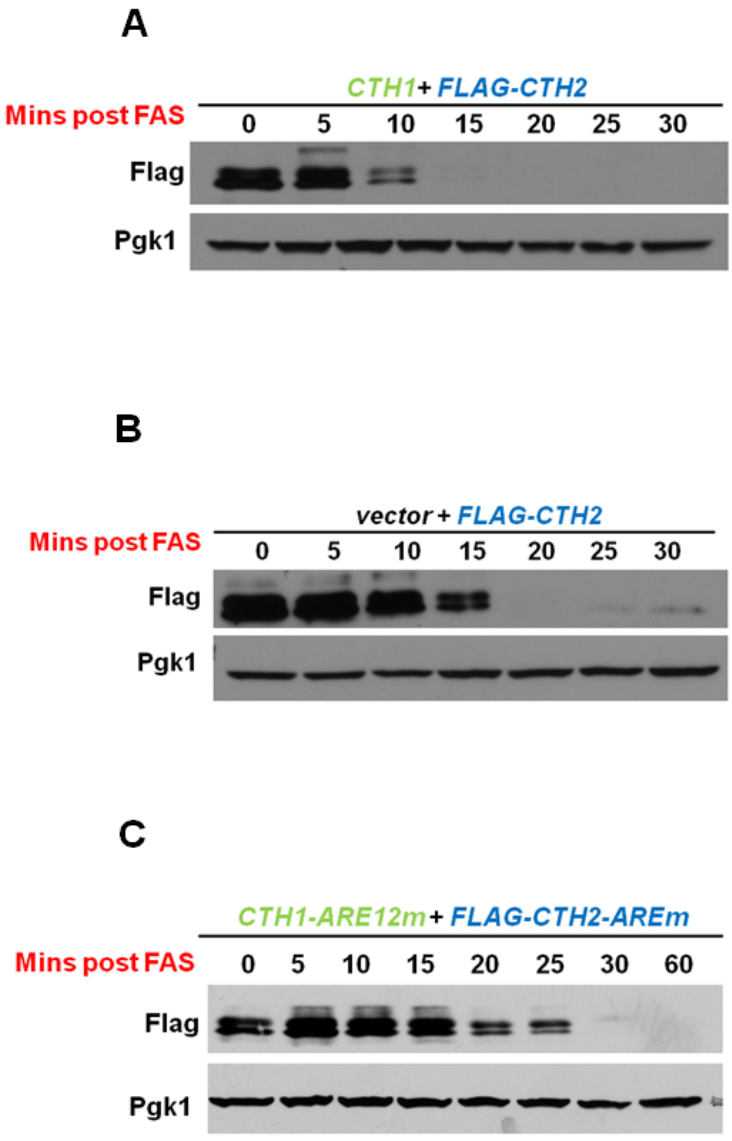

Figure 15. Auto/trans-regulation repress Cth2 expression in response to high Fe

Cells described in Figure 4D-F were grown in (Fe-) conditions for 6hr prior to re-addition of Fe. Cells were washed with water, resuspended in medium containing 300μM FAS and samples were taken at indicated times for protein extraction and immunoblotting. **A.** Flag-Cth2 expression rapidly decreases and it is no longer detectable 15mins after re-addition of Fe; **B.** Flag-Cth2 expression remains detectable at 15min in the absence of *CTH1* and at 25min in cells expressing ARE-mutant alleles of *FLAG-CTH2-AREm* and *CTH1-ARE* **(C)**.

3.3.5. Cth1/2 auto- and trans-regulation is ARE- dependent but AMD-independent

Together, our observations indicate that Cth1 and Cth2 can bind ARE-sequences within the 3'UTRs of the *CTH1* and *CTH2* mRNAs, which in turn promotes their destabilization leading to a mechanism of auto- and trans-regulation (Figures 11-13). Our data also suggest that auto- and trans-regulation are important for maintenance of steady state levels and transient expression of Cth1 during Fe-deficiency and for re-adaptation to high-Fe conditions of pre-starved cells by promoting the rapid decrease in Cth2 expression. In order to ascertain whether the auto- and trans-regulation between Cth1 and Cth2 is due to ARE-mediated mRNA decay, we analyzed the steady-state levels of the *CTH1* and *CTH2* transcripts from cells treated under the same conditions as in Figures 4 and 5. RNA blotting analyses demonstrated that *CTH1* mRNA levels do not reflect the transient pattern of expression of Cth1 protein observed in response to Fe-deficiency (Figure 16A), and *CTH1* mRNA does not hyper-accumulate in the absence of Cth2 as does Flag-Cth1 (Figure 16B, *top*). In addition, *CTH1-ARE12m* mRNA levels are also in disagreement with our Immunoblotting data, which shows increased Cth1 protein levels even prior to Fe-limitation conditions are induced (Figure 16C). Expression of *CTH2* mRNA, however, does reflect the graded increase in expression of Cth2 protein in the presence or absence of Cth1 (Figure 16A and 11B, *bottom*), as does the *CTH2-AREm* construct (Figure 16C). We analyzed expression of *CCP1*, an mRNA target

of both Cth1 and Cth2, as a biological marker for Fe-availability, and *ACT1* as loading control.

Analysis of *CTH2* in response to high-Fe conditions revealed a rapid decrease in *CTH2* mRNA within 10min of Fe exposure (Figure 16D). However, this rapid decrease in *CTH2* transcript does not appear to involve the activity of Cth1 and Cth2 activities, or the ARE-sequence (Figure 16E and 16F) indicating that ARE-dependent regulation of Flag-Cth2 is not due to changes in mRNA transcript stability and suggest an alternative ARE-independent mechanism for *CTH2* mRNA degradation in response to high Fe conditions.

Altogether, our data suggest an Fe-dependent mechanism of auto- and trans-regulation that controls Cth1 and Cth2 protein expression that is, contrary to our predictions, largely independent on their AMD-promoting activity and likely suggest a role for ARE-mediated regulation of translation by Cth1 and Cth2. In addition, the rapid decrease in *CTH2* mRNA in response to high-Fe following severe Fe-starvation suggests an ARE-independent degradation mechanism of *CTH2* mRNA.

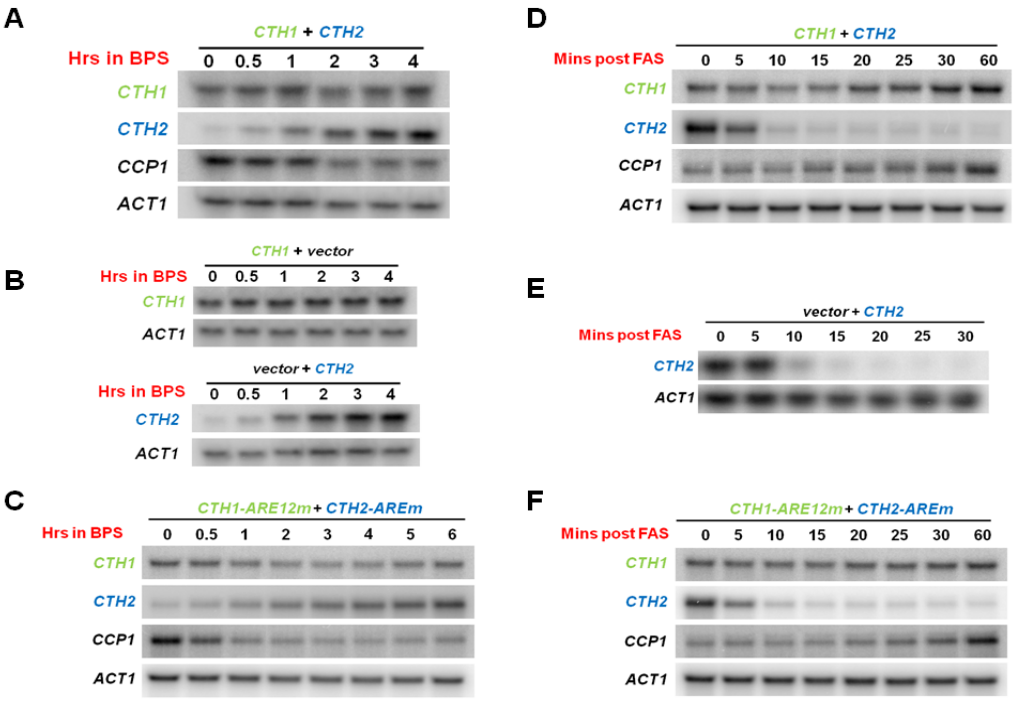

Figure 16. Auto/trans-regulation by Cth1 and Cth2 is largely independent of AMD

A – F. *CTH1* and *CTH2* mRNA expression is unaffected by disruption of auto- and trans-regulation. Total RNA extracted from cells described in Figure 4 was analyzed by RNA blotting using *CTH1*and *CTH2* probes. *CCP1* was used as biological marker of Fe-status, and *ACT1* was used as a loading control.

3.4. Discussion

Iron is an essential micronutrient for virtually all organisms; yet, Fe can be highly toxic when present in excess. As a consequence, organisms have evolved sophisticated strategies to maintain appropriate cellular Fe levels, while avoiding Fe toxicity. Cells growing in Fe-limitation not only activate mechanisms that allow them to increase cytosolic Fe concentrations, but also to prioritize the utilization of limited Fe in order to meet their metabolic demands (Puig et al., 2008; Shakoury-Elizeh et al., 2004; Vergara

and Thiele, 2008). One of such mechanisms in yeast is mediated by Cth1 and Cth2, two proteins belonging to the highly conserved $CX_8CX_5CX_3H$-family of mRNA destabilizing proteins that includes TTP, Brf1 and Brf2 (Ma and Herschman, 1995; Thompson et al., 1996). In response to Fe-deficiency, Cth1 and Cth2 promote the accelerated decay of select groups of mRNAs encoding proteins involved in highly Fe-dependent biochemical processes (Puig et al., 2005; Puig et al., 2008) that results in a genome-wide remodeling of cellular metabolism in response to Fe-deprivation that enables the cell to prioritize utilization of the available Fe. Our data revealed that a Flag-Cth1 fusion protein is expressed rapidly and transiently, reaching the highest levels of expression by 2hr of the imposed Fe-limitation. On the contrary, a Flag-Cth2 fusion becomes detectable only after approximately 2hr of Fe-starvation and it remains highly expressed over the six-hour period of the experiment (Puig et al., 2008; Figure 11A). These differences in expression suggest a role for Cth1 in the early stages of Fe-limitation and a role for Cth2 in the late, and consequently more severe, stages of Fe-starvation.

Observations described here indicate that *CTH1* and *CTH2* mRNAs are themselves regulated post-transcriptionally by Cth1 and Cth2 creating an auto- and trans-regulatory loop important in the transition from high-to-low Fe conditions. Immunoblotting analyses of Fe-deficient cells expressing Flag-Cth1 in the presence or absence of Cth2 indicate that trans-regulation by Cth2 plays a major role in the transient expression of Cth1, while auto-regulation controls its basal levels and its rate of

induction (Figure 14A-C). RNA blotting analyses, however, do not reflect our Immunoblotting data on Flag-Cth1 expression (Figure 16A and B). While this remains to be fully explored, there are at least two possible explanations for this discrepancy: first, studies have demonstrated that the transcription factor Hsf1 activates the transient expression of *CTH1* within 5 minutes of heat-exposure and by 30 minutes, *CTH1* mRNA levels are almost indistinguishable from those prior to heat-exposure (Hahn et al., 2004). Thus, it is possible that a transient elevation of *CTH1* mRNA occurs within 30 minutes of Fe-limitation, which we would have missed under our experimental conditions (Figure 16A-C). Experiments are under way to test this hypothesis; second, microarray studies demonstrated that several mRNAs encoding proteins involved in the regulation of translation are down-regulated under Fe-deficient conditions in a Cth1- and Cth2-dependent manner (Puig et al., 2008). Therefore, Cth1 and Cth2 could potentially regulate their own translation indirectly through the down-regulation of mRNAs encoding proteins involved in translation regulation. Whether or not $CX_8CX_5CX_3$-proteins play a direct role in translation is not fully understood. However, it is noteworthy that sucrose density-gradient experiments demonstrated that human TTP fractionates with polysomes (Brooks et al., 2002). Thus, Cth1 and Cth2 might play a direct role in translation regulation.

Immunoblotting analyses of Flag-Cth2 from cells expressing Cth1 or an empty vector suggest that Cth1 has little effect on the regulation of Cth2 expression during Fe-

deficiency (Figure 14D-F). However, careful quantification analyses are necessary to determine whether or not auto- and trans-regulation affect overall Cth2 protein levels during Fe-deficiency, which would be difficult to identify by simple visualization of immunoblotting data.

Iron-deprived cells shift their metabolism away from highly Fe-dependent processes to alternative Fe-independent pathways (Shakoury-Elizeh et al., 2004; Vergara and Thiele, 2008). Thus, a sudden increase in extracellular Fe concentrations can be potentially harmful to the cell if Fe-dependent processes and storage mechanisms are not rapidly restored. Our data suggest a role for Cth1 and Cth2 auto- and trans-regulation in the cellular re-adaptation from low-to-high Fe conditions. Analyses of Fe-deprived cells show a dramatic reduction in Flag-Cth2 expression 10 minutes after re-exposure to high Fe (Figure 15A). Although transcription of the *CTH2* gene is likely to cease immediately after exposure to Fe (due to the Fe-induced export of the transcription factor Aft1), the observation that Flag-Cth2 remains detectable 15 and 25 minutes after Fe-exposure in the absence of *CTH1*, or when expressed from the *FLAG-CTH2-AREm* construct, respectively, indicate that lack of transcription alone is not responsible for the rapid decrease in Flag-Cth2 expression (Figure 15B and 15C), and suggest a role for auto- and trans-regulation of Flag-Cth2 under these conditions. Surprisingly, RNA blotting analyses reveal that the *CTH2* mRNA is nearly undetectable within 10 minutes of Fe-exposure independently of auto- and trans-regulation (Figure 16D-F). These results

indicate that Flag-Cth2 protein expression is regulated in an ARE-dependent manner but not as a result of ARE-mediated mRNA decay by Cth1 and Cth2.

Studies have demonstrated that in response to high Fe levels, several mRNAs encoding members of the Fe-regulon are cleaved by the RNase III endonuclease Rnt1 and their decay mediated by the 5′→3′ Rat1 exonuclease (Lee et al., 2005). Interestingly, microarray experiments revealed that cells in which *RNT1* has been deleted express elevated levels of *CTH2* mRNA (Lee et al., 2005). In addition, strains containing a deletion of the nuclear exosome component *RRP6* or strains expressing a thermo-sensitive allele of the 5′→3′ Rat1 exonuclease (*rat1-2*) also accumulate *CTH2* mRNA levels (Ciais et al., 2008). Thus, it is possible that degradation of *CTH2* mRNA in response to high Fe exposure following growth under Fe-starvation conditions is rapidly accomplished (<10 min) by promoting its nuclear decay in a mechanism involving both nuclear mRNA degradation pathways.

Taken together, the observations described here support a mechanism of auto- and trans-regulation that controls the expression of Cth1 and Cth2 during the transitions from high-to-low Fe conditions, and during cellular re-adaptation from low-to-high Fe conditions. Furthermore, preliminary observations suggest an ARE-independent mechanism regulating *CTH2* transcript stability in response to high Fe concentrations. Experiments are currently under way to establish the importance of the mechanisms of

auto- and trans-regulation between Cth1 and Cth2, as well as the ARE-independent *CTH2* mRNA degradation pathway in response to elevated Fe-levels.

4. Early recruitment of ARE-containing mRNAs determines their cytosolic fate during iron deficiency.

4.1 Introduction

Iron participates in numerous biochemical processes of which many, but not all, are essential. Thus, under conditions of Fe-scarcity cells must ensure the appropriate allocation of Fe in order to meet essential metabolic needs, while lowering its incorporation into proteins that participate in non-essential processes, or proteins involved in metabolic pathways for which there are alternative salvage mechanisms (Shakoury-Elizeh et al, 2004; Puig et al., 2008; Vergara and Thiele, 2008). The yeast protein Cth2, and to a lesser degree Cth1, play a pivotal role in the cellular adaptation to Fe-limitation by post-transcriptionally regulating Fe-metabolism, which in turn allows the prioritization of Fe utilization. Cells that fail to prioritize Fe consumption present growth defects under limited Fe conditions (Puig et al., 2005; Puig et al., 2008).

Cth1 and Cth2 belong to the TTP (Tristetraprolin) family of mRNA-destabilizing proteins. Members of this family are characterized by an RNA-binding motif consisting of two tandem zinc-fingers (TZFs) of the $CX_8CX_5CX_3H$ type, which directly interact with AU-rich elements (AREs) within the 3'-untranslated region (3'UTR) of select groups of mRNAs (Carballo et al., 1998, 2000; Stoecklin et al., 2002; Stoecklin et al., 2001) This interaction leads to the rapid destabilization of the bound transcript in a process termed ARE-mediated mRNA decay, or AMD. In response to mitogenic stimulation, mammalian TTP promotes AMD of the TNF-α and GM-CSF mRNAs in the cytosol by

inducing poly-A tail removal, followed by decapping and mRNA decay from both 5′→ 3′ and 3′→5′ directions (Carballo et al., 2000; Chen et al., 2001; Fenger-Gron et al., 2005; Lai et al., 1999; Lai et al., 2003; Lykke-Andersen and Wagner, 2005). Though only a few ARE-containing mRNAs have been identified as direct targets of TTP, it is estimated that up to 8% of all human mRNAs contain AREs (Bakheet et al., 2006). In addition, recent genome-wide analyses from macrophages and fibroblasts indicate that TTP may regulate over 100 mRNAs suggesting that AMD may be a widespread gene regulatory mechanism in humans (Lai et al., 2006; Stoecklin et al., 2008). Despite our progress in the understanding of AMD in mammals, it remains largely unknown where TTP recruits target transcripts, or how it can discriminate *bona fide* target transcripts from any other ARE-bearing mRNA. Interestingly, subcellular localization experiments revealed that members of the TTP family are nucleocytoplasmic shuttling proteins (Murata et al., 2002; Phillips et al., 2002) and although the importance of shuttling in the regulation of TTP-dependent AMD is not understood, it is interesting to note that stimulatory signals that activate TTP-dependent AMD (e.g. serum and lipopolysaccharide) also cause changes in the subcellular localization of TTP (Carballo et al., 1998; Taylor et al., 1996b). Therefore, nucleocytoplasmic shuttling of TTP may potentially play a role in the mechanism of recognition of ARE-containing mRNAs destined for degradation.

In response to Fe-starvation, yeast Cth1 and Cth2 coordinately promote AMD of a group of ~100 mRNAs, many of which encode proteins with functions in highly Fe-

demanding processes such TCA cycle, electron transport chain, heme and Fe-S cluster biogenesis among others (Puig et al., 2005; Puig et al., 2008; Vergara and Thiele, 2008). Studies have demonstrated that yeast AREs modulate poly-A tail removal of a reporter mRNA followed by decapping (Vasudevan and Peltz, 2001). In addition, recent studies demonstrated that Cth2-dependent AMD is catalyzed from the 5′→ 3′ end by the exonuclease Xrn1 in cytoplasmic Processing Bodies (PBs)(Pedro-Segura et al., 2008; Prouteau et al., 2008). These observations suggest a mechanistic conservation of AMD between yeast and mammals.

Here we demonstrate that the yeast homolog of TTP, Cth2, is a nucleocytoplasmic shuttling protein whose nuclear export is mediated by both Crm1/Xpo1 and the general mRNA exporter Mex67 (known as TAP in metazoans). Cth2 nuclear import information is contained within the TZF domain, but it is independent on mRNA-binding function. We also demonstrate that shuttling is important for Cth2-dependent AMD, as disruption of shuttling leads to defects in AMD and a growth defect under Fe-deficient conditions. In addition, we present evidence that under Fe-limitation Cth2 travels into the nucleus to recruit ARE-containing transcripts destined for cytosolic degradation, and that Cth2-recruitment of target mRNAs occurs at or near the site of transcription. Most importantly, we believe that the study of the molecular mechanisms by which Cth2 regulates the response to Fe-deficiency in yeast provides an outstanding model for understanding the intricacies of AMD in higher eukaryotes. First, while

studies on AMD in mammalian systems frequently rely on overexpression systems or reporter constructs, yeast allows the study of AMD under biologically-relevant conditions, namely Fe-deficiency, providing a range of target mRNAs and easy to analyze phenotypes; second, with the exception of the miRNA-mediated AMD pathway, many aspects of AMD in yeast are conserved in mammals including deadenylation, decapping and 5′→ 3′ degradation (Parker and Song, 2004; Pedro-Segura et al., 2008; Vasudevan and Peltz, 2001); third, yeast provides exceptional genetic and biochemical resources such deletion strains, temperature-sensitive alleles of essential genes, epitope-tagged proteins, and a large number of genome-wide databases on protein-protein interactions, gene regulatory mechanisms, post-translational modifications and subcellular localization among others.

4.2 Materials and methods

Plasmids

For visualization of Cth2, the GFP sequence was inserted between the *CTH2* promoter and the *CTH2* coding sequence in a pRS416 plasmid backbone to produce a functional amino-terminus GFP-Cth2 fusion protein, assessed by the ability to promote the degradation of two well-characterized target mRNAs of Cth2 under Fe-limitation. Fusing either epitope sequence at the carboxy terminus rendered Cth2 non-functional (data not shown). We used the forced localization cassettes described in Edgington and Futcher (2001), containing either two copies of the SV40 NLS or two copies of the PKI

NES to generate the *NLS$_2$-GFP-CTH2* and *NES$_2$-GFP-CTH2* fusions, respectively. Mutations within each cassette were introduced using site-directed mutagenesis to revert the effect of the localization cassettes. The *FLAG-CTH2* fusion has been previously described (Puig et al. 2005). The *DCP2-RFP* fusion was a kind gift from Dr. Roy Parker at the University of Arizona.

Live-cell microscopy

All microscopy experiments were done in live cultures using an AxioImager.A1 (Carl Zeiss, Thornwood, NY) with a 100×/1.4 Plan Apochromat oil immersion objective, an ORCA CCD camera (Hamamatsu, Bridgewater, NJ), and images were captured using the Metamorph 7.5 software. Overnight liquid cultures were re-inoculated to an optical density A_{600}=0.2 in selective medium with 100μM BPS to induce the robust expression of GFP-Cth2 fusion proteins. Temperature sensitive strains were visualized at 24°C and after 1hr incubation at 37°C. Thiolutin (Sigma T3450) was used at a concentration of 5μg/ml for 30m at 30°C. Cells were incubated for 30 min with 10 μg/ml 4'6-diamidino-2-phenylindole (DAPI) to stain yeast nuclei.

Yeast strains and growth assay

Strains *xpo1-1, mex67-5, xpo1-1/mex67-5,* and *XPO1/MEX67* (isogenic wild type) were kindly provided by Dr. Karsten Weis at the University of California at Berkeley. The *xrn1Δ* (BY4741 *xrn1::KanMX4*) strain was obtained from Research Genetics. Strain *cth1Δcth2Δ* has been previously described (Puig et al., 2005). For growth assay in Figure

18D, overnight cultures from *cth1Δcth2Δ* cells expressing *pRS415* and the *pRS416-GFP-CTH2 (WT)* fusion protein, as well as fusions with the appended NLS and NES cassettes, and their inactivated forms were re-inoculated to A_{600}=0.05 in of SC-Ura-Leu in the presence of either 300μM FAS (+Fe) or 100μM BPS (-Fe). The A_{600} after 24hr of three independent transformants was used as a measure of growth.

Nuclear fractionation and RNA analyses

Nuclei were separated from cytosolic fraction by differential centrifugation. Overnight cultures of *cth1Δcth2Δ* cells co-transformed with plasmids *pRS416-FLAG-CTH2* and *pRS415* were re-inoculated to A_{600}=0.2 in 200mL of SC-Ura-Leu, split into two 100mL subcultures to which either 300μM FAS (+Fe) or 100μM BPS (-Fe) was added and grown at 30°C for 6hr. Spheroplasts and cell lysis were carried out using reagents from MITOISO3 kit from Sigma. Differential centrifugation was carried out at 3500g for 10min to obtain unlysed whole cells, 20000g for 20m to isolate nuclei, the cytosolic fraction was collected, and the fractions were analyzed by Immunoblotting using antibodies against the FLAG-epitope (Sigma F-8592), the nuclear resident protein Nop1 (Covance MMS-581), and the cytosolic protein Pgk1 (Molecular Probes A6457). RNA analyses were performed as previously described in Puig et al. (2005).

4.3 Results and Discussion

4.3.1. Cth2 is a nucleocytoplasmic shuttling protein

TTP promotes AMD by interacting with members of the cytosolic general mRNA decay machinery (Chen et al., 2001; Lai et al., 1999; Lai et al., 2003; Lykke-Andersen and Wagner, 2005). Yet, experiments revealed that TTP shuttles between the nucleus and cytosol (Murata et al., 2002; Phillips et al., 2002). Similarly, Cth2 can promote AMD by recruiting the cytosolic 5′→ 3′ decay machinery (Pedro-Segura et al., 2008). However, the subcellular localization of Cth2 has not been determined. We carried out a combination of live microscopy and biochemical fractionation experiments using functional GFP- or FLAG-epitope tagged constructs (Materials and Methods) to conclusively establish the subcellular localization of Cth2. Cells expressing a *GFP-CTH2* fusion were grown under Fe-limitation conditions to induce the expression of the protein and observed by live fluorescence microscopy, which revealed that GFP-Cth2 is localized diffusely throughout cells (Figure 17A, top). We have previously demonstrated that mutations in two cysteine residues within the TZF domain of Cth2 (C190 and C213) eliminate the interaction between Cth2 and ARE-sequences within target mRNAs, which in turn abolishes the ability of Cth2 to promote AMD (Puig et al. 2005). To determine whether the inability of Cth2 to interact with mRNA had an effect on its localization, we observed the GFP-Cth2-C190, 213A mutant fusion protein, which appears to be largely localized to the nucleus (Figure 17A, *bottom*). In order to independently assess the

localization of Cth2, cells expressing a *FLAG-CTH2* fusion were grown under Fe-replete or Fe-deficient conditions, and nuclei separated from cytosol by differential centrifugation. As previously demonstrated, Flag-Cth2 is readily detected in extracts from cells treated only under Fe-deficiency conditions (Puig et al. 2005; Figure 17B). Immunoblotting analysis of fractions enriched for nuclei show that Flag-Cth2 co-fractionates with the nuclear resident protein Nop1. In addition, both Flag-Cth2 and the cytosolic protein Pgk1 can be detected in the cytosolic fraction (Figure 17B).These data demonstrate that Cth2 is both a cytosolic and nuclear resident protein, and also suggest that the Cth2:mRNA interaction is important for maintenance of steady state localization of Cth2.

Localization experiments for TTP and related proteins (Phillips et al. 2002; Murata et al., 2002) demonstrated that these proteins actively shuttle between the nucleus and the cytosol, and that their export from the nucleus relies on the export receptor Crm1/Xpo1. We tested whether translocation of Cth2 out of the nucleus was also Crm1/Xpo1-dependent by visualizing the GFP-Cth2 fusion in a yeast strain harboring a temperature sensitive allele of the nuclear export receptor Crm1/Xpo1 (*xpo1-1ts).* As shown in Figure 17C, the GFP-Cth2 fusion protein is partially retained in the nucleus of the *xpo1-1ts* strain at the restrictive temperature (37°C), but not in cells grown at 24°C or in a wild type strain at either temperature (data not shown), consistent with the notion that Cth2 export from the nucleus is at least partially dependent on

Crm1/Xpo1. The regions of TTP containing both the NES and NLS sequences are not conserved in yeast Cth2.Therefore, in order to identify the NES and NLS sequences we made truncations of the amino terminus, carboxy terminus or both termini of Cth2 (Figure 17D, top) and fused them to the GFP-epitope in order to visualize their localization. However, none of the truncations had an apparent defect in localization in wild-type cells (data not shown). This observation raised two possibilities: one, either the intact protein is required for nuclear import and consequently none of the truncated versions of GFP-Cth2 can be transported into the nucleus, which is difficult to ascertain by microscopy alone; or two, the truncation constructs are exported via an alternative nuclear export pathway, perhaps bound to mRNA, precluding us from identifying a region containing the nuclear export information important for Crm1/Xpo1-dependent export. To test the latter possibility, we asked whether full-length Cth2 localization was defective in a strain harboring a temperature sensitive allele of the general mRNA exporter, Mex67. As shown in Figure 17C, GFP-Cth2 is retained in the nucleus of the *mex67-5ts* strain at the restrictive temperature, but not in cells grown at room temperature. Furthermore, the nuclear retention defect of GFP-Cth2 is exacerbated in a strain harboring both *xpo1-1* and *mex67-5* mutations, suggesting that Cth2 is exported via both pathways. Visualization of the truncation constructs in the *mex67-5* strain at the restrictive temperature allowed us to determine the nuclear import information within Cth2. As shown in Figure 17D, none of the truncations showed an obvious difference in

localization compared to GFP-Cth2 in cells grown at 24°C, but inactivation of the mRNA-export activity of *mex67-5* by incubation at 37°C for 1hr clearly showed nuclear accumulation of GFP-Cth2 and the three partial deletions. These results demonstrate that the minimal nuclear import information in Cth2 resides at the TZF motif (Figure 17D). A GFP-epitope fused to a NLS and NES sequence was used a control, and showed no nuclear accumulation under the same conditions.

The data present here suggest that Cth2 is a nucleocytoplasmic shuttling protein whose export from the nucleus is mediated by the bulk mRNA transporter Mex67, as well as the nuclear export factor, Xpo1. An interesting observation is that contraire to the evenly distributed nucleoplasmic localization of the non-mRNA binding mutant GFP-Cth2-C190, 213A (Figure 17A), GFP-Cth2 is enriched in subnuclear regions in the mRNA-export deficient *mex67-5* strain (Figure 17C). This localization likely corresponds to sites of retained polyA mRNAs previously described in this strain (Hilleren and Parker, 2001; Segref et al., 1997). These observations suggest that Cth2 export from the nucleus is at least partially, though not completely, dependent on its ability to interact with mRNA further supporting a role for both the Xpo1- and Mex67-dependent pathways.

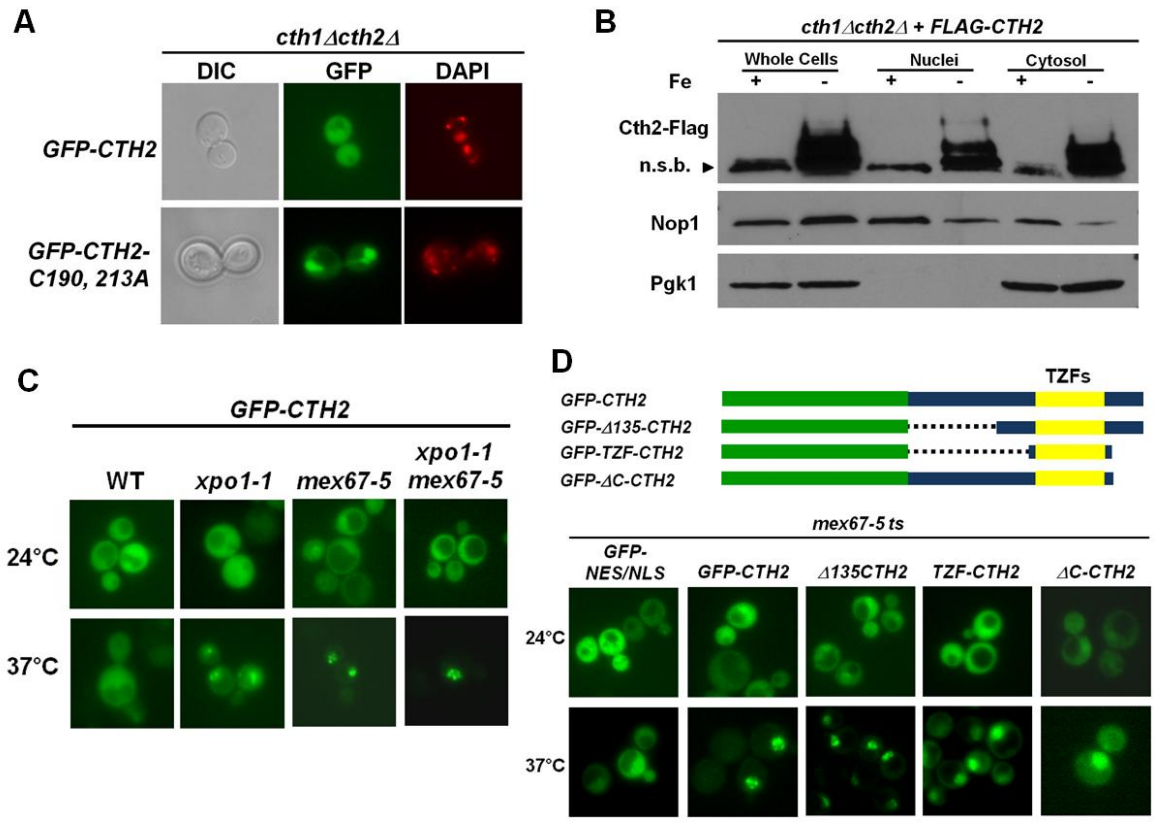

Figure 17. Cth2 is a nucleo-cytoplasmic shuttling protein

A. GFP-Cth2 is expressed diffusely throughout cells, while a non-mRNA binding mutant is largely localized to the nucleus. c*th1Δcth2Δ* cells transformed with pRS416-*GFP-CTH2* (top) or pRS416-*GFP-CTH2-C190, 213A* (bottom) were visualized by live fluorescence microscopy. 4',6-diamidino-2-phenylindole (DAPI) was used to stain nuclei. **B.** Cth2 is a nuclear and cytosolic resident protein. Nuclear and cytosolic fractions were obtained from c*th1Δcth2Δ* cells expressing pRS416-*FLAG-CTH2* grown in medium containing 300μM Ferrous Ammonium Sulfate (FAS; Fe+) or 100μM BPS (Fe-) and analyzed by immunoblotting. The anti-FLAG-HRP conjugated antibody used to detect Flag-Cth2 also detects a non-specific band (n.s.b.) indicated by the arrow head. Nuclear and cytosolic fractions were identified by incubation with antibodies against Nop1 and Pgk1 proteins, respectively. **C.** Cth2 export from the nucleus is mediated by Xpo1 and Mex67 pathways. Wild-type and thermosensitive strains *xpo1-1*, *mex67-5*, and *xpo1-1/mex67-5* double mutants transformed with pRS416-*GFP-CTH2* were visualized at 24°C and after a shift to 37°C for one hour to disrupt function of the Xpo1-1 and Mex67-5 mutant proteins. **D.** (*Top*). Representation of the *GFP-CTH2* construct and truncations made at the amino- and carboxy-termini, or both. Tandem zinc finger domain (TZFs) is indicated; (*Bottom*). *mex67-5* cells were transformed with plasmid *GFP-NES/NLS* as control, and plasmids containing full length *GFP-CTH2* and the truncations described above. All cells were visualized after six hours of growth in selective medium containing 100μM of the Fe-chelator Bathophenanthroline disulfonate (BPS) to induce Fe-deficiency. Vacuoles (one or more per cell) may appear as clear indentations in DIC images and correspond to regions devoid of fluorescence signal.

4.3.2. Cth2 nucleocytoplasmic shuttling is important for function

The observation that Cth2 leaves the nucleus via two export pathways made mapping of a possible NES sequence in Cth2 difficult. Furthermore, while we identified the TZF as the region containing the minimal nuclear import information, mutations within this domain abolish the mRNA-binding activity of Cth2 (data not shown) precluding the determination of whether localization plays a role on Cth2 function. Thus, we disrupted the steady state localization of Cth2 by attaching "forced localization" cassettes (Edgington and Futcher, 2001) consisting of two copies of the SV40 NLS sequence or two copies of the PKI NES sequence at the amino terminus of the GFP-Cth2 fusion (*NLS_2-GFP-CTH2* and *NES_2-GFP-CTH2*, respectively). As controls, we used localization cassettes in which we introduced mutations within key residues, thus rendering the localization sequences inactive (*inac-NLS_2-GFP-CTH2* and *inacNES_2-GFP-CTH2*; Figure 18A and 18B, top). In order to assay the effectiveness of the appended sequences we visualized the localization of the NLS_2-GFP-Cth2 fusion and its inactive form in a nuclear export competent strain by fluorescence live microscopy. As shown in Figure 18A, the NLS_2-GFP-Cth2 construct appears mostly localized to the nucleus, while the GFP-Cth2 and the inac-NLS_2-GFP-Cth2 constructs are localized all throughout the cell. Due to the difficulty of visualizing empty nuclei by live microscopy in yeast, we observed the efficacy of the NES_2-GFP-Cth2 fusion in a *mex67-5* strain at 37°C in order to disrupt mRNA export (as in Figure 17C), and thus determine if the appended NES

cassette can successfully increase the rate of nuclear export of GFP-Cth2. As shown in Figure 18B, cytosolic localization of the NES_2-GFP-Cth2 construct is higher than GFP-Cth2 or the inac-NES_2-GFP-Cth2 fusions. These data demonstrate that both of the appended localization sequences can successfully disrupt the native localization of GFP-Cth2, and fusions harboring mutations within the forced localization cassettes behave like GFP-Cth2.

We assessed how localization influences Cth2 function by evaluating the steady state levels of the *SDH4* mRNA in cells competent for mRNA export and degradation, but expressing the fusion constructs described in Figure 18A and 18B. In addition, we examined whether altering the native localization of Cth2 affects cell growth under Fe-deficiency conditions. As shown in Figure 18C, cells expressing the unmodified GFP-Cth2 (*WT*) construct show a three-fold decrease in *SDH4* mRNA levels. Interestingly, cells expressing the appended NLS_2 and NES_2 cassettes present a defect in the down-regulation of *SDH4* (only 1.5 and 1.7 fold, respectively), while inactivation of these sequences (*inacNLS* and *inacNES*) rescues the down-regulation close to wild type levels (roughly 2.8 fold). Fold down-regulation was calculated after normalization to *ACT1* mRNA. Consistent with these data, cells expressing the NLS_2-GFP-Cth2 and NES_2-GFP-Cth2 constructs grow less well under Fe-deficiency conditions compared to cells expressing the unmodified GFP-Cth2 construct, or the inactivated NLS_2 and NES_2 forms (Figure 18D, light gray bars). Cells expressing any of these constructs grow equally well

if grown in the presence of abundant Fe in the medium (Figure 18D, dark gray bars), conditions under which Cth2 activity is not required, and it is therefore not expressed. The ability of the inactivated sequences to rescue both the down-regulation defect of *SDH4* mRNA and the growth phenotype suggest that the appended sequences do not interfere with mRNA-binding.

Recent studies demonstrated that Cth2 promotes Fe deficiency-dependent degradation of the *SDH4* mRNA in the 5′→ 3′ direction, which is catalyzed by the PB resident exonuclease, Xrn1 (Pedro-Segura, 2008). Deletion of the *XRN1* gene causes the accumulation of PBs as mRNAs get trapped within these structures but fail to be degraded. While GFP-Cth2 localizes all throughout wild type cells, it accumulates in PBs in strains deleted for the *XRN1* gene, suggesting that the function of Cth2 in promoting AMD may be the delivery of the target transcripts to PBs (Pedro-Segura, 2008; Figure 19A), and that degradation of the target mRNA is required for release of Cth2 from this site, perhaps to engage in another round of mRNA delivery. Altering the steady state localization of Cth2 affects its ability to promote AMD of the *SDH4* transcript (Figure 18C and D) suggesting that disruption of shuttling may hinder the Cth2 interaction with the mRNA-decay machinery. We visualized the NLS_2-GFP-Cth2 and NES_2-GFP-Cth2 constructs (as well as inactivated forms) in the *xrn1Δ* strain in order to ascertain if disruption of shuttling affects Cth2 localization to PBs. As we have previously demonstrated and shown in Figure 18E, GFP-Cth2 co-localizes with the PB resident

protein Dcp2-RFP in the *xrn1Δ* strain (Pedro-Segura, 2008). Visualization of the NLS_2-GFP-Cth2 and NES_2-GFP-Cth2 constructs revealed that forced re-localization of Cth2 greatly impaired its ability to localize to PBs (Figure 18E). The constructs containing the inactivated sequences, on the other hand, resembled the localization of the GFP-Cth2 construct, consistent with their ability to rescue both the down-regulation of the *SDH4* mRNA and the growth defect under Fe-deficient conditions (Figure 18C and 18D). Together, these results suggest that like its mammalian counter parts, Cth2 actively moves between the nucleus and the cytosol, and demonstrate that the ability of Cth2 to move between both compartments is important for function, suggesting that nucleocytoplasmic shuttling might be part of the mechanism of its AMD-promoting activity.

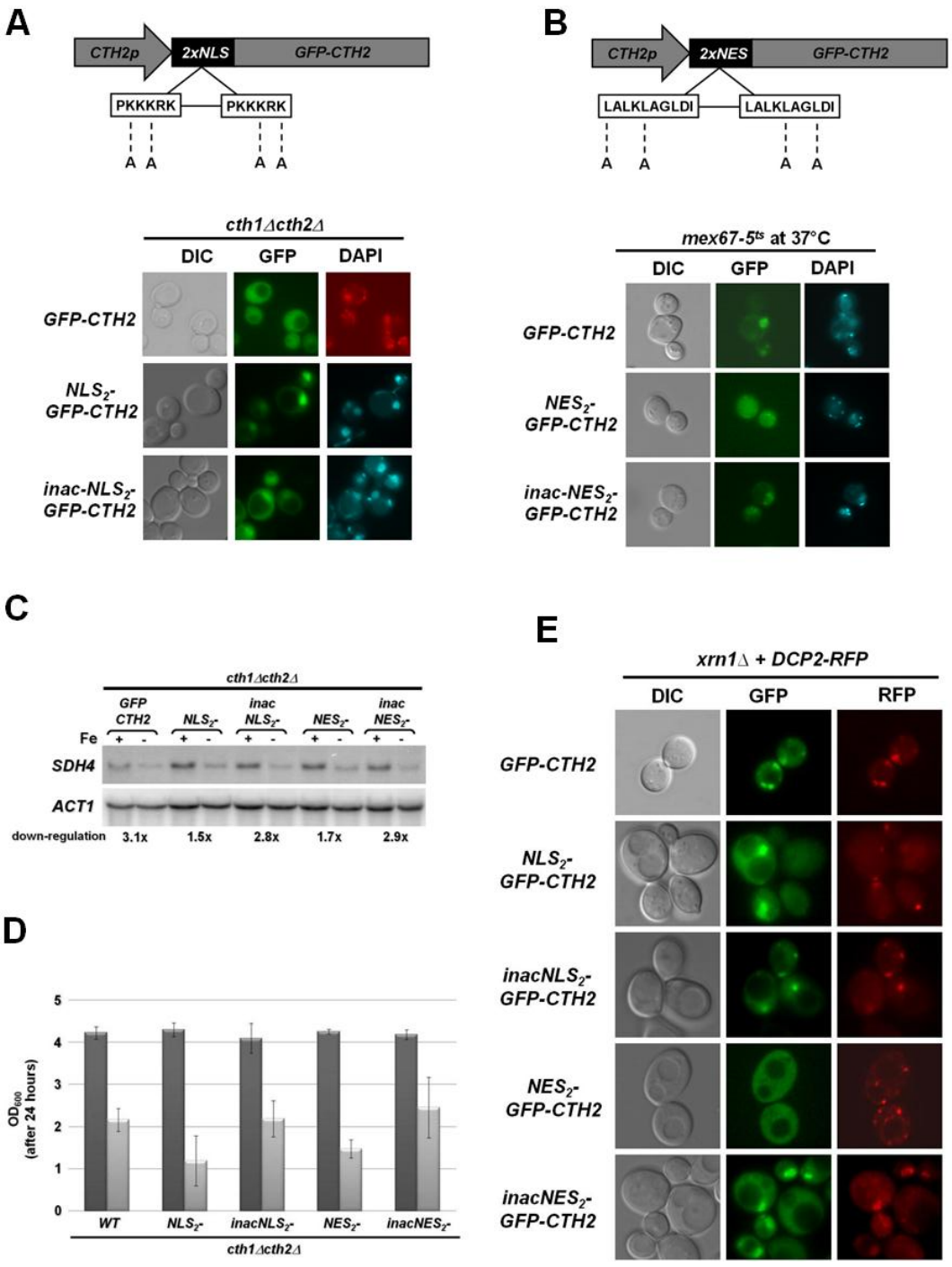

Figure 18. Nucleo-cytoplasmic shuttling of Cth2 is important for function

A. (*top*) Representation of the forced nuclear localization construct. Two tandem copies of the SV40 NLS sequence were inserted between the *CTH2* promoter and the *GFP-CTH2* fusion. The active SV40 NLS

sequence is shown the box, and specific lysines mutated to alanines to inactivate the NLS sequence are shown; (*bottom*) c*th1Δcth2Δ* cells transformed with p416-*CTH2p-GFP-CTH2,* p416-*CTH2p-NLS*$_2$*-GFP-CTH2,* or p416-*CTH2p*-inac*NLS*$_2$*-GFP-CTH2* were visualized by live fluorescence microscopy. DAPI was used to stain nuclei. **B.** Representation of the forced nuclear export construct. Two tandem copies of the PKI NES sequence were inserted between the *CTH2* promoter and the *GFP-CTH2* fusion. The active PKI NES sequence is shown the box, and specific leucines mutated to alanines to inactivate the NES sequence are shown; (*bottom*) *mex67-5ts* cells transformed with p416-*CTH2p-GFP-CTH2,* p416-*CTH2p-NES*$_2$*-GFP-CTH2,* or p416-*CTH2p*-inac*NES*$_2$*-GFP-CTH2* were grown at 24°C and visualized after 1hr shift to 37°C by fluorescence live microscopy. DAPI was used to stain nuclei. **C. and D.** Alterations in steady-state localization compromises Cth2 function. c*th1Δcth2Δ* cells were transformed with p416-*CTH2p-GFP-CTH2 (WT)* or the forced localization constructs described above and referred to as: *NLS*$_2$- and *inacNLS*$_2$-, and *NES*$_2$- and *inacNES*$_2$-. Transformants were grown in Fe(+) or Fe(-) conditions, and steady-state levels of the *SDH4* transcript were analyzed by RNA blotting and fold down-regulation of the *SDH4* mRNA under Fe(-) conditions was calculated after normalization to *ACT1* (**C**). Optical density of cells grown in Fe(+)(dark grey bars) or Fe(-)(light grey bars) conditions was measured 24hr after initial re-inoculation. Experiment was done in triplicate; error bars represent standard deviation (**D**). **E.** *xrn1Δ* cells were co-transformed with pRS416-*DCP2-RFP* and p416-*CTH2p-GFP-CTH2 (WT)* or the forced localization constructs. Cells were visualized by fluorescence live microscopy after six hours of growth under Fe(-) conditions.

4.3.3. Cytosolic localization of Cth2 depends on RNA synthesis

In addition to disrupting mRNA-binding, mutation of cysteine residues within the TZF domain of TTP and Cth2 causes their nuclear accumulation in wild type cells (Murata el al., 2002)(Figure 17A), indicating that the interaction of TTP and Cth2 with cognate target mRNAs is important for nuclear export. Interestingly, visualization of the GFP-Cth2-C190, 213A allele in the *xrn1Δ* strain demonstrated that localization to PBs also depends on the Cth2:mRNA interaction. Figure 19A shows that while GPF-Cth2 colocalizes with the PB-resident protein Dcp2-RFP in *xrn1Δ* cells, GFP-Cth2-C190, 213A remains largely retained in the nucleus similarly to its localization in wild-type cells (Figure 19A and 17A). These data suggest that Cth2 binding to mRNA and shuttling through the nucleus precedes localization to cytosolic PBs.

We hypothesized that if Cth2 binds target mRNAs in the nucleus, disruption of RNA synthesis by inhibiting transcription should prevent Cth2 nucleocytoplasmic shuttling, and consequently, it should also prevent localization of Cth2 to PBs. We tested this hypothesis by using a strain expressing a temperature sensitive allele of the largest subunit of RNA polymerase II (*rpb1-1*), and by using a pharmacological inhibitor of transcription (thiolutin) to ascertain GFP-Cth2 localization in the absence of on-going mRNA synthesis. As shown in Figure 19B, GFP-Cth2 accumulates in the nucleus of *rpb1-1* cells incubated at 37°C, while it remains diffusely localized throughout cells grown at the permissive temperature. Incubation of wild-type cells with the transcription inhibitor thiolutin also causes nuclear retention of GFP-Cth2, while a GFP epitope fused to an NLS/NES sequence does not show nuclear accumulation under the same conditions (Figure 19C). Pab1 (polyA binding protein 1) is also a nucleocytoplasmic shuttling protein, whose nuclear export is mediated by Mex67 and Xpo1. However, inhibition of transcription in *rpb1-1* cells (Dunn et al., 2005), or by incubation with thiolutin (Figure 19C) does not cause nuclear accumulation of Pab1-GFP, suggesting that nuclear retention upon transcription inhibition is not a phenotype affecting all shuttling proteins.

Interestingly, we noticed that nuclear GFP-Cth2 accumulation occurs into punctate structures of thiolutin-treated cells (Figure 19C and D), and localization of Cth2 to these structures is independent on its ability to interact with mRNA since the non-

mRNA binding mutant GFP-Cth2-C190, 213A (Figure 19D) accumulates into similar structures upon exposure to thiolutin. Lastly, transcription inhibition also prevents GFP-Cth2 localization to PBs in the *xrn1Δ* strain as shown in Figure 19E. Together, these data are consistent with nucleocytoplasmic shuttling of Cth2 being important for the early recruitment of target mRNAs for escort to cytosolic PBs.

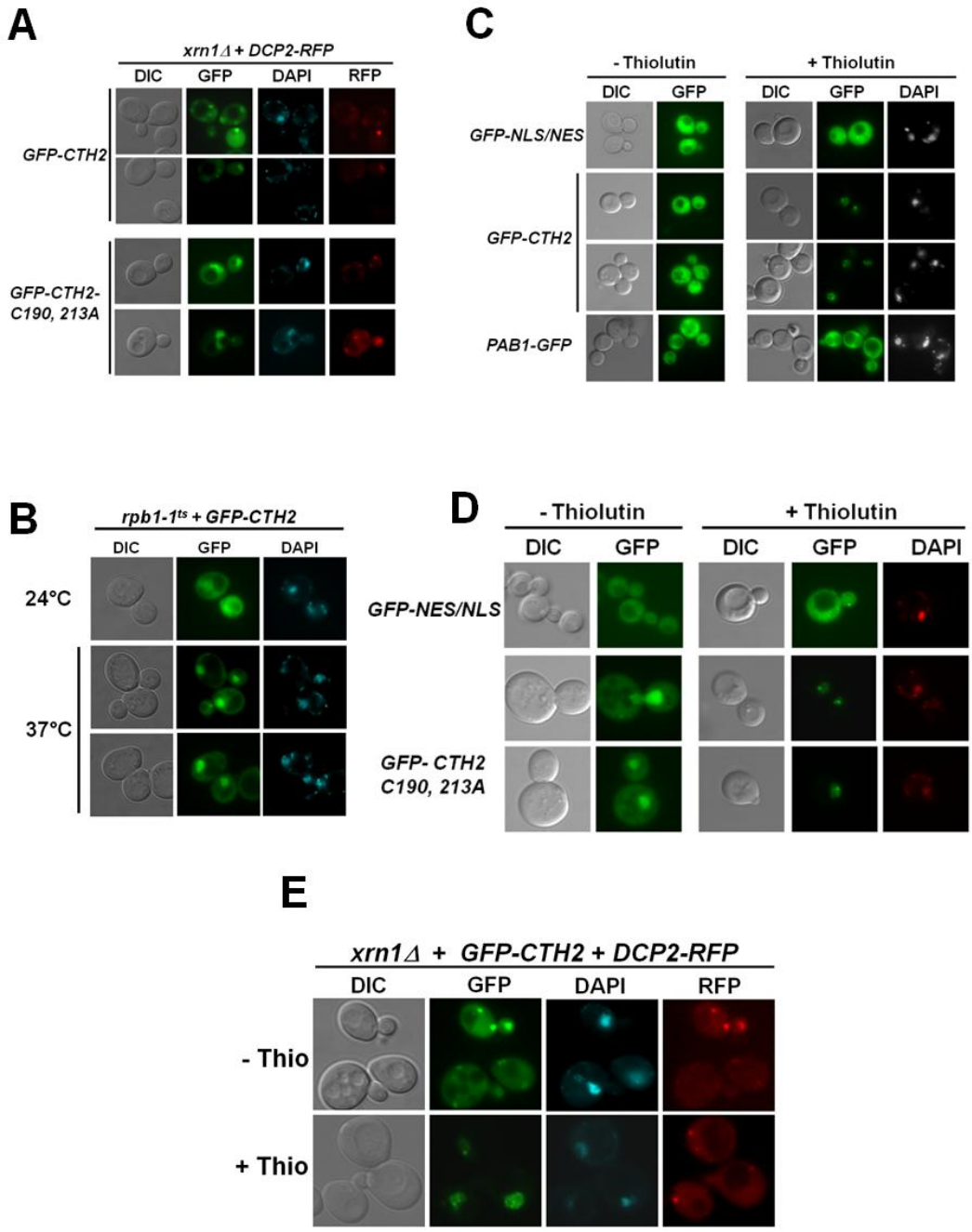

Figure 19. Transcription-dependent shuttling of Cth2

A. PB localization of Cth2 requires interaction with mRNA. *xrn1Δ* cells expressing PB body marker pRS416-*DCP2-RFP* co-transformed with pRS416-*GFP-CTH2* or non-mRNA binding mutant pRS416-*GFP-CTH2-C190, 213A*. **B. and C.** GFP-Cth2 is retained in the nucleus of cells defective in transcription. *rbp1-1* cells transformed with pRS416-*GFP-CTH2* were visualized at 24°C, and after a 1hr shift to 37°C to disrupt the

activity of the thermosensitive allele of the largest subunit of RNA polymerase II, Rpb1-1 (**B**). c*th1Δcth2Δ* cells transformed with plasmids *GFP-NLS/NES* or *PAB1-GFP* were visualized before and after treatment with 5μL/mL thiolutin for 30m. Thiolutin blocks transcription from RNA pol I, II, and III (Tipper, 1973) (**C**). **D. and E.** Transcription-inhibition disrupts Cth2 localization to PBs. Transcription of *xrn1Δ* cells co-expressing pRS416-*DCP2-RFP* and pRS416-*GFP-CTH2* (**D**) or non-mRNA binding mutant pRS416-*GFP-CTH2-C190, 213A* (**E**) were observed in the presence or absence of thiolutin treatment. All cells were visualized after six hours of growth under Fe(-) conditions and DAPI was used to stain nuclei.

4.3.4. Nuclear recruitment of ARE-containing mRNAs targeted for degradation during Fe-deficiency

Although several steps in the mechanisms of AMD have been characterized in mammals and in yeast, where TTP and family members first encounter their cognate target mRNAs for recruitment and subsequent cytosolic degradation remains an unresolved question (Chen et al., 2001; Lai et al., 1999; Lai et al., 2003; Lykke-Andersen and Wagner, 2005). Interestingly, studies revealed that TTP and family members are nucleocytoplasmic shuttling proteins; however, neither the function of nuclear TTP, nor a role for TTP shuttling on AMD has been uncovered (Murata et al., 2002; Phillips et al., 2002). Our data indicate that Cth2 is expressed in the nucleus and in the cytosol and that like TTP, Cth2 translocates between both compartments. Our data also suggest that Cth2 recruits target mRNAs in the nucleus for escort to the cytosol for degradation. Our hypothesis is further supported by the recently identified function of Cth2 in the nucleus (Prouteau et al., 2008).

Recent studies identified Cth2 as a factor that regulates 3'-end processing by interfering with normal poly-A site selection leading to the formation of extended mRNAs that are highly unstable (Prouteau et al., 2008). Cells expressing an allele of Cth2

in which the first 86 amino acids have been deleted accumulate extended *SDH4* transcripts suggesting that this truncation can efficiently bind and promote the formation of the extended mRNA, but fails to induce its rapid turnover (Prouteau et al., 2008). As shown in Figure 20A (*top*), the amino terminus truncation of Cth2, GFP-Δ89Cth2, does not have any apparent defect in subcellular localization. Furthermore, treatment with thiolutin induces its nuclear retention in a manner comparable to full length GFP-Cth2 (Figure 20A, *bottom*), and it does not have a defect in PB localization in *xrn1Δ* cells (Figure 20B). These observations suggest that truncation of the amino terminus of Cth2 acts as a separation-of-function mutation that can efficiently induce the formation of extended mRNA and localize to PBs, but fails to promote degradation of the extended transcripts, perhaps due to its inability to recruit the deadenylase machinery. NMR studies on the TZF domain of the TTP family member Tis11D bound to the nonameric sequence 5′- $U_1U_2A_3U_4U_5U_6A_7U_8U_9$-3′ revealed that the second TZF interacts with the 5′-most $U_2A_3U_4U_5$ sequence, while the first TZF of the protein interacts with the 3′-most $U_6A_7U_8U_9$ region of the sequence (Hudson et al., 2004). Therefore, the amino terminus of Tis11D faces the poly-A tail of the bound transcript. This observation may suggest that the deadenylase is brought to the ARE-containing transcript through a direct or indirect interaction with the amino terminus of Cth2.

Our data guided us to propose the following four-step model for AMD in yeast: (1) Docking: Cth2 is recruited to the nascent mRNA before polyadenylation takes place;

(2) Recognition: the proximity to the 3'-end allows Cth2 to be deposited onto the nascent ARE sequence; (3) Transport: target mRNA bound by Cth2 continues to be packaged into a mature mRNP and exported to the cytosol via two independent pathways, Mex67 and Xpo1; and (4) Decay: Cth2 directs the bound transcript to the site of degradation in the cytosol (Figure 20C).

The observation that Cth2 affects polyA-site selection (Prouteau et al., 2008) suggests that Cth2 binds target ARE-mRNAs at a step before polyadenylation. Factors involved in polyA tail regulation and mRNP export (e.g. Nab2 and Npl3) are co-transcriptionally recruited to the nascent mRNPs and experiments showed that incubation with thiolutin disrupt their shuttling activity (Lee et al., 1996). Consistently, thiolutin treatment disrupts Cth2 shuttling and causes the retention of Cth2 into nuclear foci independently of mRNA-binding, suggesting a step whereby Cth2 docks onto a site near the 3'end in anticipation of the nascent ARE sequence. Once the ARE sequence is transcribed, Cth2 recognizes it and binds preventing normal polyA site selection thus inducing extended transcripts.

Messenger RNA surveillance mechanisms ensure that only properly processed mRNPs are exported to the cytoplasm. Our data suggest that while Cth2 promotes the formation of extended transcripts, these appear to be packaged into mature mRNPs and exported to the cytosol for degradation into PBs. Evidence for this comes from the observation that the separation-of-function mutant, GFP-Δ89Cth2, is efficiently recruited

to PBs though it fails to promote deadenylation and subsequent 5′→ 3′ degradation of the target mRNA. Thus, it is possible that mRNPs containing extended polyA tails bound by Cth2 are selectively delivered to the cytosol for degradation under conditions of Fe-deficiency.

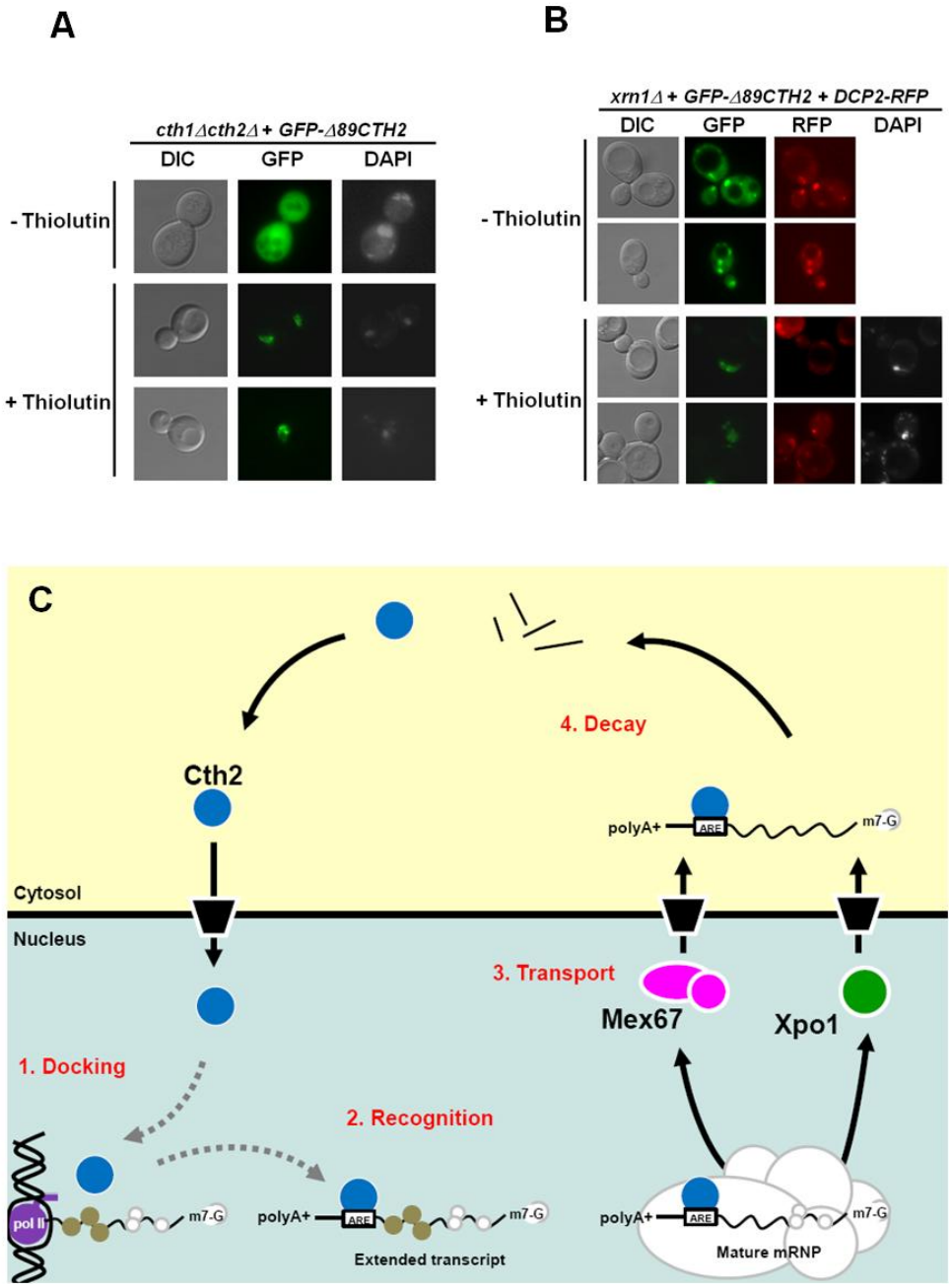

Figure 20. Nucleo-cytoplasmic shuttling working model.

A. and B. *cth1Δcth2Δ* (**A**) and *xrn1Δ* (**B**) cells transformed with plasmid p416-*CTH2p-GFP-Δ89CTH2* visualized before or after treatment with 5µL/mL thiolutin for 30m.**C. Working model: Cth2 recruits target**

mRNAs in the nucleus for degradation in the cytosol during Fe-deficiency. Steps in ARE-mRNA recruitment: (1) *Docking:* Cth2 (blue circle) is brought to target mRNAs by 3'-end processing factors; (2) *Recognition:* Cth2 binds AREs within target transcripts. Cth2 binding causes readthrough of normal polyadenylation site resulting in extended transcript formation; (3) *Transport:* mature mRNP containing extended target transcript bound by Cth2 is exported via two independent pathways: Mex67 and Xpo1; (4) *Decay:* Cth2 bound transcript is deadenylated and degraded in the cytosol. Factors involved in processing and cytosolic mRNA decay have been omitted for simplicity.

5. Other observations and future directions

5.1 Cth1 and Cth2 localization to the mitochondria

5.1.1. Introduction

Mitochondria are essential organelles involved in numerous cellular processes including energy generation and apoptosis, as well as biosynthesis of heme and Fe-S clusters and the metabolism of amino acids and fatty acids (Sheftel and Lill, 2009). Mitochondrial abnormalities are associated with diseases such cancer, diabetes, Friedrich's ataxia, Amyotrophic Lateral Sclerosis (ALS) and age-related neurodegenerative diseases like Alzheimer's and Parkinson's disease (Lill and Muhlenhoff, 2008; Rouault, 2006). Since their successful isolation in the 1940s, mitochondrial function, biogenesis and physiology have been under extensive investigation (Sheftel and Lill, 2009). It is now well established that while mitochondria contain their own DNA, 80-95% of mitochondrial proteins are nuclear encoded and translated on cytosolic ribosomes, and thus necessitate a mechanism of transport across the outer and inner mitochondrial membranes into the site of endogenous localization. The first mitochondrial protein transport system described involves an amino-terminal mitochondrial targeting sequence that interacts with the translocase of the outer membrane complex (TOM) and the translocase of the inner complex (TIM)(Neupert, 1997; Schatz and Dobberstein, 1996). However, studies pioneered by the Butow Laboratory in the 1970s suggested that mitochondrial protein transport might also occur

co-translationally. Their studies in yeast demonstrated that cytosolic ribosomes loaded with mRNAs encoding mitochondrial proteins were associated with the outer mitochondrial membrane in a manner analogous to the ribosome coating of the rough endoplasmic reticulum of higher eukaryotes (Kellems et al., 1974, 1975; Kellems and Butow, 1972, 1974). This observation, in addition to kinetic analyses of [^{35}S]-methionine incorporation into cytosolic versus mitochondrial matrix proteins and peptidase analyses, lead to the model that mitochondrial proteins translated by cytosolic polysomes can be imported post-translationally as well as co-translationally (Ades and Butow, 1980a, b). Furthermore, studies in yeast indicated that some mRNAs encoding mitochondrial proteins are localized in the vicinity of the mitochondria and that localization requires *cis*-acting information within the transcript (Corral-Debrinski et al., 2000). Recent genome-wide analyses revealed that there is an asymmetric partition of mRNAs encoding mitochondrial peptides between free and mitochondria-bound polysomes (Marc et al., 2002). cDNAs from mRNAs isolated from free- and mitochondrial-bound polysomes were Cy3/Cy5 labeled and hybridized to DNA microarrays. Based on microarray hybridization data, genes were given Mitochondrial Localization of RNA (MLR) values; the higher the MLR value, the more likely it is localized in the vicinity of the mitochondria (Marc et al., 2002; Sylvestre et al., 2003a; Sylvestre et al., 2003b). The recent identification of the Pumilio family RNA-binding protein, Puf3, as a *trans*-acting factor controlling mitochondrial localization has allowed

the classification of 480 identified mitochondria localized mRNAs (MLR-mRNAs) into two classes: Class I MLR-mRNAs, whose localization is directed by Puf3 through an interaction with Puf3-bindings sites within their 3'-UTRs; and Class II MLR-mRNAs, which do not contain Puf3 sites, and as a consequence are unaffected by Puf3 activity. In addition, these data established which mRNAs encoding mitochondrial proteins were translated by free-cytosolic polysomes. As expected, Puf3 localizes to the cytosolic face of the mitochondrial outer membrane (Garcia-Rodriguez et al., 2007). Interestingly, Class I MLR-mRNAs mostly encode assembly factors of the respiratory chain and mitochondrial translational machinery, while Class II MLR-mRNAs encode mainly proteins involved in mitochondrial metabolic pathways, including the TCA cycle and the electron transport chain (Saint-Georges et al., 2008).

5.1.2. Preliminary results and conclusions

Cth1 and Cth2 localization to mitochondria during Fe-deficiency

In response to Fe-limitation, the yeast $CX_8CX_5CX_3H$-proteins Cth1 and Cth2 accelerate the rate of decay of select groups of mRNAs that encode proteins involved highly Fe-demanding processes by binding to ARE-sequences within their 3'UTRs (Ma and Herschman, 1994; Thompson et al., 1996). Some of these processes include metabolic pathways that take place in the mitochondria such TCA cycle, electron transport chain, heme and Fe-S biosynthesis, sterol and amino acid metabolism. While both proteins are capable of binding the same 3'ARE sequences, Cth1 appears to have a preference for a

small group of mRNAs (~20) encoding Fe-requiring mitochondrial proteins, whereas Cth2 promotes the down-regulation of a much larger group of mRNAs (~100) that encode both mitochondrial and non-mitochondrial Fe-utilizing proteins (Puig et al., 2005; Puig et al., 2008). Subcellular localization experiments described in Chapter 4 demonstrated that GFP-Cth2 is localized all throughout cells under Fe-deficient conditions. The same studies demonstrated that Cth2 is a nucleocytoplasmic shuttling protein, whose shuttling into the nucleus is important for efficient down-regulation of the *SDH4* target mRNA in cytosolic P-bodies. Nuclear export of Cth2 appears to involve the protein export pathway mediated by Xpo1, as well as the bulk mRNA export pathway mediated by Mex67.

In contrast to Cth2, however, preliminary localization experiments of a *GFP-CTH1* fusion in cells expressing thermo-sensitive alleles of Xpo1 or Mex67 (*xpo1-1* and *mex67-5*) did not show nuclear retention of GFP-Cth1 at the restrictive temperature (data not shown). Moreover, due to low fluorescence levels of the GFP-Cth1 fusion in the *xrn1Δ* strain, we were unable to determine whether GFP-Cth1 localizes to P-bodies under Fe-deficiency (data not shown). Interestingly, fluorescence live microscopy and mitochondrial fractionation experiments from *cth1Δ* cells expressing a functional *GFP-CTH1* or *FLAG-CTH1* fusion constructs, respectively, demonstrated that Cth1 localizes in the vicinity of mitochondria in cells grown under Fe-deficiency. As shown in Figure 21A, GFP-Cth1 accumulates in structures that co-localize with the mitochondrial marker

mitoRFP – a fusion protein consisting of RFP and the targeting sequence of subunit 9 of the F_0 ATPase (Figure 21A)(Frederick et al., 2004). In addition, immunoblotting analysis from differential centrifugation fractions demonstrated that Flag-Cth1 co-fractionates with the mitochondrial marker porin. Both Flag-Cth1 and the cytosolic protein Pgk1 can be detected in the cytosolic fraction (Figure 21B).

During the course of the studies described in Chapter 4, we observed that shifting the steady-state localization of GFP-Cth2 fusions to the cytosol by means of attaching a strong NES_2 motif at their amino-terminus induced their cytosolic accumulation into structures that resembled mitochondria. Co-localization experiments with the mitochondrial marker mitoRFP confirmed that NES_2-GFP-Δ89Cth2 (Figure 21C) and NES_2-GFP-Cth2 (data not shown) fusions localize in the vicinity of mitochondria in some cells. Therefore, we isolated mitochondria from *FLAG-CTH2* expressing cells under Fe-deficiency. As shown in Figure 21B, Flag-Cth2 is detected in fractions expressing the mitochondrial marker porin, suggesting that both Cth1 and Cth2 localize to mitochondria.

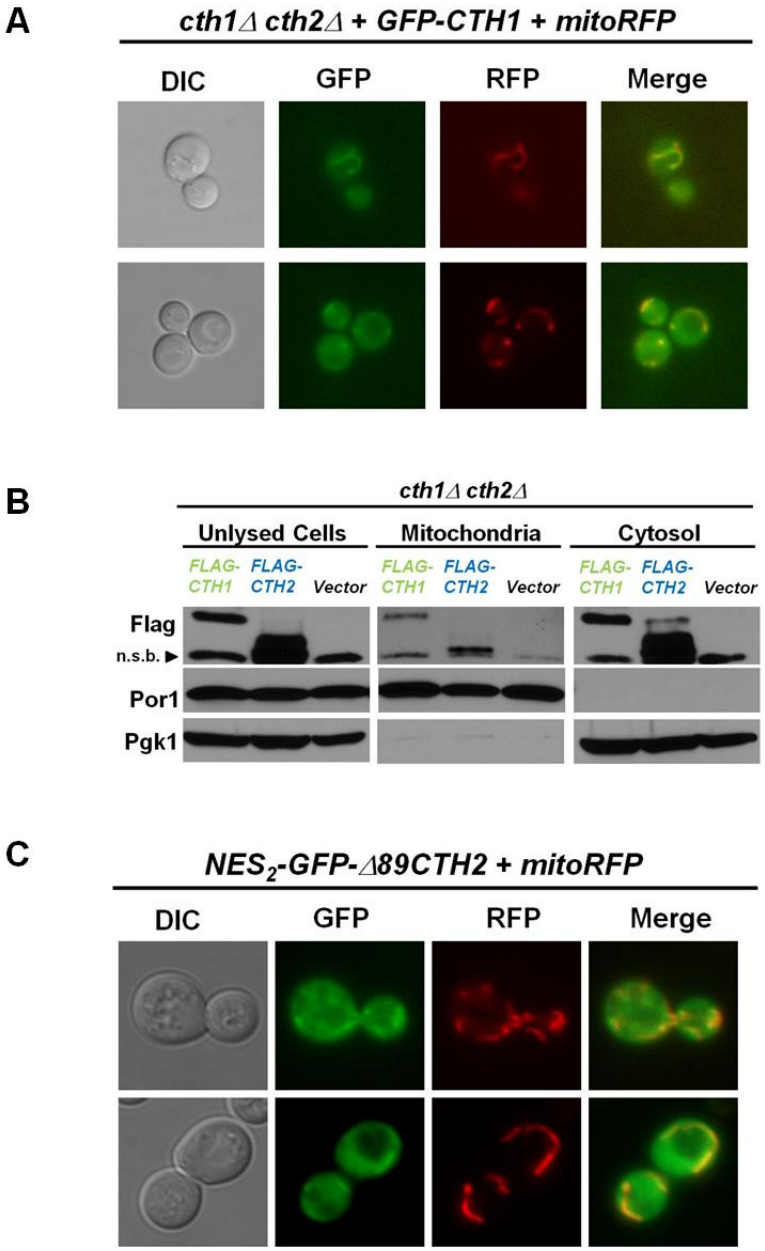

Figure 21. Cth1 and Cth2 partially localize to mitochondria

cth1Δcth2Δ cells co-transformed with p415-Su9 (aa l-69)-RFPff (Janet Shaw, University of Utah) and pRS416-*GFP-CTH1* (**A**), and with pRS416-*NES2-GFP-Δ89-CTH2* (**C**) were visualized by live fluorescence microscopy. **B.** Mitochondrial and cytosolic fractions were obtained from *cth1Δcth2Δ* cells expressing pRS416-*FLAG-CTH1*, pRS416-*FLAG-CTH2*, or vector alone grown in medium containing 100μM BPS (Fe-) and analyzed by immunoblotting. The anti-FLAG-HRP conjugated antibody used to detect Flag-Cth1 and Flag-Cth2 also detects a non-specific band (n.s.b.) indicated by the arrow head. Mitochondrial and cytosolic fractions were identified by incubation with antibodies against Porin and Pgk1 proteins, respectively.

Messenger RNAs targeted for degradation by Cth1 are localized in the vicinity of mitochondria

We analyzed the MLR classification of the putative targets of both Cth1 and Cth2 based on published work by Saint-Georges et al. (2008). Table 10 shows that 8 of 16 mRNAs encoding mitochondrial proteins targeted by Cth1 are MLR-mRNAs, representing 40% of the total pool of Cth1 targets identified in previous studies (Puig et al., 2008). Similarly, Table 11 shows 26 of the 49 mRNAs encoding mitochondrial proteins targeted by Cth2 are MLR-mRNAs, representing 28% of the total mRNA targets of Cth2. Messenger RNAs encoding mitochondrial proteins translated by free-polysomes are labeled as non-MLR-mRNAs, and mRNAs encoding non-mitochondrial proteins were omitted from tables. The observation that almost half of the Cth1 targets, whereas only 28% of the total targets of Cth2 are MLR-mRNAs might explain the predominant localization of Cth1 in the vicinity of mitochondria, while Cth2 localization appears distributed all throughout cells. Though recruitment of target mRNAs could explain the mitochondrial localization of Cth1 and Cth2, our recent findings indicate that Cth2 recruits mRNAs in the nucleus prior to export (Chapter 4), and preliminary data suggest that the NES_2-GFP-Δ89-Cth2 loses mitochondrial localization in cells treated with the transcription inhibitor thiolutin and remains trapped in the nucleus (data not shown). A possible explanation for both observations (mitochondrial localization and nuclear recruitment) may be that Cth1 and Cth2 bind their target mRNAs in the nucleus without altering their final localization in the cytosol. Once the

mRNP is in its native localization, Cth1 and Cth2 can promote turnover by inducing deadenylation and degradation of the bound transcripts. One problem with this hypothesis is the observation that we have been unable to fully determine shuttling of Cth1 or its localization to P-bodies. However, these experiments were done after 6hr of Fe-starvation at which point Cth1 expression is much lower. Some of the immediate questions that should be addressed in order to accelerate our understanding of the role of Cth1 and Cth2 localization to the mitochondria include whether mRNA-binding is required or if a non-mRNA binding mutant forced to the cytoplasm also localizes to the mitochondria. Moreover, the issue with Cth1 shuttling and P-body localization should be addressed through fluorescence microscopy and biochemical fractionations at earlier times during the imposed Fe deficiency.

Table 10: Putative MLR-mRNAs targeted by Cth1

ORF	Gene	Class
YKL148C	***SDH1***	**I**
YER182W	***FMP10***	**I**
YJR016C	***ILV3***	**II**
YKR066C	***CCP1***	**II**
YJR048W	***CYC1***	**II**
YOR356W		II
YLL041C	***SDH2***	**II**
YLR304C	***ACO1***	**II**
YNL052W	***COX5A***	**non-MLR**
YLR355C	*ILV5*	non-MLR
YDL171C	***GLT1***	**non-MLR**
YLR193C	*UPS1*	non-MLR
YDR178W	***SDH4***	**non-MLR**
YDR529C	***QCR7***	**non-MLR**
YJL166W	***QCR8***	**non-MLR**
YNL111C	*CYB5*	non-MLR

MLR-mRNAs identified by Saint-Georges et al., (2008). mRNAs in bold are targets of Cth1 and Cth2. Class I: MLR-mRNAs containing 3'UTR Puf3-sites; Class II: MLR-mRNAs that do not contain Puf3-sites. Non-MRL: mRNAs encoding mitochondrial proteins translated by free polysomes

Table 11: Putative MLR-mRNAs targeted by Cth2

ORF	Gene	Class
YGR255C	*COQ6*	I
YER017C	*AFG3*	I
YDR079W	*PET100*	I
YER141W	*COX15*	I
YPL215W	*CBP3*	I
YKL148C	*SDH1*	I
YER182W	*FMP10*	I
YNL104C	*LEU4*	II
YJR016C	*ILV3*	II
YDR234W	*LYS4*	II
YDR232W	*HEM1*	II
YBR163W	*DEM1*	II
YIL125W	*KGD1*	II
YDR148C	*KGD2*	II
YOR176W	*HEM15*	II
YKR066C	*CCP1*	II
YJR048W	*CYC1*	II
YPR002W	*PDH1*	II
YOR196C	*LIP5*	II
YGR049W	*SCM4*	II
YKL141W	*SDH3*	II
YLL041C	*SDH2*	II
YLR304C	*ACO1*	II
YOR136W	*IDH2*	II
YOR065W	*CYT1*	II
YEL052W	*AFG1*	II
YDL067C	*COX9*	non-MLR
YGL187C	*COX4*	non-MLR
YHR051W	*COX6*	non-MLR
YLR395C	*COX8*	non-MLR
YNL052W	*COX5A*	non-MLR
YLL027W	*ISA1*	non-MLR
YKL040C	*NFU1*	non-MLR
YGR174C	*CBP4*	non-MLR
YDL171C	*GLT1*	non-MLR
YJL026W	*RNR2*	non-MLR
YGR180C	*RNR4*	non-MLR
YOR045W	*TOM6*	non-MLR
YDR044W	*HEM13*	non-MLR
YGL256W	*ADH4*	non-MLR
YOR241W	*MET7*	non-MLR
YDR178W	*SDH4*	non-MLR
YEL024W	*RIP1*	non-MLR
YPR191W	*QCR2*	non-MLR
YDR529C	*QCR7*	non-MLR
YFR033C	*QCR6*	non-MLR
YGR183C	*QCR9*	non-MLR
YJL166W	*QCR8*	non-MLR
YDR070C	*FMP16*	non-MLR

Class I: MLR-mRNAs containing 3'UTR Puf3-sites; Class II: MLR-mRNAs that do not contain Puf3-sites. Non-MRL: mRNAs encoding mitochondrial proteins translated by free polysomes

5.2 Expression of Cth2 in response to glucose-limitation

5.2.1. Introduction

Glucose is the preferred source of chemical energy for most organisms and the biochemical reactions in the dissimilation of glucose are extraordinarily well conserved from bacteria to human. Generally speaking, glucose (a six-carbon sugar) is metabolized into two three-carbon molecules of pyruvate through the biochemical reactions of glycolysis, which also generates 2 net molecules of ATP, several intermediate metabolites and reducing power in the form of NADH and $FADH_2$. Pyruvate represents a central metabolic branch point as it can be further metabolized for energy production via two pathways, which are regulated mostly by oxygen and glucose availability: fermentation (under anaerobic and glucose-rich conditions) or respiration (under aerobic and glucose-limited conditions)(Dickinson and Schweizer, 2004).

During fermentation in animal cells and lactic acid bacteria, pyruvate is reduced to lactic acid in a one-step reaction that involves the re-oxidation of NADH generated in glycolysis back to NAD^+ by lactate dehydrogenase. During alcoholic fermentation carried out by yeasts, pyruvate is first decarboxylated by pyruvate decarboxylase to produce acetyladehyde, followed by its reduction to ethanol by ethanol dehydrogenase. As in lactic acid fermentation, NADH is re-oxidized to NAD^+. The final products of fermentation have the same oxidation state as the starting substrate (glucose) and consequently, little of the potential energy stored in glucose is liberated. The second fate

of pyruvate is respiration. In the presence of oxygen, pyruvate is transported into the mitochondrial matrix where it is oxidatively decarboxylated to Acetyl-CoA by pyruvate dehydrogenase. Acetyl-CoA is subsequently fully oxidized to generate two molecules of CO_2, NADH and $FADH_2$ through the tricarboxylic acid cycle, or TCA cycle. The TCA cycle is an amphibolic pathway, and thus, it generates intermediate metabolites used in the biosynthesis of amino acids, nucleotides, and heme. The NADH and $FADH_2$ redox carriers are re-oxidized in the electron transport chain (ETC) in the inner mitochondrial membrane. The energy liberated from the electron transfer reactions is coupled to oxidative phosphorylation to generate ATP from ADP and inorganic phosphate by ATP synthase. The combined TCA cycle and ETC reactions are highly efficient energy generators, producing 36 ATPs per molecule of pyruvate, and as a consequence is the preferred dissimilation pathway for energy production in most cells living in aerobic environments. While glycolysis and fermentation are highly Fe-independent pathways, the TCA cycle and ETC rely heavily on Fe (and Cu) for the reactions that lead to the full oxidation of Acetyl-CoA to CO_2 (Matthews et al., 2000).

Unlike most cells, the yeast *Saccharomyces cerevisiae* is a facultative aerobic fermenter – it switches from respiratory to mixed respiro-fermentative metabolism in concentrations higher than 0.8mM glucose, even in the presence of oxygen (Verduyn et al., 1992). The relative catalytic capacities of the initial steps in fermentative versus respiratory pathways are thought to favor aerobic fermentation in yeast. First, the

enzyme catalyzing the reduction of pyruvate for entry into fermentation, pyruvate decarboxylase, has greater catalytic capacity than its counterpart, pyruvate dehydrogenase, which catalyzes the oxidation of pyruvate for entry into respiration (Figure 22A); second, high glucose represses many of the genes encoding proteins involved in TCA cycle and oxidative phosphorylation, and as a consequence these enzymes are lowly expressed in cells grown in high glucose concentrations. Mitochondrial respiration is the main producer of reactive oxygen species (ROS) in the cell. Thus, it is possible that high levels of glucose repress respiration as a protective mechanism from unleashed ROS generation. In addition, the production of ethanol may confer a selective advantage against competing micro-organisms.

Because glucose fermentation is a highly inefficient energy generator, yeast must consume copious amounts of glucose in order to produce enough ATP to meet their cellular needs, and therefore produce lavish amounts of ethanol and glycerol that accumulate in the medium (represented by thick arrows in Figure 22A) (Dickinson and Schweizer, 2004). As the glucose concentration in the medium drops, cells undergo metabolic changes such the strong activation of TCA cycle and mitochondrial electron transport chain, enabling them to obtain ATP from the full oxidation of ethanol and glycerol through respiration (Figure 22B). This metabolic switch is called the diauxic shift. Therefore, while respiration is dispensable in cells grown under glucose-rich

conditions, it is indispensable for their growth during the diauxic shift, or in cells grown in non-fermentable carbon source.

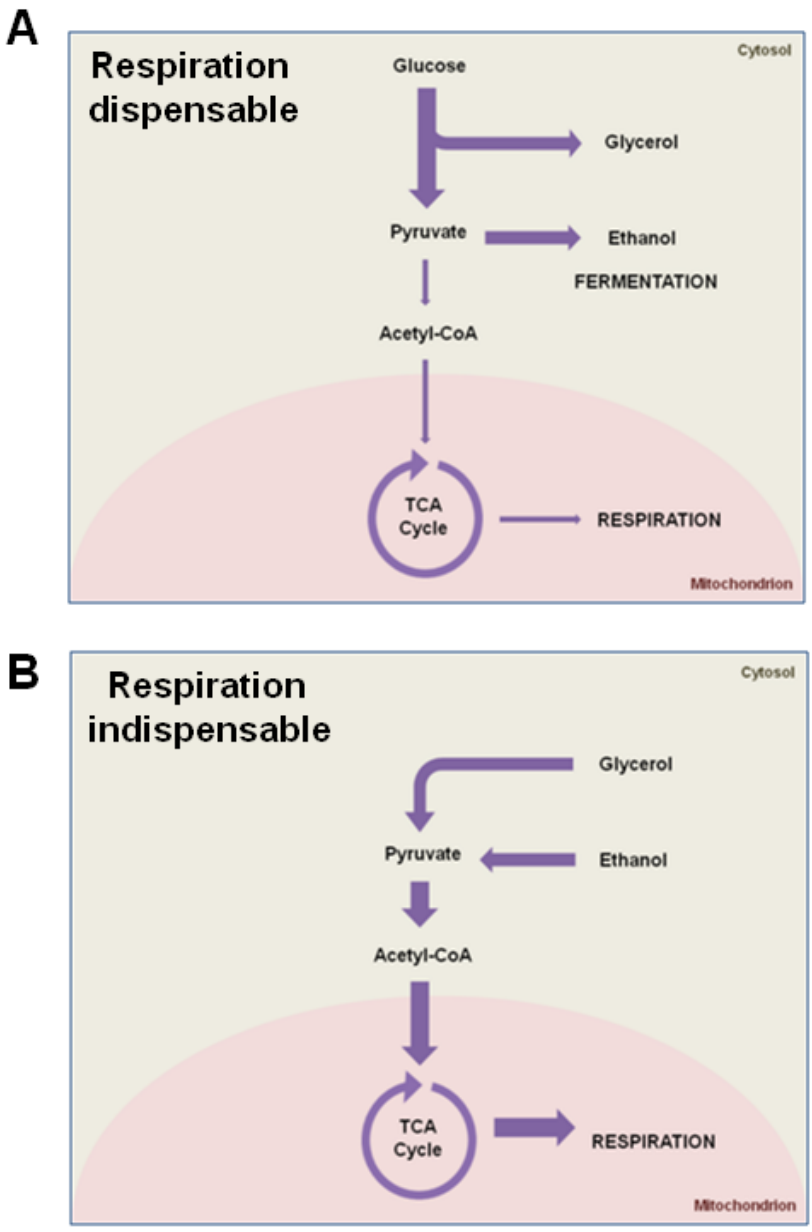

Figure 22. Glucose metabolism in yeast.

A. Respiro-fermentative metabolism of yeast grown in glucose-rich conditions. Thick arrows represent favored pathways. Under glucose-rich conditions, fermentation is favored even in the presence of oxygen

and respiration is dispensable. **B.** Respiratory metabolism under glucose limitation or non-fermentable carbon sources. Respiration is indispensable.

5.2.2. Preliminary results and conclusions

Iron is a key co-factor in the catalysis of countless biochemical reactions, including those involved in energy generation. Not surprisingly, there appears to be an intricate relationship between glucose availability and Fe-homeostasis. Studies in yeast have revealed that a small group of genes belonging to the Fe-regulon are controlled by two key regulators of glucose metabolism: Snf1 and PKA kinases (Haurie et al., 2003; Robertson et al., 2000). The Snf1 kinase plays a crucial role in the transition from fermentative to respiratory metabolism during the diauxic shift, and in growth in non-fermentable carbon sources by promoting the activation of genes involved in the utilization of alternative carbon sources, gluconeogenesis, and mitochondrial respiration among many others. Conversely, PKAs (protein kinase A) are important for the transition back into fermentative metabolism and away from respiration when glucose is added to cells at diauxic shift or growing in non-fermentable carbon sources. Microarrays and RNA blotting analyses from cells grown in glucose limitation demonstrated that the Fe-regulon genes *FET3, FTR1, ARN3, FIT2* and *CTH2* are highly expressed (Haurie et al., 2003). Their transcriptional activation was demonstrated to be regulated by Aft1, but in response to a signal that is independent of Fe-levels, since Fe-supplementation of glucose-starved cultures did not suppress *FET3, FTR1, ARN3, FIT2* and *CTH2* expression. In addition, activation of Aft1 in response to glucose limitation

depends indirectly on Snf1 activity (Haurie et al., 2003). Moreover, microarray analyses showed that strains in which the PKA genes *TPK1*or *TPK2* have been deleted express high levels of Fe-regulon genes involved in the high-affinity uptake of Fe (*FET3, FTR1* and *CCC2*) and siderophore uptake (*ARN3*), suggesting that Tpk1/2 repress the expression of these genes in cells grown in glucose-rich medium (Robertson et al., 2000). Together, these observations suggest that in response to glucose abundance, PKA represses the expression of members of the Fe-regulon involved in Fe-uptake, while their expression is induced by Aft1 via Snf1 activation during glucose limitation. Expression of the Fe-uptake genes may be consistent with an increased need of Fe at diauxic shift or in the presence of non-fermentable carbon sources when respiratory metabolism is essential.

We have previously established that during Fe-limitation, the transcription factor Aft1 activates the robust expression of the *CTH2* gene. In turn, Cth2 functions during Fe-limitation to promote the accelerated turnover of many mRNAs encoding proteins involved in TCA cycle and respiration among many others (Puig et al., 2005; Puig et al., 2008). Thus, during Fe deficiency (even in the presence of glucose) Cth2 is expressed and it works towards repressing respiration, as respiration is dispensable under these conditions (Figure 23B). The observation that the *CTH2* mRNA is highly expressed in cells grown in medium containing non-fermentable carbon sources or at diauxic shift is therefore somewhat paradoxical given that cells rely on respiration under these

conditions (Figure 23A)(Ma and Herschman, 1994; Haurie et al., 2003). What, then, is the role of Cth2 during glucose deficiency? It seems contradictory that Cth2 would target for degradation mRNAs encoding mitochondrial energy generation and preliminary data suggest that at least for the *SDH4* transcript this may not be the case. As shown in Figure 23A, *aft1Δaft2Δ* or *cth2Δ* cells grown in ethanol/glycerol medium express similar *SDH4* levels as *WT* cells, suggesting that under these conditions Cth2 does not mediate its degradation. It would be interesting to address whether Cth2 targets different sets of mRNAs under different conditions. At least four mRNAs down-regulated in response to low glucose contain putative ARE sequences within their 3'-UTRs: *HXK2*, *FBA1*, *RP23*, and *ADH4* (DeRisi et al., 1997). Hexokinase 2 (*HXK2*) catalyzes the first irreversible step of glycolysis, the phosphorylation of glucose to glucose-6-phosphate. Hxk2 is highly expressed in glucose-rich medium, but dramatically repressed during glucose-limitation. *FBA1* encodes fructose 1,6 bisphosphate aldolase required for glycolysis; *RP23* encodes a protein component of the large (60S) ribosomal subunit; and *ADH4* encodes an alcohol dehydrogenase family member that converts acetylaldehyde to ethanol in glucose-rich medium. Thus, while Cth2 promotes the degradation of mRNAs encoding respiratory proteins in response to Fe-deficiency, it would be interesting to ascertain whether Cth2 can also promote the degradation of mRNAs involved in glycolysis and fermentation during glucose-deficiency.

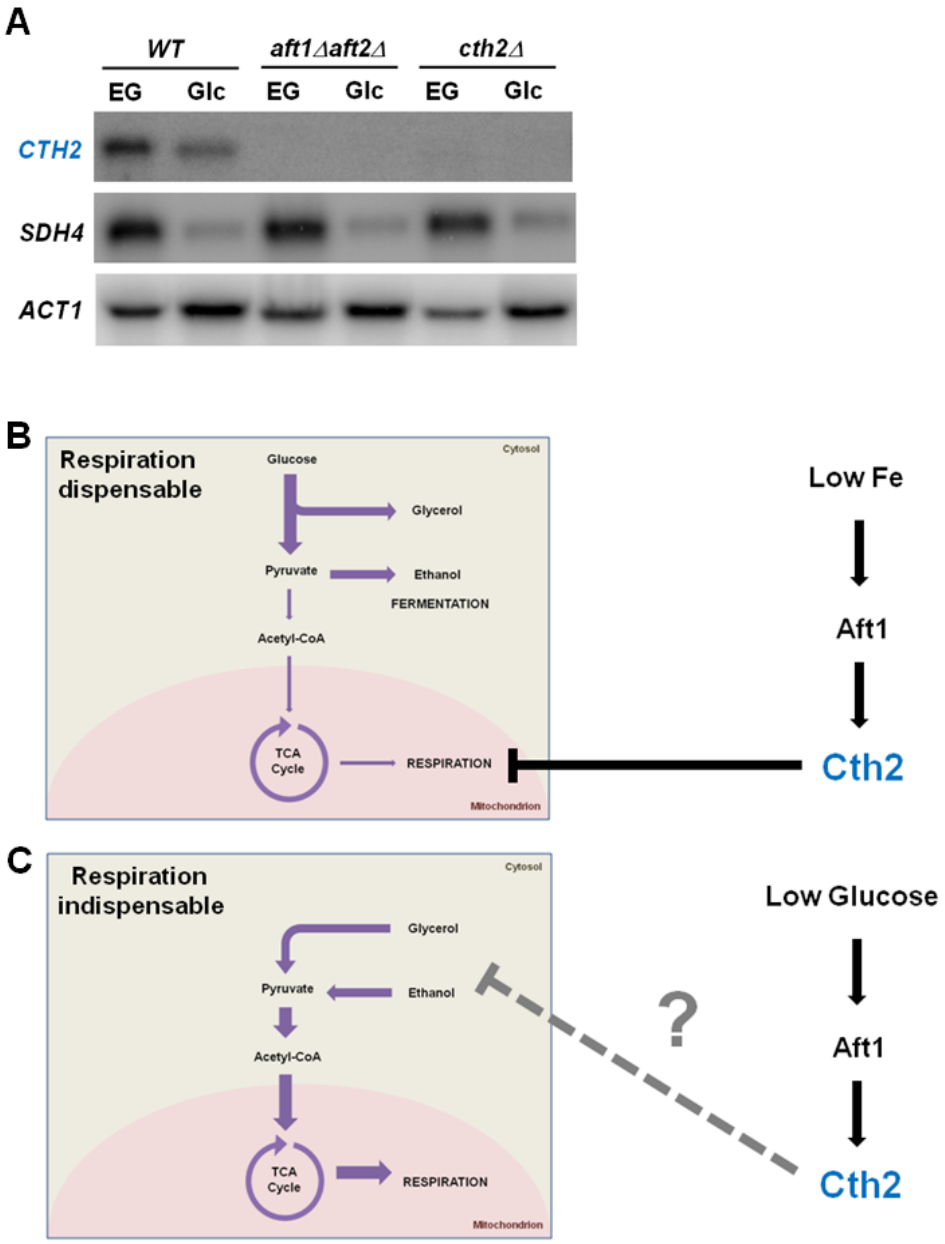

Figure 23. Cth2 expression in response to different respiratory requirements.

A. Cth2 is highly expressed under glucose-limitation. EG: ethanol/glycerol medium. Glc: glucose-rich medium. **B.** In response to Fe-limitation, Aft1 activates the expression of *CTH2*. In the presence of oxygen and in glucose-rich medium, mitochondrial energy generation is dispensable. Thus, as a response to Fe-deficiency, Cth2 promotes the degradation of mRNAs encoding proteins involved in mitochondrial energy generation pathways. **C.** Paradoxically, Aft1 is also activated in response to glucose-limitation inducing the expression of *CTH2*. Cth2 could potentially regulate mRNAs encoding proteins involved in glucose-rich metabolism, such those in glycolysis and fermentation.

5.3. Materials and methods

Live-cell microscopy

c*th1Δcth2Δ* cells co-transformed with pRS416-*GFP-CTH1* or pRS416-*NES*$_2$*-GFP-Δ89-CTH2* and p415-Su9 (aa l-69)-RFPff (Janet Shaw, University of Utah) to mark mitochondria were re-inoculated to an optical density A_{600}=0.2 in selective medium with 100μM BPS. Microscopy experiments were done in live cultures using an AxioImager.A1 (Carl Zeiss, Thornwood, NY) with a 100×/1.4 Plan Apochromat oil immersion objective, an ORCA CCD camera (Hamamatsu, Bridgewater, NJ), and images were captured using the Metamorph 7.5 software.

Mitochondria isolation

Mitochondria were separated from cytosolic fraction by differential centrifugation. Overnight cultures of *cth1Δcth2Δ* cells co-transformed with plasmids *pRS416-FLAG-CTH1* and *pRS415;* or, *pRS416-FLAG-CTH2* and *pRS415; or*, *pRS416* and *pRS415* were re-inoculated to A_{600}=0.2 in 100mL of SC-Ura-Leu and 100μM BPS (-Fe) was added and grown at 30°C for 6hr. Spheroplasts and cell lysis were carried out using reagents from MITOISO3 kit from Sigma. Differential centrifugation was carried out at 3500g for 10min to obtain unlysed whole cells, 6500g for 15m to isolate mitochondria, the cytosolic fraction was collected, and the fractions were analyzed by Immunoblotting using antibodies against the FLAG-epitope (Sigma F-8592), the mitochondria resident

protein porin (Molecular Probes A6449), and the cytosolic protein Pgk1 (Molecular Probes A6457).

RNA blotting

Overnight cultures of BY4741 (WT), *aft1Δaft2Δ*, and *cth2Δ* cells were in glucose-rich medium were re-inoculated to OD_{600}=0.1 in medium containing Ethanol/Glycerol as sole carbon source, or in glucose rich medium. Cells were incubated for 6hr prior to harvesting for total RNA extraction using the glass beads method. Twenty-five micrograms of total RNA were resolved in 1.5% agarose/MOPS gels, transferred overnight on nytran membranes, and mRNAs were detected using DNA probes radiolabeled with ^{32}P-dCTP using random primers (invitrogen).

Works cited

Ades, I.Z., and Butow, R.A. (1980a). The products of mitochondria-bound cytoplasmic polysomes in yeast. J Biol Chem *255*, 9918-9924.

Ades, I.Z., and Butow, R.A. (1980b). The transport of proteins into yeast mitochondria. Kinetics and pools. J Biol Chem *255*, 9925-9935.

Anderson, G.J., Lesuisse, E., Dancis, A., Roman, D.G., Labbe, P., and Klausner, R.D. (1992). Ferric iron reduction and iron assimilation in Saccharomyces cerevisiae. J Inorg Biochem *47*, 249-255.

Andreini, C., Bertini, I., Cavallaro, G., Holliday, G.L., and Thornton, J.M. (2008). Metal ions in biological catalysis: from enzyme databases to general principles. J Biol Inorg Chem *13*, 1205-1218.

Andrews, S.C. (1998). Iron storage in bacteria. Adv Microb Physiol *40*, 281-351.

Archibald, F.S., and Duong, M.N. (1984). Manganese acquisition by Lactobacillus plantarum. J Bacteriol *158*, 1-8.

Argaman, L., Hershberg, R., Vogel, J., Bejerano, G., Wagner, E.G., Margalit, H., and Altuvia, S. (2001). Novel small RNA-encoding genes in the intergenic regions of Escherichia coli. Curr Biol *11*, 941-950.

Arredondo, M., and Nunez, M.T. (2005). Iron and copper metabolism. Mol Aspects Med *26*, 313-327.

Bakheet, T., Frevel, M., Williams, B.R., Greer, W., and Khabar, K.S. (2001). ARED: human AU-rich element-containing mRNA database reveals an unexpectedly diverse functional repertoire of encoded proteins. Nucleic Acids Res *29*, 246-254.

Bakheet, T., Williams, B.R., and Khabar, K.S. (2006). ARED 3.0: the large and diverse AU-rich transcriptome. Nucleic Acids Res *34*, D111-114.

Baou, M., Jewell, A., and Murphy, J.J. (2009). TIS11 family proteins and their roles in posttranscriptional gene regulation. J Biomed Biotechnol *2009*, 634520.

Barreau, C., Paillard, L., and Osborne, H.B. (2005). AU-rich elements and associated factors: are there unifying principles? Nucleic Acids Res *33*, 7138-7150.

Baynes, R.D., and Bothwell, T.H. (1990a). Iron deficiency. Annu Rev Nutr *10*, 133-148.

Baynes, R.D., and Bothwell, T.H. (1990b). Iron deficiency. Annu Rev Nutr *10*, 133-148.

Beard, J.L. (2001). Iron biology in immune function, muscle metabolism and neuronal functioning. J Nutr *131*, 568S-579S; discussion 580S.

Bertini, I., Gray, H.B., Stiefel, E.I., and Valentine, J.S. (2007). Biological inorganic chemistry : structure and reactivity (Sausalito, Calif., University Science Books).

Blackshear, P.J. (2002). Tristetraprolin and other CCCH tandem zinc-finger proteins in the regulation of mRNA turnover. Biochem Soc Trans *30*, 945-952.

Brengues, M., Teixeira, D., and Parker, R. (2005). Movement of eukaryotic mRNAs between polysomes and cytoplasmic processing bodies. Science *310*, 486-489.

Brennan, C.M., and Steitz, J.A. (2001). HuR and mRNA stability. Cell Mol Life Sci *58*, 266-277.

Brooks, S.A., Connolly, J.E., and Rigby, W.F. (2004). The role of mRNA turnover in the regulation of tristetraprolin expression: evidence for an extracellular signal-regulated kinase-specific, AU-rich element-dependent, autoregulatory pathway. J Immunol *172*, 7263-7271.

Bullen, J.J., Rogers, H.J., and Griffiths, E. (1978). Role of iron in bacterial infection. Curr Top Microbiol Immunol *80*, 1-35.

Carballo, E., Lai, W.S., and Blackshear, P.J. (1998). Feedback inhibition of macrophage tumor necrosis factor-alpha production by tristetraprolin. Science *281*, 1001-1005.

Carballo, E., Lai, W.S., and Blackshear, P.J. (2000). Evidence that tristetraprolin is a physiological regulator of granulocyte-macrophage colony-stimulating factor messenger RNA deadenylation and stability. Blood *95*, 1891-1899.

Cartron, M.L., Maddocks, S., Gillingham, P., Craven, C.J., and Andrews, S.C. (2006). Feo--transport of ferrous iron into bacteria. Biometals *19*, 143-157.

Cartwright, G.E., Lauritsen, M.A., Humphreys, S., Jones, P.J., Merrill, I.M., and Wintrobe, M.M. (1946). The Anemia Associated With Chronic Infection. Science *103*, 72-73.

Chen, C.Y., Del Gatto-Konczak, F., Wu, Z., and Karin, M. (1998). Stabilization of interleukin-2 mRNA by the c-Jun NH2-terminal kinase pathway. Science *280*, 1945-1949.

Chen, C.Y., Gherzi, R., Ong, S.E., Chan, E.L., Raijmakers, R., Pruijn, G.J., Stoecklin, G., Moroni, C., Mann, M., and Karin, M. (2001). AU binding proteins recruit the exosome to degrade ARE-containing mRNAs. Cell *107*, 451-464.

Chen, C.Y., and Shyu, A.B. (1995). AU-rich elements: characterization and importance in mRNA degradation. Trends Biochem Sci *20*, 465-470.

Chen, C.Y., Xu, N., and Shyu, A.B. (1995). mRNA decay mediated by two distinct AU-rich elements from c-fos and granulocyte-macrophage colony-stimulating factor transcripts: different deadenylation kinetics and uncoupling from translation. Mol Cell Biol *15*, 5777-5788.

Chen, O.S., Crisp, R.J., Valachovic, M., Bard, M., Winge, D.R., and Kaplan, J. (2004). Transcription of the yeast iron regulon does not respond directly to iron but rather to iron-sulfur cluster biosynthesis. J Biol Chem *279*, 29513-29518.

Ciais, D., Bohnsack, M.T., and Tollervey, D. (2008). The mRNA encoding the yeast ARE-binding protein Cth2 is generated by a novel 3' processing pathway. Nucleic Acids Res *36*, 3075-3084.

Corral-Debrinski, M., Blugeon, C., and Jacq, C. (2000). In yeast, the 3' untranslated region or the presequence of ATM1 is required for the exclusive localization of its mRNA to the vicinity of mitochondria. Mol Cell Biol *20*, 7881-7892.

Courel, M., Lallet, S., Camadro, J.M., and Blaiseau, P.L. (2005). Direct activation of genes involved in intracellular iron use by the yeast iron-responsive transcription factor Aft2 without its paralog Aft1. Mol Cell Biol *25*, 6760-6771.

Cowart, R.E. (2002). Reduction of iron by extracellular iron reductases: implications for microbial iron acquisition. Arch Biochem Biophys *400*, 273-281.

Dancis, A. (1998). Genetic analysis of iron uptake in the yeast Saccharomyces cerevisiae. J Pediatr *132*, S24-29.

De Domenico, I., McVey Ward, D., and Kaplan, J. (2008). Regulation of iron acquisition and storage: consequences for iron-linked disorders. Nat Rev Mol Cell Biol *9*, 72-81.

De Freitas, J., Wintz, H., Kim, J.H., Poynton, H., Fox, T., and Vulpe, C. (2003). Yeast, a model organism for iron and copper metabolism studies. Biometals *16*, 185-197.

DeRisi, J.L., Iyer, V.R., and Brown, P.O. (1997). Exploring the metabolic and genetic control of gene expression on a genomic scale. Science *278*, 680-686.

Dickinson, J.R., and Schweizer, M. (2004). The metabolism and molecular physiology of Saccharomyces cerevisiae, 2nd edn (Boca Raton, CRC Press).

Dunn, E.F., Hammell, C.M., Hodge, C.A., and Cole, C.N. (2005). Yeast poly(A)-binding protein, Pab1, and PAN, a poly(A) nuclease complex recruited by Pab1, connect mRNA biogenesis to export. Genes Dev *19*, 90-103.

Dunn, L.L., Rahmanto, Y.S., and Richardson, D.R. (2007). Iron uptake and metabolism in the new millennium. Trends Cell Biol *17*, 93-100.

Dupont, C.L., Yang, S., Palenik, B., and Bourne, P.E. (2006). Modern proteomes contain putative imprints of ancient shifts in trace metal geochemistry. Proc Natl Acad Sci U S A *103*, 17822-17827.

Edgington, N.P., and Futcher, B. (2001). Relationship between the function and the location of G1 cyclins in S. cerevisiae. J Cell Sci *114*, 4599-4611.

Escolar, L., Perez-Martin, J., and de Lorenzo, V. (1999). Opening the iron box: transcriptional metalloregulation by the Fur protein. J Bacteriol *181*, 6223-6229.

Felice, M.R., De Domenico, I., Li, L., Ward, D.M., Bartok, B., Musci, G., and Kaplan, J. (2005). Post-transcriptional regulation of the yeast high affinity iron transport system. J Biol Chem *280*, 22181-22190.

Fenger-Gron, M., Fillman, C., Norrild, B., and Lykke-Andersen, J. (2005). Multiple processing body factors and the ARE binding protein TTP activate mRNA decapping. Mol Cell *20*, 905-915.

Fernandes, L., Rodrigues-Pousada, C., and Struhl, K. (1997). Yap, a novel family of eight bZIP proteins in Saccharomyces cerevisiae with distinct biological functions. Mol Cell Biol *17*, 6982-6993.

Fillman, C., and Lykke-Andersen, J. (2005). RNA decapping inside and outside of processing bodies. Curr Opin Cell Biol *17*, 326-331.

Frederick, R.L., McCaffery, J.M., Cunningham, K.W., Okamoto, K., and Shaw, J.M. (2004). Yeast Miro GTPase, Gem1p, regulates mitochondrial morphology via a novel pathway. J Cell Biol *167*, 87-98.

Garcia-Rodriguez, L.J., Gay, A.C., and Pon, L.A. (2007). Puf3p, a Pumilio family RNA binding protein, localizes to mitochondria and regulates mitochondrial biogenesis and motility in budding yeast. J Cell Biol *176*, 197-207.

Garneau, N.L., Wilusz, J., and Wilusz, C.J. (2007). The highways and byways of mRNA decay. Nat Rev Mol Cell Biol *8*, 113-126.

Georgatsou, E., Georgakopoulos, T., and Thireos, G. (1992). Molecular cloning of an essential yeast gene encoding a proteasomal subunit. FEBS Lett *299*, 39-43.

Hahn, J.S., Hu, Z., Thiele, D.J., and Iyer, V.R. (2004). Genome-wide analysis of the biology of stress responses through heat shock transcription factor. Mol Cell Biol *24*, 5249-5256.

Hall, H.K., and Foster, J.W. (1996). The role of fur in the acid tolerance response of Salmonella typhimurium is physiologically and genetically separable from its role in iron acquisition. J Bacteriol *178*, 5683-5691.

Hansch, R., and Mendel, R.R. (2009). Physiological functions of mineral micronutrients (Cu, Zn, Mn, Fe, Ni, Mo, B, Cl). Curr Opin Plant Biol *12*, 259-266.

Hantke, K. (1981). Regulation of ferric iron transport in Escherichia coli K12: isolation of a constitutive mutant. Mol Gen Genet *182*, 288-292.

Haurie, V., Boucherie, H., and Sagliocco, F. (2003). The Snf1 protein kinase controls the induction of genes of the iron uptake pathway at the diauxic shift in Saccharomyces cerevisiae. J Biol Chem *278*, 45391-45396.

Hentze, M.W., Muckenthaler, M.U., and Andrews, N.C. (2004). Balancing acts: molecular control of mammalian iron metabolism. Cell *117*, 285-297.

Hilleren, P., and Parker, R. (2001). Defects in the mRNA export factors Rat7p, Gle1p, Mex67p, and Rat8p cause hyperadenylation during 3'-end formation of nascent transcripts. RNA *7*, 753-764.

Horton, S., and Ross, J. (2003). The economics of iron deficiency. Food policy *28*, 51-75.

Hudson, B.P., Martinez-Yamout, M.A., Dyson, H.J., and Wright, P.E. (2004). Recognition of the mRNA AU-rich element by the zinc finger domain of TIS11d. Nat Struct Mol Biol *11*, 257-264.

Johnson, B.A., Stehn, J.R., Yaffe, M.B., and Blackwell, T.K. (2002). Cytoplasmic localization of tristetraprolin involves 14-3-3-dependent and -independent mechanisms. J Biol Chem *277*, 18029-18036.

Kaplan, J., McVey Ward, D., Crisp, R.J., and Philpott, C.C. (2006). Iron-dependent metabolic remodeling in S. cerevisiae. Biochim Biophys Acta *1763*, 646-651.

Kehres, D.G., and Maguire, M.E. (2002). Structure, properties and regulation of magnesium transport proteins. Biometals *15*, 261-270.

Kellems, R.E., Allison, V.F., and Butow, R.A. (1974). Cytoplasmic type 80 S ribosomes associated with yeast mitochondria. II. Evidence for the association of cytoplasmic ribosomes with the outer mitochondrial membrane in situ. J Biol Chem *249*, 3297-3303.

Kellems, R.E., Allison, V.F., and Butow, R.A. (1975). Cytoplasmic type 80S ribosomes associated with yeast mitochondria. IV. Attachment of ribosomes to the outer membrane of isolated mitochondria. J Cell Biol *65*, 1-14.

Kellems, R.E., and Butow, R.A. (1972). Cytoplasmic-type 80 S ribosomes associated with yeast mitochondria. I. Evidence for ribosome binding sites on yeast mitochondria. J Biol Chem *247*, 8043-8050.

Kellems, R.E., and Butow, R.A. (1974). Cytoplasmic type 80 S ribosomes associated with yeast mitochondria. 3. Changes in the amount of bound ribosomes in response to changes in metabolic state. J Biol Chem *249*, 3304-3310.

Lai, W.S., Carballo, E., Strum, J.R., Kennington, E.A., Phillips, R.S., and Blackshear, P.J. (1999). Evidence that tristetraprolin binds to AU-rich elements and promotes the deadenylation and destabilization of tumor necrosis factor alpha mRNA. Mol Cell Biol *19*, 4311-4323.

Lai, W.S., Kennington, E.A., and Blackshear, P.J. (2003). Tristetraprolin and its family members can promote the cell-free deadenylation of AU-rich element-containing mRNAs by poly(A) ribonuclease. Mol Cell Biol *23*, 3798-3812.

Lai, W.S., Parker, J.S., Grissom, S.F., Stumpo, D.J., and Blackshear, P.J. (2006). Novel mRNA targets for tristetraprolin (TTP) identified by global analysis of stabilized transcripts in TTP-deficient fibroblasts. Mol Cell Biol *26*, 9196-9208.

Lee, A., Henras, A.K., and Chanfreau, G. (2005). Multiple RNA surveillance pathways limit aberrant expression of iron uptake mRNAs and prevent iron toxicity in S. cerevisiae. Mol Cell *19*, 39-51.

Lee, M.S., Henry, M., and Silver, P.A. (1996). A protein that shuttles between the nucleus and the cytoplasm is an important mediator of RNA export. Genes Dev *10*, 1233-1246.

Lee, T.I., Rinaldi, N.J., Robert, F., Odom, D.T., Bar-Joseph, Z., Gerber, G.K., Hannett, N.M., Harbison, C.T., Thompson, C.M., Simon, I., *et al.* (2002). Transcriptional regulatory networks in Saccharomyces cerevisiae. Science *298*, 799-804.

Lesuisse, E., Santos, R., Matzanke, B.F., Knight, S.A., Camadro, J.M., and Dancis, A. (2003). Iron use for haeme synthesis is under control of the yeast frataxin homologue (Yfh1). Hum Mol Genet *12*, 879-889.

Li, L., Bagley, D., Ward, D.M., and Kaplan, J. (2008). Yap5 is an iron-responsive transcriptional activator that regulates vacuolar iron storage in yeast. Mol Cell Biol *28*, 1326-1337.

Lill, R., and Muhlenhoff, U. (2008). Maturation of iron-sulfur proteins in eukaryotes: mechanisms, connected processes, and diseases. Annu Rev Biochem *77*, 669-700.

Lippard, S.J., and Berg, J.M. (1994). Principles of bioinorganic chemistry (Mill Valley, Calif., University Science Books).

Litwin, C.M., and Calderwood, S.B. (1993). Role of iron in regulation of virulence genes. Clin Microbiol Rev *6*, 137-149.

Lykke-Andersen, J., and Wagner, E. (2005). Recruitment and activation of mRNA decay enzymes by two ARE-mediated decay activation domains in the proteins TTP and BRF-1. Genes Dev *19*, 351-361.

Ma, Q., and Herschman, H.R. (1995). The yeast homologue YTIS11, of the mammalian TIS11 gene family is a non-essential, glucose repressible gene. Oncogene *10*, 487-494.

Marc, P., Margeot, A., Devaux, F., Blugeon, C., Corral-Debrinski, M., and Jacq, C. (2002). Genome-wide analysis of mRNAs targeted to yeast mitochondria. EMBO Rep *3*, 159-164.

Masse, E., and Arguin, M. (2005). Ironing out the problem: new mechanisms of iron homeostasis. Trends Biochem Sci *30*, 462-468.

Masse, E., and Gottesman, S. (2002). A small RNA regulates the expression of genes involved in iron metabolism in Escherichia coli. Proc Natl Acad Sci U S A *99*, 4620-4625.

Masse, E., Salvail, H., Desnoyers, G., and Arguin, M. (2007). Small RNAs controlling iron metabolism. Curr Opin Microbiol *10*, 140-145.

Masse, E., Vanderpool, C.K., and Gottesman, S. (2005). Effect of RyhB small RNA on global iron use in Escherichia coli. J Bacteriol *187*, 6962-6971.

Ming, X.F., Kaiser, M., and Moroni, C. (1998). c-jun N-terminal kinase is involved in AUUUA-mediated interleukin-3 mRNA turnover in mast cells. EMBO J *17*, 6039-6048.

Murata, T., Yoshino, Y., Morita, N., and Kaneda, N. (2002). Identification of nuclear import and export signals within the structure of the zinc finger protein TIS11. Biochem Biophys Res Commun *293*, 1242-1247.

Neupert, W. (1997). Protein import into mitochondria. Annu Rev Biochem *66*, 863-917.

Niederhoffer, E.C., Naranjo, C.M., Bradley, K.L., and Fee, J.A. (1990). Control of Escherichia coli superoxide dismutase (sodA and sodB) genes by the ferric uptake regulation (fur) locus. J Bacteriol *172*, 1930-1938.

Parker, R., and Song, H. (2004). The enzymes and control of eukaryotic mRNA turnover. Nat Struct Mol Biol *11*, 121-127.

Pedro-Segura, E., Vergara, S.V., Rodriguez-Navarro, S., Parker, R., Thiele, D.J., and Puig, S. (2008). The Cth2 ARE-binding protein recruits the Dhh1 helicase to promote the decay of succinate dehydrogenase SDH4 mRNA in response to iron deficiency. J Biol Chem *283*, 28527-28535.

Peng, S.S., Chen, C.Y., Xu, N., and Shyu, A.B. (1998). RNA stabilization by the AU-rich element binding protein, HuR, an ELAV protein. EMBO J *17*, 3461-3470.

Phillips, R.S., Ramos, S.B., and Blackshear, P.J. (2002). Members of the tristetraprolin family of tandem CCCH zinc finger proteins exhibit CRM1-dependent nucleocytoplasmic shuttling. J Biol Chem *277*, 11606-11613.

Philpott, C.C., and Protchenko, O. (2008). Response to iron deprivation in Saccharomyces cerevisiae. Eukaryot Cell *7*, 20-27.

Philpott, C.C., Protchenko, O., Kim, Y.W., Boretsky, Y., and Shakoury-Elizeh, M. (2002). The response to iron deprivation in Saccharomyces cerevisiae: expression of siderophore-based systems of iron uptake. Biochem Soc Trans *30*, 698-702.

Philpott, C.C., Rashford, J., Yamaguchi-Iwai, Y., Rouault, T.A., Dancis, A., and Klausner, R.D. (1998). Cell-cycle arrest and inhibition of G1 cyclin translation by iron in AFT1-1(up) yeast. EMBO J *17*, 5026-5036.

Posey, J.E., and Gherardini, F.C. (2000). Lack of a role for iron in the Lyme disease pathogen. Science *288*, 1651-1653.

Protchenko, O., and Philpott, C.C. (2003). Regulation of intracellular heme levels by HMX1, a homologue of heme oxygenase, in Saccharomyces cerevisiae. J Biol Chem *278*, 36582-36587.

Prouteau, M., Daugeron, M.C., and Seraphin, B. (2008). Regulation of ARE transcript 3' end processing by the yeast Cth2 mRNA decay factor. EMBO J *27*, 2966-2976.

Puig, S., Askeland, E., and Thiele, D.J. (2005). Coordinated remodeling of cellular metabolism during iron deficiency through targeted mRNA degradation. Cell *120*, 99-110.

Puig, S., Vergara, S.V., and Thiele, D.J. (2008). Cooperation of two mRNA-binding proteins drives metabolic adaptation to iron deficiency. Cell Metab *7*, 555-564.

Ratledge, C., and Dover, L.G. (2000). Iron metabolism in pathogenic bacteria. Annu Rev Microbiol *54*, 881-941.

Robertson, L.S., Causton, H.C., Young, R.A., and Fink, G.R. (2000). The yeast A kinases differentially regulate iron uptake and respiratory function. Proc Natl Acad Sci U S A *97*, 5984-5988.

Rouault, T.A. (2006). The role of iron regulatory proteins in mammalian iron homeostasis and disease. Nat Chem Biol *2*, 406-414.

Rouault, T.A., and Tong, W.H. (2005). Iron-sulphur cluster biogenesis and mitochondrial iron homeostasis. Nat Rev Mol Cell Biol *6*, 345-351.

Rutherford, J.C., Jaron, S., Ray, E., Brown, P.O., and Winge, D.R. (2001). A second iron-regulatory system in yeast independent of Aft1p. Proc Natl Acad Sci U S A *98*, 14322-14327.

Rutherford, J.C., Jaron, S., and Winge, D.R. (2003). Aft1p and Aft2p mediate iron-responsive gene expression in yeast through related promoter elements. J Biol Chem *278*, 27636-27643.

Saint-Georges, Y., Garcia, M., Delaveau, T., Jourdren, L., Le Crom, S., Lemoine, S., Tanty, V., Devaux, F., and Jacq, C. (2008). Yeast mitochondrial biogenesis: a role for the PUF RNA-binding protein Puf3p in mRNA localization. PLoS One *3*, e2293.

Sandler, H., and Stoecklin, G. (2008). Control of mRNA decay by phosphorylation of tristetraprolin. Biochem Soc Trans *36*, 491-496.

Schaible, U.E., and Kaufmann, S.H. (2004). Iron and microbial infection. Nat Rev Microbiol *2*, 946-953.

Schatz, G., and Dobberstein, B. (1996). Common principles of protein translocation across membranes. Science *271*, 1519-1526.

Segref, A., Sharma, K., Doye, V., Hellwig, A., Huber, J., Luhrmann, R., and Hurt, E. (1997). Mex67p, a novel factor for nuclear mRNA export, binds to both poly(A)+ RNA and nuclear pores. EMBO J *16*, 3256-3271.

SenGupta, D.J., Zhang, B., Kraemer, B., Pochart, P., Fields, S., and Wickens, M. (1996). A three-hybrid system to detect RNA-protein interactions in vivo. Proc Natl Acad Sci U S A *93*, 8496-8501.

Shakoury-Elizeh, M., Tiedeman, J., Rashford, J., Ferea, T., Demeter, J., Garcia, E., Rolfes, R., Brown, P.O., Botstein, D., and Philpott, C.C. (2004). Transcriptional remodeling in response to iron deprivation in Saccharomyces cerevisiae. Mol Biol Cell *15*, 1233-1243.

Sheftel, A.D., and Lill, R. (2009). The power plant of the cell is also a smithy: the emerging role of mitochondria in cellular iron homeostasis. Ann Med *41*, 82-99.

Sheth, U., and Parker, R. (2003). Decapping and decay of messenger RNA occur in cytoplasmic processing bodies. Science *300*, 805-808.

Stadler, J.A., and Schweyen, R.J. (2002). The yeast iron regulon is induced upon cobalt stress and crucial for cobalt tolerance. J Biol Chem *277*, 39649-39654.

Stipanuk, M.H. (2000). Biochemical and physiological aspects of human nutrition (Philadelphia, W.B. Saunders).

Stoecklin, G., Colombi, M., Raineri, I., Leuenberger, S., Mallaun, M., Schmidlin, M., Gross, B., Lu, M., Kitamura, T., and Moroni, C. (2002). Functional cloning of BRF1, a regulator of ARE-dependent mRNA turnover. EMBO J *21*, 4709-4718.

Stoecklin, G., Stoeckle, P., Lu, M., Muehlemann, O., and Moroni, C. (2001). Cellular mutants define a common mRNA degradation pathway targeting cytokine AU-rich elements. RNA *7*, 1578-1588.

Stoecklin, G., Stubbs, T., Kedersha, N., Wax, S., Rigby, W.F., Blackwell, T.K., and Anderson, P. (2004). MK2-induced tristetraprolin:14-3-3 complexes prevent stress granule association and ARE-mRNA decay. EMBO J *23*, 1313-1324.

Stoecklin, G., Tenenbaum, S.A., Mayo, T., Chittur, S.V., George, A.D., Baroni, T.E., Blackshear, P.J., and Anderson, P. (2008). Genome-wide analysis identifies interleukin-10 mRNA as target of tristetraprolin. J Biol Chem *283*, 11689-11699.

Stojiljkovic, I., and Hantke, K. (1994). Transport of haemin across the cytoplasmic membrane through a haemin-specific periplasmic binding-protein-dependent transport system in Yersinia enterocolitica. Mol Microbiol *13*, 719-732.

Sylvestre, J., Margeot, A., Jacq, C., Dujardin, G., and Corral-Debrinski, M. (2003a). The role of the 3' untranslated region in mRNA sorting to the vicinity of mitochondria is conserved from yeast to human cells. Mol Biol Cell *14*, 3848-3856.

Sylvestre, J., Vialette, S., Corral Debrinski, M., and Jacq, C. (2003b). Long mRNAs coding for yeast mitochondrial proteins of prokaryotic origin preferentially localize to the vicinity of mitochondria. Genome Biol *4*, R44.

Tardat, B., and Touati, D. (1993). Iron and oxygen regulation of Escherichia coli MnSOD expression: competition between the global regulators Fur and ArcA for binding to DNA. Mol Microbiol *9*, 53-63.

Taylor, G.A., Carballo, E., Lee, D.M., Lai, W.S., Thompson, M.J., Patel, D.D., Schenkman, D.I., Gilkeson, G.S., Broxmeyer, H.E., Haynes, B.F., *et al.* (1996a). A pathogenetic role for TNF alpha in the syndrome of cachexia, arthritis, and autoimmunity resulting from tristetraprolin (TTP) deficiency. Immunity *4*, 445-454.

Taylor, G.A., Thompson, M.J., Lai, W.S., and Blackshear, P.J. (1996b). Mitogens stimulate the rapid nuclear to cytosolic translocation of tristetraprolin, a potential zinc-finger transcription factor. Mol Endocrinol *10*, 140-146.

Tchen, C.R., Brook, M., Saklatvala, J., and Clark, A.R. (2004). The stability of tristetraprolin mRNA is regulated by mitogen-activated protein kinase p38 and by tristetraprolin itself. J Biol Chem *279*, 32393-32400.

Teixeira, D., and Parker, R. (2007). Analysis of P-body assembly in Saccharomyces cerevisiae. Mol Biol Cell *18*, 2274-2287.

Thompson, M.J., Lai, W.S., Taylor, G.A., and Blackshear, P.J. (1996). Cloning and characterization of two yeast genes encoding members of the CCCH class of zinc finger proteins: zinc finger-mediated impairment of cell growth. Gene *174*, 225-233.

Tipper, D.J. (1973). Inhibition of yeast ribonucleic acid polymerases by thiolutin. J Bacteriol *116*, 245-256.

Van Ho, A., Ward, D.M., and Kaplan, J. (2002). Transition metal transport in yeast. Annu Rev Microbiol *56*, 237-261.

Vasudevan, S., and Peltz, S.W. (2001). Regulated ARE-mediated mRNA decay in Saccharomyces cerevisiae. Mol Cell *7*, 1191-1200.

Verduyn, W.H., Hilt, J., Roberts, M.A., and Roberts, R.J. (1992). Multiple partial seizure-like symptoms following 'minor' closed head injury. Brain Inj *6*, 245-260.

Vergara, S.V., and Thiele, D.J. (2008). Post-transcriptional regulation of gene expression in response to iron deficiency: co-ordinated metabolic reprogramming by yeast mRNA-binding proteins. Biochem Soc Trans *36*, 1088-1090.

Waldron, K.J., Rutherford, J.C., Ford, D., and Robinson, N.J. (2009). Metalloproteins and metal sensing. Nature *460*, 823-830.

Wassarman, K.M., Repoila, F., Rosenow, C., Storz, G., and Gottesman, S. (2001). Identification of novel small RNAs using comparative genomics and microarrays. Genes Dev *15*, 1637-1651.

West, A.R., and Oates, P.S. (2008). Mechanisms of heme iron absorption: current questions and controversies. World J Gastroenterol *14*, 4101-4110.

Wienk, K.J., Marx, J.J., and Beynen, A.C. (1999). The concept of iron bioavailability and its assessment. Eur J Nutr *38*, 51-75.

Williams, R.J., and Frausto Da Silva, J.J. (2003). Evolution was chemically constrained. J Theor Biol *220*, 323-343.

Wilusz, C.J., Wormington, M., and Peltz, S.W. (2001). The cap-to-tail guide to mRNA turnover. Nat Rev Mol Cell Biol *2*, 237-246.

Winzen, R., Kracht, M., Ritter, B., Wilhelm, A., Chen, C.Y., Shyu, A.B., Muller, M., Gaestel, M., Resch, K., and Holtmann, H. (1999). The p38 MAP kinase pathway signals for cytokine-induced mRNA stabilization via MAP kinase-activated protein kinase 2 and an AU-rich region-targeted mechanism. EMBO J *18*, 4969-4980.

Wolfe, K.H., and Shields, D.C. (1997). Molecular evidence for an ancient duplication of the entire yeast genome. Nature *387*, 708-713.

Yamaguchi-Iwai, Y., Ueta, R., Fukunaka, A., and Sasaki, R. (2002). Subcellular localization of Aft1 transcription factor responds to iron status in Saccharomyces cerevisiae. J Biol Chem *277*, 18914-18918.

Zaharik, M.L., and Finlay, B.B. (2004). Mn2+ and bacterial pathogenesis. Front Biosci *9*, 1035-1042.

Biography

Sandra Viviana Vergara was born on October 2nd, 1977 in southwestern Colombia. After graduating from high school, she moved to the United States to pursue her college education. She obtained an Associate of Arts degree from Santa Fe Community College in Gainesville (Florida) in 2000, and a Bachelor of Science in Microbiology and Cell Science with a minor in French from the University of Florida in 2003 (Go Gators!). During her tenure at the University of Florida, she participated in a study abroad program at the Institute for American Universities in Avignon, France. In 2001, she joined the laboratory of Dr. Stephen Gluck in the Division of Nephrology, Department of Medicine at the University of Florida and worked under the direct supervision of Dr. Ming Lu on the function, transport and regulation of the Vacuolar (H+)-ATPases in yeast. She later joined the laboratory of Dr. Shannon L. Holliday in the Department of Orthodontics, School of Dentistry where she studied the interactions of yeast Vacuolar (H+)-ATPases with the actin cytoskeleton. Sandra joined the matriculating class of 2004 in the University Program in Genetics and Genomics at Duke University, and in 2005 she joined the laboratory of Dr. Dennis J. Thiele in the Department of Pharmacology and Cancer Biology to pursue her dissertation research. Her work has focused in elucidating the molecular mechanisms by which yeast cells adapt to iron deficiency. She is a co-author in seven publications: "Ironing out a midlife crisis" (Cell, 2009), "Post-transcriptional regulation of gene expression in response to

iron deficiency: coordinated metabolic reprogramming by yeast mRNA-binding proteins" (Biochem.Soc.Trans., 2008), "The Cth2 ARE-binding protein recruits the Dhh1 helicase to promote the decay of succinate dehydrogenase SDH4 mRNA in response to iron deficiency" (J. Biol Chem., 2008), "Cooperation of two mRNA-binding proteins drives metabolic adaptation to iron deficiency" (Cell Metab., 2008), "Biochemical and functional characterization of the actin-binding activity of the B subunit of yeast vacuolar H+-ATPase" (J Exp Biol., 2008), ''Actin binding activity of subunit B of vacuolar H(+)-ATPase is involved in its targeting to ruffled membranes of osteoclasts" (J Bone Miner Res., 2006), "The amino-terminal domain of the E subunit of vacuolar H^+-ATPase (V-ATPase) interacts with the H subunit and is required for V-ATPase function" (J Biol Chem., 2002). Sandra is the recipient of a NRSA pre-doctoral fellowship from the National Institutes of Health (NIH / NIDDK. No. FDK081304A), a National Science Foundation Graduate Research Honorable Mention (2005), and the Robert J. Fitzgerald Scholar Award (Duke University, 2008). She is also the recipient of student travel awards and poster awards from the American Society of Biochemistry and Molecular Biology (2010), the International BioIron Society (2009), and the Carl Storm Underrepresented Minority Fellowship Program (2005).